SANDIA REPORT
SAND2011-9320
Unlimited Release
Printed December 2011

An Evaluation of Possible Next-Generation High-Temperature Molten-Salt Power Towers

Gregory J. Kolb

Prepared by
Sandia National Laboratories
Albuquerque, New Mexico 87185 and Livermore, California 94550

Sandia National Laboratories is a multi-program laboratory managed and operated by Sandia Corporation, a wholly owned subsidiary of Lockheed Martin Corporation, for the U.S. Department of Energy's National Nuclear Security Administration under contract DE-AC04-94AL85000.

Issued by Sandia National Laboratories, operated for the United States Department of Energy by Sandia Corporation.

Available to DOE and DOE contractors from
U.S. Department of Energy
Office of Scientific and Technical Information
P.O. Box 62
Oak Ridge, TN 37831

Telephone: (865) 576-8401
Facsimile: (865) 576-5728
E-Mail: reports@adonis.osti.gov
Online ordering: http://www.osti.gov/bridge

Available to the public from
U.S. Department of Commerce
National Technical Information Service
5285 Port Royal Rd.
Springfield, VA 22161

Telephone: (800) 553-6847
Facsimile: (703) 605-6900
E-Mail: orders@ntis.fedworld.gov
Online order: http://www.ntis.gov/help/ordermethods.asp?loc=7-4-0#online

SAND2011-9320
Unlimited Release
Printed December 2011

An Evaluation of Possible Next-Generation High Temperature Molten-Salt Power Towers

Gregory J. Kolb
National Solar Thermal Test Facility (NSTTF)
Sandia National Laboratories
P.O. Box 5800
Albuquerque, New Mexico 87185-1127

Abstract

Since completion of the Solar Two molten-salt power tower demonstration in 1999, the solar industry has been developing initial commercial-scale projects that are 3 to 14 times larger. Like Solar Two, these initial plants will power subcritical steam-Rankine cycles using molten salt with a temperature of 565 °C. The main question explored in this study is whether there is significant economic benefit to develop future molten-salt plants that operate at a higher receiver outlet temperature. Higher temperatures would allow the use of supercritical steam cycles that achieve an improved efficiency relative to today's subcritical cycle (~50% versus ~42%). The levelized cost of electricity (LCOE) of a 565 °C subcritical baseline plant was compared with possible future-generation plants that operate at 600 or 650 °C. The analysis suggests that ~8% reduction in LCOE can be expected by raising salt temperature to 650 °C. However, most of that benefit can be achieved by raising the temperature to only 600 °C. Several other important insights regarding possible next-generation power towers were also drawn: (1) the evaluation of receiver-tube materials that are capable of higher fluxes and temperatures, (2) suggested plant reliability improvements based on a detailed evaluation of the Solar Two experience, and (3) a thorough evaluation of analysis uncertainties.

ACKNOWLEDGMENTS

I would like to thank several of my colleagues who provided support to this work and kept me from "reinventing the wheel," which I hate to do.

Bruce Kelly (Abengoa) gave me an initial set of GateCycle power-block models he developed under another recent Department of Energy project. He was always there to answer my persistent questions to allow me to successfully modify the models to meet the needs of the current study.

Mike Wagner (National Renewable Energy Laboratory) developed a detailed multi-node receiver thermal model as part of his recent Master's Thesis. I decided to use Mike's model, rather than the one developed during the Solar Two project, to avoid recoding the defunct Solar Two model and because Mike's model is similar to the one now in the System Advisor Model (SAM). Mike also made several modifications to this model to meet the needs of the current study.

I obtained an algorithm developed by Siri Khalsa (Sandia National Laboratories [SNL] contractor) for another project that allowed me to quickly run SOLERGY the hundreds of times necessary to perform the uncertainty analysis. He is a mathematical genius who wants to use his analytical skills to save lives! He left SNL in the summer of 2011 and is now in medical school.

Cliff Ho (SNL) ran the Latin-Hypercube sampling and stepwise-rank-regression software for me to support the uncertainty analysis. The last time I used this software was in 1992 and I did not want to relearn it, especially when I have an expert right down the hall.

Finally, Bob Bradshaw (SNL, now retired) provided a concise table of expected corrosion rates for proposed receiver tube materials when exposed to molten salt. This avoided my review (and likely misinterpretation) of experimental results he has published in countless reports over the last 30 years. He was also willing to use his expert judgment to "fill in the blanks" when data were lacking.

CONTENTS

FIGURES

TABLES

ACRONYMS

ATS	Advanced Thermal Systems Company
CDF	cumulative distribution function
DNI	direct normal irradiation
DOE	Department of Energy
DP	Design Point
DPD	discrete-probability distribution
EPRI	Electric Power Research Institute
FCR	fixed charge rate
FCV	flow control valve
HT	Incoloy 800 product designator
IPP	Independent Power Producer
ITC	investment tax credit
ITD	initial-temperature difference
LBL	Lawrence Berkeley Laboratory
LCF	low-cycle fatigue
LCOE	levelized cost of electricity
LHS	Latin Hypercube sampling
MDT	mean downtime
MTBF	mean time between failures
MW_e	megawatt electric
MW_t	megawatt thermal
NSTTF	National Solar Thermal Test Facility
O&M	operations and maintenance
OD	outer diameter
R&D	research and development
SAM	System Advisor Model
SNL	Sandia National Laboratories
SRC	standardized regression coefficient

Chapter 1
Introduction

Development programs for central receiver technology in the United States have produced a large amount of valuable information regarding the design of plants intended to produce electric power. Although the emphasis has been on components and subsystems, much has been learned regarding full system design, fabrication erection, and operation.

Solar One, a 10-megawatt electric (MW_e) water-steam receiver project, operated from 1982 to 1988 to prove the viability of power tower technology. Plant operation continually improved, culminating in a 95% plant availability during the final operating year. Three commercial power towers using this first-generation technology are in operation today: Abengoa's PS 10 and PS 20 plants in Spain, and eSolar's 5-MW_e Sierra plant in California. Much larger steam power towers with power ratings greater than 100 MW_e are currently under construction by Brightsource at their Ivanpah site in California.

After shutdown of Solar One, the United States and Europe compared second-generation concepts. The United States was promoting salt, the Europeans air. The results of the study convinced the United States to continue to pursue molten salt [1]. A few years later, the Solar One steam-receiver plant was redesigned into a power tower plant named Solar Two, which employed a molten-salt receiver and thermal storage system. The change was made from steam to molten salt primarily because of the ease of integrating a highly efficient (~99%) and low-cost energy storage system into the plant design. Solar Two operated from 1996 to 1999 and helped validate nitrate salt technology, reduce the technical and economic risks of power towers, and stimulate the commercialization of second-generation power tower technology.

1.1 Overview of Molten-Salt Power Towers

A molten-salt central receiver power system uses a tubular-type receiver mounted on top of a tower. Reflected solar energy from a field of heliostats heats the receiver; molten salt is the heat-transfer fluid, and it also cools the receiver. Figure 1 shows a flow schematic of this system. The molten salt used in this system is a mixture of 60 wt% sodium nitrate and 40 wt% potassium nitrate. It is heated from 290 °C to 565 °C in the receiver and then flows in pipes to thermal storage. Hot salt is extracted from the storage system to generate steam within a molten-salt steam generator. The steam feeds a Rankine-cycle turbine to produce electricity. The cooled salt is returned through the thermal storage system to the receiver.

In the configuration shown in Figure 1 the thermal storage system buffers the steam generator from solar transients and also supplies energy during periods of no insolation, at night or on partly cloudy days. Since the salt remains in a single liquid phase throughout the process, and because of its relatively high heat capacity, it can be stored in compact storage tanks. The hot-salt temperature of 565 °C enables steam production at temperatures and pressures typical of those used in conventional subcritical Rankine plants. Depending on the availability of cooling water at the site, the condenser in Rankine plant is cooled with either wet or dry cooling towers. Wet-cooled plants are somewhat more efficient than dry ones (43% versus 41%).

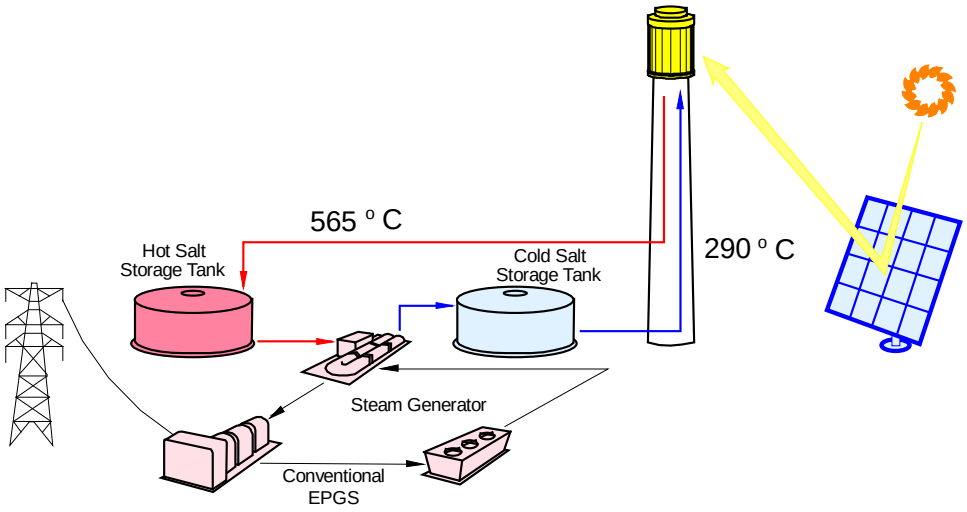

Figure 1. Flow schematic of a molten-salt central receiver system.

The molten salts used as the heat transfer fluid are in the same family as molten salts used in commercial heat-treating and industrial process plants. Extensive operational experience has been accumulated for these salt mixtures over the last 60 years. Because the molten salt has a freezing point near 220 °C, each subsystem containing salt must be trace-heated and/or easily drained to assure the salt does not freeze.

The molten salts are not toxic and, when properly protected from overheating, are compositionally stable over an extended period of time. These salts have a low vapor pressure at high temperature and do not react chemically with water/steam; hence no unusual safety hazards are expected. The relatively inert characteristics of this fluid permit the design of the solar receiver, storage tanks, and steam generator using standard ASME codes for high-temperature containment and flow systems. These characteristics and the relative low cost and commercial availability of the molten salt make this fluid attractive for use with solar central receivers. This is particularly true for systems with large amounts of thermal storage.

The basic salt receiver investigated in this study was demonstrated at Solar Two, as depicted in Figure 2. The salt flows through thin-walled metal tubes with a diameter in the 20- to 80-mm range. The exteriors of the tubes are painted black to enhance absorptance. Tubes are assembled into panels and configured in a cylindrical geometry. There are two flow circuits and 14 to 24 panels. The salt in each circuit passes through 7 to 12 panels in a series manner.

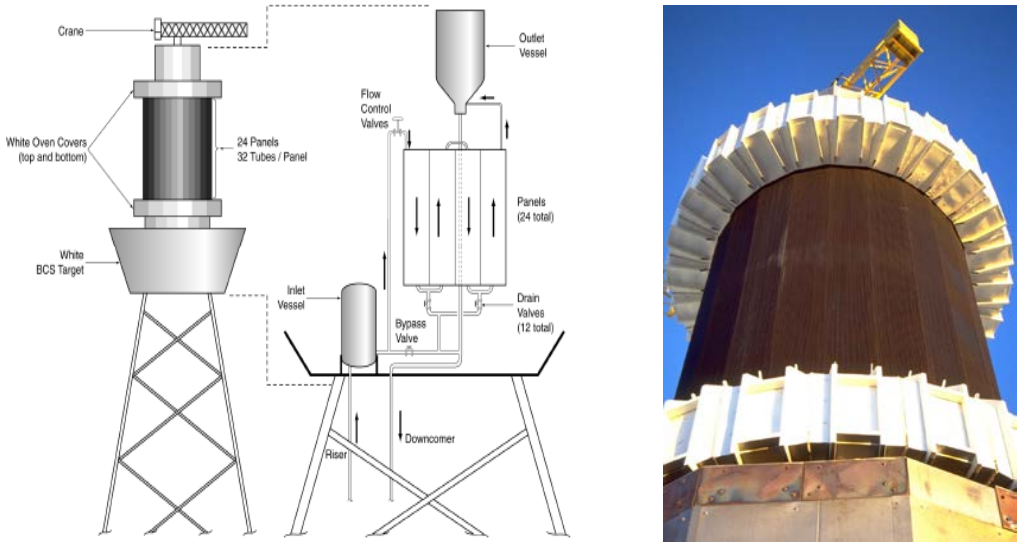

Figure 2. In the Solar Two receiver, molten salt flowed through 20-mm tubes arranged within 24 panels. There were two flow paths, each containing 12 panels.

Salt receivers have been demonstrated in the United States at a 5-megawatt thermal (MW_t) scale (Sandia National Laboratories [SNL]) and at a 40-MW_t scale (Solar Two). In Europe, a 10-MW_t receiver was demonstrated in France (Themis). These receiver experiments were completed in the 1980s and 1990s and no longer exist. However, the first commercial plant began operating in Spain in 2011; the Gemasolar project built by Torresol Energy uses a 120-MW_t receiver and 15 hours of thermal storage to power a 19.9-MW_e turbine, both day and night.

The three power plant types investigated in this report are:

1. 565 °C receiver salt temperature powering a subcritical steam-Rankine cycle;
2. 600 °C receiver salt temperature powering a supercritical steam-Rankine cycle; and
3. 650 °C receiver salt temperature powering an ultrasupercritical steam-Rankine cycle.

The construction of the first 565 °C commercial-scale molten-salt plant in the United States is now under way near Tonopah, Nevada. The plant, built by SolarReserve, will combine a 580-MW_t receiver with 11 hours of thermal storage to power a 110-MW_e subcritical steam-Rankine cycle. The plant represents a factor of 14 scaleup from Solar Two. SolarReserve intends to deploy several of these initial-generation plants throughout the world.

The three plant types listed above are possible second- third-, and fourth-generation configurations. The receiver thermal rating investigated here is the maximum practical size originally identified by the US Utility Studies (~1000 MW_t) [2]. Larger molten-salt receivers are predicted to enjoy an improved economy of scale. In addition, if the receiver salt temperature can be raised to 600 °C and higher, it is feasible to interface with higher-efficiency supercritical

and ultrasupercritical steam cycles. The scaleup and efficiency improvement is expected to result in a significant reduction in the levelized cost of electricity (LCOE).

1.2 Overview of Study Tasks

The study tasks and the interrelationships among them are depicted in Figure 3. In general, each task is the subject of a separate chapter of this report.

"Plant Design Definition" consisted of optimizing the size of the receiver, tower, heliostat field, thermal storage, and steam-Rankine equipment to achieve the lowest LCOE, given a receiver thermal rating of 1000 MW_t. Each of the three power plant types described in Section 1.1 were explored, either with wet or dry condenser cooling, for a total of six designs. For each design, an "Annual Performance Analysis" was performed to obtain a prediction of the annual net electricity produced by the plant. The performance analysis was conducted assuming plant outages due to equipment malfunctions did not occur, i.e., 100% availability. Equipment malfunctions will cause the plant to be unavailable for power production during a fraction of the calendar year. The "Reliability Analysis" determined this unavailability fraction, and the energy lost while the plant was down was subtracted from the performance analysis. A first-order "Analysis of Capital and O&M Costs" was performed; the costs were primarily derived from the power tower roadmap [3] recently developed for the Department of Energy (DOE). The results of these three parallel analyses were then used to calculate the LCOE for each of the six designs assuming plant ownership by an independent power producer. Next, an "Uncertainty Analysis" was performed to identify the analysis parameters that are most important to the uncertainty in the LCOEs. Since the purpose of research and development (R&D) is to reduce uncertainty, the resulting importance ranking is useful in planning and prioritizing future research efforts. The final task was to interpret the analysis and to draw appropriate "Results and Conclusions."

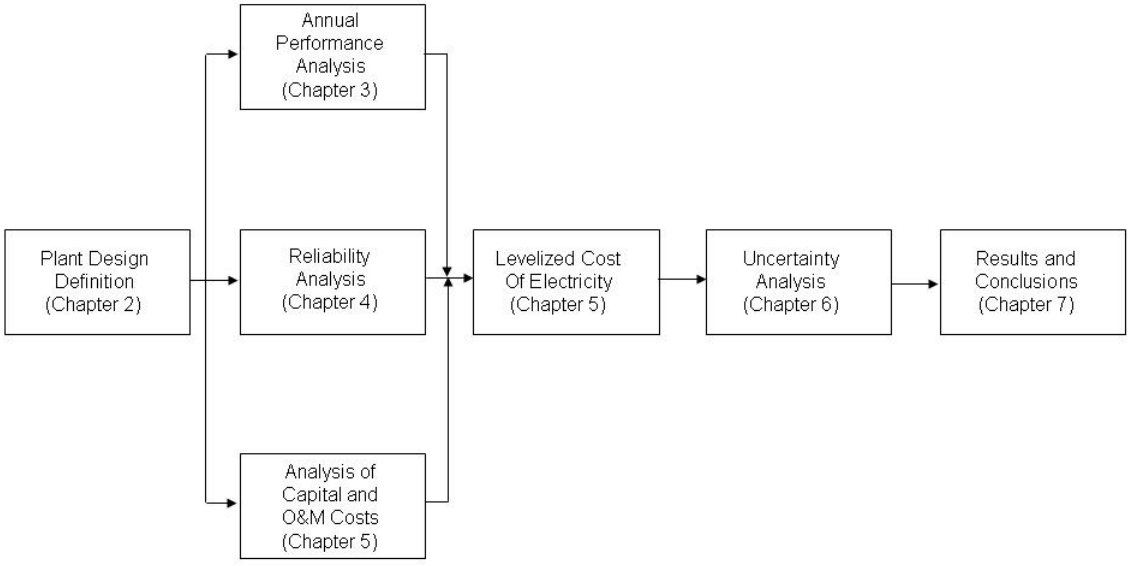

Figure 3. Study tasks.

1.3 Overview of Methodology and Data

The best available methods and data should be used when assessing proposed improvements in power tower technology. Many models exist with varying degrees of detail. However, the predictions of a model will only be accepted if it has been fully validated with experimental data. For example, a recent evaluation of 10 parabolic trough annual-performance models showed a +/- 6.5 to 13% variation in the prediction of annual performance even when all models supposedly used the same weather data and input parameters [4]. Further investigation revealed that most of the models with the highest variation relative to the mean had not been validated with data from real solar plants. Every effort has been made to use validated models and applicable experimental data within this study, as noted in Table 1. However, since the plants being modeled have not yet been built, complete validation is not possible and significant uncertainty remains in the results.

The methods, main system parameters, and data sources used in this study are summarized in Table 1. How they were applied is fully described in the subsequent chapters.

Table 1. Study Methods, Parameters, and Notes/Assumptions.

	Methods, Parameters	**Notes/Assumptions**
PLANT DESIGN DEFINITION		
Optical design tool	DELSOL used to determine tower height and field size	DELSOL was used to design the PS-10 and PS-20 commercial power towers.
Plant configuration	Molten nitrate salt and a two-tank thermal storage	Basic design demonstrated at Solar Two.
Receiver thermal rating	1000 MW_t (565 ^oC) 1000 MW_t (600 ^oC) 1000 MW_t (650 ^oC)	Size is similar to optimum in the Utility Study [2]. Perform three case studies with different salt temperatures.
Receiver peak solar flux	1 MW/m^2	Solar Two was 0.80 but current salt receivers have higher flux limit [5].
Plant gross power rating	Varies from 139 MW_e to 167 MW_e	Subcritical plants exist with this size. However, today's supercritical plants are >400 MW_e and must be scaled down[1].
Capacity factors	~70%	Includes plant outages due to scheduled and unscheduled maintenance.
Solar multiple	3.0	Solar Two had a solar multiple of 1.2 but lowest LCOE occurs at ~3 [6].
Solar plant design point	Equinox noon, 950 W/m^2	Typical value.
Power generation design tool	Use GateCycle 6.0 to determine sizes of steam plant components	Code has been a power industry standard tool for many years [7].

[1] Ansaldo is offering a 200 MW supercritical steam turbine but detailed information about it could not be found. See www.ansaldoenergia.com.

Table 1. Study Methods, Parameters, and Notes/Assumptions (continued)

	Methods, Parameters	Notes/Assumptions
Power cycle case studies	Subcritical 540 ^{o}C/125 bar Supercrit 591 ^{o}C/300 bar Ultrasuper 630 ^{o}C/330 bar	There are many new supercritical coal plants with >600 ^{o}C steam temperature.
Dry cooling equipment and design point condition	Use industry vendor information to calibrate GateCycle air-cooled condenser model	Assume use of an SPX air-cooled condenser [8]. Design condition is hottest time of year to optimize annual performance [9].
Tower type	Concrete	Steel tower used at Solar Two. However, for taller towers, concrete is lower cost [10].
Plant design life	30 years	Typical value.
Redundancy in design	Redundant molten-salt cold and hot pumps	Utility plants typically have redundant pumps.
Land constraints	None	Assume flat land.
Heliostat type/size	95 m^2 Advanced Thermal Systems Company (ATS) glass/metal with 16 mirror modules	An ATS heliostat has reliably operated at SNL for >20 years. Similar to DELSOL default heliostat.
Heliostat optical specs (pointing-type errors)	94% Reflectivity 95% Cleanliness 1.33 mrad mirror slope. 0.75 mrad tracking. All mirror modules are canted to slant range. All mirror modules are focused to six tower heights.	Typical specs [11].
PERFORMANCE ANALYSIS		
Annual energy	Use SOLERGY	SOLERGY was validated with data from Solar One [12] and Solar Two [13].
Optical performance	Use DELSOL to develop field efficiency versus sun position matrix used by SOLERGY	DELSOL validated against other optical codes [10] and Solar Two [13] data.
Receiver heat loss	For 565 ^{o}C receiver, use Solar Two heat loss data. For higher-temperature receivers, use model.	Heat losses measured at Solar Two for a 565 ^{o}C receiver. Model [14] calibrated with Solar Two data [15].
Rankine cycle performance	Use GateCycle 6.0 to develop thermodynamic efficiencies used by SOLERGY	Code has been a power industry standard tool for many years [7].
Site insolation, temperature, pressure, humidity, wind	1977 Aerospace file, 15-minute average data	Measured in Barstow, CA. Annual DNI 2.707 MWh/m^2.

Table 1. Study Methods, Parameters, and Notes/Assumptions (continued)

	Methods, Parameters	Notes/Assumptions
ANALYSIS OF COSTS		
Capital cost estimates	Heliostats \$120/m^2 Receiver/tower \$150/kWt Storage \$25/kWh_t Steam generator \$250/kW_e Rankine power block \$800/kW_e with increased cost for supercritical and dry cooling features	Year 2020 Power Tower Roadmap values [3]. DELSOL tower cost algorithm with ctow1=1650000 and ctow2=0.0113 [10].
Accounting structure for capital costs	Utility Study [2] method	Abengoa also used this method [16].
O&M costs	\$50/kW-yr	Year 2020 Power Tower Roadmap value [3].
Price Year	2010	
Land cost	\$2/m^2	
RELIABILITY ANALYSIS		
Calculation of plant availability	Use SNL's Pro-Opta reliability analysis software [17]	Pro-Opta validated with Solar One data, as described in Chapter 4.
Component MTBFs and MDTs	Use data from Solar Two, Themis, Electric Power Research Institute (EPRI), and Solar One	
Heliostat field availability	99%	Solar One data [51].
LEVELIZED COST OF ENERGY CALCULATION		
LCOE Method	Use Lawrence Berkeley Laboratory (LBL) Non-Utility Generator Cash Flow Model [18]	This is the basis for the System Advisor Model (SAM) [19] Independent Power Producer (IPP)model.
LCOE Economic Parameters	Use 2020 Power Tower Roadmap Values. See parameters in Chapter 5.	
UNCERTAINTLY ANALYSIS		
Uncertainty analysis method	Stepwise regression [20] and Latin-Hybercube Sampling [21]	
Parameter estimation techniques	Parameters are generally "best estimates" within a plausible range	Not all parameters are data-based. Many parameters and plausible ranges are developed using expert judgment.

Chapter 2
Plant Design Definition

The conceptual designs of possible next-generation 1000-MW_t subcritical (565 ^oC), supercritical (600 ^oC), and ultra-supercritical (650 ^oC) molten-salt power plants are presented in this chapter. A Design Basis Document [11], issued shortly after conclusion of the Solar Two project, provided several recommended characteristics of a next-generation subcritical plant based on lessons learned from Solar Two. This information was reviewed and extended to include the designs considered here.

2.1 Plant Optical Designs

The DELSOL3 computer code [10] was used to develop the optical designs. The code determined the number of heliostats, receiver dimensions, and tower height necessary to absorb 1000 MW_t into the salt flowing through the receiver. When running DELSOL a flux constrained aiming strategy for the heliostats was employed such that peak flux on the receiver was limited to ~1 MW/m^2 (1000 suns). This value is somewhat larger than the 800-sun limit adopted at Solar Two but is predicted to be acceptable using advanced receiver materials and less conservative design methods, as described in detail in Section 2.2.

A surround heliostat field was chosen because the Utility Studies [2] showed that it resulted in a lower LCOE than a north heliostat field for very large plants, like those studied here. The optimum optical design selected by DELSOL is the one that results in the lowest LCOE. The optimization considers the cost of heliostats, the receiver, and the tower (versus height). The costs for these items were taken from industry information included in the Power Tower Roadmap[2] [3]. The optimization also considers the annual optical performance of the heliostat field as well as the thermal losses of the receiver. In the latter trade-off, DELSOL compared the thermal losses versus beam-spillage losses to select the receiver dimensions (height and diameter) that produce the highest combined optical and thermal efficiency, given the 1000-sun flux limit. Based on the receiver thermal model described in Section 2.2, the thermal losses used in the optimizations were 30 kW_t/m^2 (565 ^oC), 36 kW_t/m^2 (600 ^oC), and 40 kW_t/m^2 (650 ^oC)[3].

All plants are assumed to use glass/metal heliostats similar to the 95-m^2 Generation 3 version made by Advanced Thermal Systems Company (ATS) in the 1980s (see Figure 4). This size was selected because SNL's analysis of heliostat cost versus size [22] indicated that the heliostats with sizes greater than 50 m^2 will likely result in the lowest installed cost on a $\$/m^2$ basis. SNL has successfully operated a 148-m^2 heliostat (also built by ATS) for more than 20 years, but the performance during windy conditions is not as stable as has been observed for somewhat smaller heliostats. Thus, the 95-m^2 version was selected as the preferred heliostat. The optical error for the heliostat (expressed as pointing type) was taken from the Design Basis Document as 1.53 mrad root-mean-square (RMS). Of this, 0.75 mrad is due to tracking error and the remainder

[2] The year 2020 cost values were used: heliostats ($\$120/m^2$), receiver and tower ($\$150/kW_t$). The latter was achieved by setting DELSOL parameters CREC1=125e6, XREC=0.0, CTOW1=1.65E6, and CTOW2=0.013.

[3] Thermal losses of 30 kW_t/m^2 were measured at Solar Two [15] given a 565 ^oC outlet temperature. The losses at 600 ^oC and 650 ^oC were estimated using the model. The model was calibrated to match the Solar Two data at 565 ^oC.

(1.33 mrad) are beam quality errors (slope, alignment, gravity sag, etc.).[4] Mirror reflectivity was assumed to be 89.3%. Solar mirrors are available today that are 94%; this was reduced by an assumed cleanliness factor of 95%.

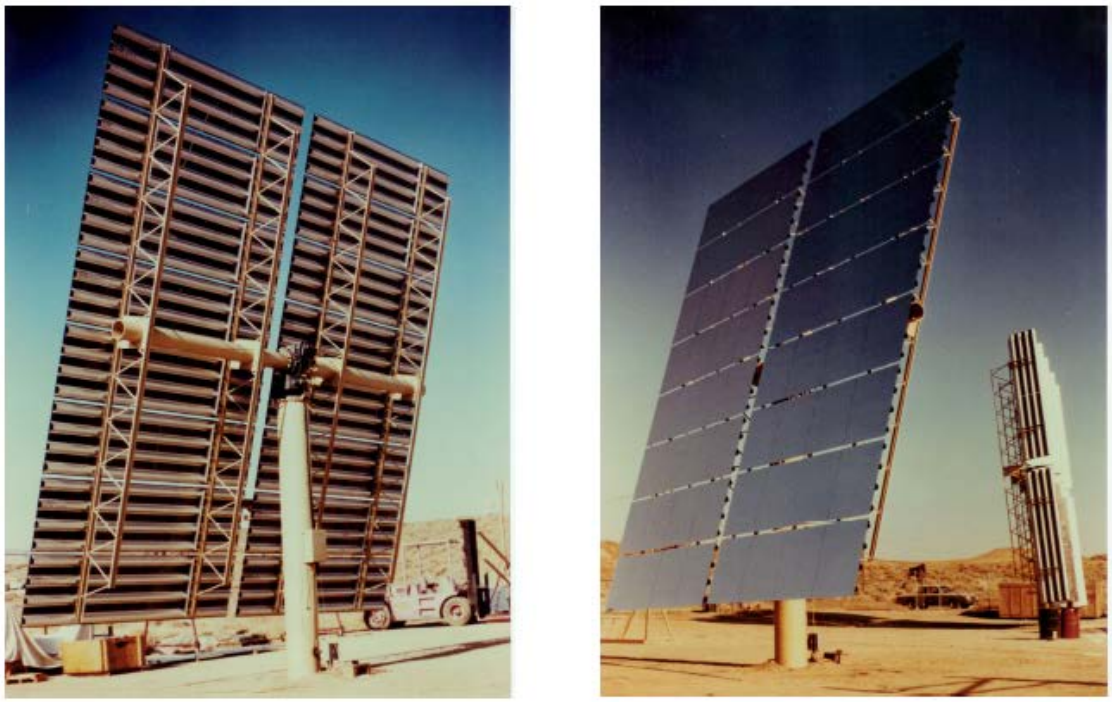

Figure 4. The 95-m^2 Generation 3 heliostat built by ATS in the 1980s is similar to the default heliostat described in the DELSOL User's Manual [10].

When laying out the heliostat fields, the optimizations were constrained to maintain a ratio of approximately 2 between the power on the north and south receiver panels. A similar value for this parameter was implemented at Solar Two. In addition, the height-to-diameter ratio of the receiver was fixed at ~1.2, according to the acceptable 1.2-to-1.5 guidance given in the Design Basis Document.

The DELSOL optical designs are depicted in Table 2. The tower height (275 m) and receiver dimensions (26.8 m H X 22 m D) are shown to be the same for all three case studies. However, it can be seen that the heliostat field is slightly larger for the higher-temperature receivers; since higher-temperature receivers incur higher thermal losses, this is compensated for by adding some additional heliostats.

[4] $1.53 = SQRT(0.75^2+1.33^2)$.

Table 2. Design Characterization of 1000-MW_t Receiver Power Tower Plants.

	565 °C	600 °C	650 °C
Collector System			
# of heliostats	19917	20183	20410
Reflective area (m^2)	1.90e6	1.93e6	1.95e6
Total plant land area (km^2)	10.8	11.0	11.1
Field boundaries			
North boundary from tower (m)	1788	1788	1788
South boundary from tower (m)	1213	1213	1213
East/West width (m)	1644	1788	1788
Receiver System			
Design point (DP) day	equinox	same	same
Solar multiple	3.0	same	Same
Optical tower height (m)	275	same	same
Absorber size – L x D (m)	26.8 x 22.0	same	same
Absorber area (m^2)	1854	same	same
Aspect ratio (L/D)	1.22	same	same
Tube size – OD x wall (mm)			
I-800 HT material	82.3/1.85	85.3/2.87	N/A
I-625-LCF material	80.8/1.38	N/A	N/A
Haynes 230 material	80.3/1.27	81.5/1.68	83.8/2.37
Design point power (MW_t)	1000	same	same
Inlet/outlet fluid temp (°C)	288/566	336/600	336/650
# of flow control zones	2	same	same
# of panels/zone	8	same	same
DP flow rate (kg/sec)	2390	2520	2230
DP friction loss (psi)	165	same	same
Inc. flux limit - N (kW/m^2)	1000	same	same
N/S panel power/flux ratio	2.17	2.11	2.03
Tube absorptance (Pyromark)	0.94	same	same
Thermal Storage System			
Capacity (MWh_t)	5000	same	same
Hot/cold tank ΔT (°C)	277	264	314
Active volume per tank (m^3)	23900	25300	21400
Tank height/diameter (m)	20.9/38.2	20.9/39.2	20.9/36.1
Full load equivalent hours (h)	15	same	same
# of storage tanks	2	same	same
Oxygen blanket?	No	No	Yes
Steam Generation System			
Rating (MW_t)	337	same	same
Type	subcritical	supercritical	ultra-supercritical
Turbine Generator System			
Design pt conditions			
Dry bulb temperature (°C)	43	same	same
Wet bulb temperature (°C)	22	same	same
Atmospheric Pressure (bar)	0.95	same	same
Turbine-cycle type	Rankine	same	same

Table 2. Design Characterization of 1000-MW_t Receiver Power Tower Plants (continued).

	565 °C	**600 °C**	**650 °C**
Gross Turbine Power (MW_e)			
Wet-cooled condenser	145	163	167
Dry-cooled condenser	139	158	162
Steam conditions (bar/°C)	125/537	301/591	331/630
Condenser pressure (bar)			
Wet-cooled condenser	0.087	same	same
Dry-cooled condenser	0.17	same	same
Cycle efficiency at design pt (%)			
Wet-cooled condenser	43.0	48.4	49.6
Dry-cooled condenser	41.2	46.8	48.0
Design pt parasitics (MW_e) Wet-cooled condenser			
FW pumps	2.14	5.70	5.93
Circ water pumps	0.75	0.77	0.76
Cooling tower fans	1.14	1.18	1.15
Condensate pumps	0.12	0.20	0.19
Total	**4.14**	**7.85**	**8.04**
Dry-cooled condenser			
FW pumps	2.14	5.70	5.93
Circ water pumps	N/A	N/A	N/A
Cooling tower fans	3.55	3.32	3.26
Condensate pumps	0.11	0.20	0.19
Total	**5.81**	**9.22**	**9.39**

2.2 Receiver Designs

The receiver system design is assumed to be similar to that demonstrated at Solar Two. A system schematic is shown in Figure 5. Molten salt is pumped up the tower, fills a cold-surge tank that is pressurized with air,[5] and then flows through the receiver.

Receiver absorber materials of historical and current interest were studied: Incoloy 800H (I-800H), Inconel 625-LCF, and Haynes 230. Incoloy was selected because it was the tube material used in a salt receiver test at SNL [23] before Solar Two[6] and was also used in the Solar One steam receiver. Inconel 625-LCF was selected because it was extensively studied by industry and SNL after Solar Two as a possible next-generation material [25]. Haynes 230 was selected because it has been recently promoted as an excellent candidate material for solar dish and tower receivers by the material manufacturer.[7] These materials were also selected because they are identified as candidate high-temperature tube materials within the ASME Boiler and Pressure Vessel Code. The chemical compositions of these three materials are shown in Table 3.

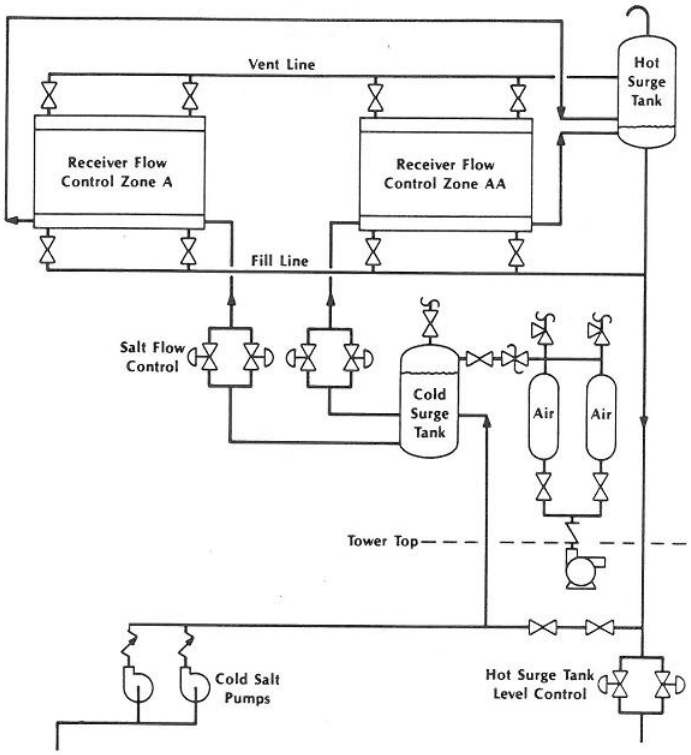

Figure 5. Receiver system schematic.

[5] The primary function of the cold surge tank (also known as inlet tank) is to provide emergency receiver cooling for a few minutes during station blackout. Given loss of AC power, the cold salt pumps will trip and the emergency power system will be used to quickly remove the heliostat beams from the receiver.

[6] The tube material used at Solar Two was 316H SS. This material is not recommended in future salt receivers because it was found to be susceptible to stress-corrosion cracking [24].

[7] According to data and analysis presented by Dr. Henry White (Haynes International) to SNL in August 2010, Haynes 230 is more thermally stable than I800 and Inconel 625-LCF alloys. Thus, the creation of deleterious phases that lead to embrittlement are less of a concern when operating above 600 ^{o}C.

Table 3. Receiver Tube Material Composition. [26], [27], [28]

	Incoloy 800 HT	Inconel 625-LCF	Haynes 230
Nickel	30-35%	58%	57%
Chromium	19-23%	20-23%	22%
Tungsten			14%
Molybdenum		8-10%	2%
Iron	39.5%	5%	3%
Cobalt		1%	5%
Manganese		0.5%	0.5%
Silicon		0.15%	0.4%
Aluminum	0.25-0.6%	0.40%	0.3%
Carbon	0.06-0.1%	0.03%	0.1%
Lanthanum			0.02%
Boron			0.015%
Titanium	0.25-0.6%	0.4%	
Niobium		3.15-4.15%	
Sulfur		0.015%	
Phosphorus		0.015%	
Nitrogen		0.02%	

When the metal that comprises the tubes of the receiver is heated, it expands.[8] Some of this expansion is accommodated in the receiver design by allowing the panels to grow in length. Some of this expansion, however, cannot be accommodated and so produces mechanical strains as heated metal constrained by colder material. These strains are termed "thermal strains" and result from "self constraint." A solar receiver must, by its nature, operate cyclically. The receiver is heated to operating temperature and then allowed to relax to thermal equilibrium at least daily, and more often due to the passage of clouds over the plant. This cyclic operation results in thermal fatigue damage to the receiver tubes. This fatigue damage must be limited to a tolerable level over the 30-year lifetime of the receiver.

Fatigue damage data were compiled from several sources; low-cycle fatigue (LCF) experimental data were adapted and used. The LCF data for the alloys investigated in this study appear in Table 4. It can be seen that the number of cycles to failure decreases as strain and/or temperature increases. Of the three alloys, I-800 has (by far) the most available data since it is the oldest alloy. The LCF data apply to relatively short strain cycles; a few-second strain cycle was typical. Strain cycles within a power tower typically last several hours, which calls into question the applicability of the few-second LCF data available in the literature. Previous experimental studies have shown that cyclic fatigue life is significantly reduced given long hold periods of an hour or more [31] [32] [33]. To obtain an answer to this question, longer cycle LCF data were

[8] This section follows much of the general methodology described in Reference 29, and some of the text from that paper has been reused here.

sought. Five-hour hold data were found for I-800 [33], but only four data points were identified. In Figure 6 these four points are plotted on top of the short-cycle LCF data published on the Special Metals website for I-800 type alloys [26]. The average of these plots suggests that fatigue life can be expected to be reduced by an approximate factor of 4 due to long hold times. This factor is also suggested by data in a paper comparing 10-second and 60-minute hold times for I-800 [32], and comparing 0- and 30-minute hold times for Inconel 625 [34]. Thus, in this study the cycles-to-failure shown in Table 4 were multiplied by a factor of ¼. These reduced values represent the allowable number of cycles for a given strain range and temperature.

Table 4. Number of Fatigue Cycles to Failure for I-800H [26], Inconel 625-LCF [27 and 29], and Haynes 230 [30] as a Function of Strain at Temperature. (These values were multiplied by ¼ in the analysis.)

		Strain									
I800H		0.001	0.002	0.003	0.004	0.005	0.006	0.007	0.008		
	70	1.00E+07	1.00E+06	1.00E+05	7.00E+04	5.00E+04	2.50E+04	1.70E+04	1.30E+04		
Temp F	1000	1.00E+07	1.00E+06	1.00E+05	7.00E+04	2.60E+04	1.40E+04	1.00E+04	8.00E+03		
	1200	1.00E+06	1.00E+05	5.00E+04	2.50E+04	1.30E+04	8.00E+03	6.00E+03	4.00E+03		
	1400	7.00E+05	9.00E+04	2.30E+04	1.00E+04	7.00E+03	4.00E+03	3.20E+03	2.50E+03		
		Strain									
Inconel 625 LCF		0.002	0.004	0.006	0.008	0.01	0.02				
	1000	1.00E+09	1.00E+07	1.00E+06	9.33E+04	3.63E+04	1.12E+03				
Temp F	1200	1.00E+08	3.63E+05	1.66E+04	3.72E+03	1.38E+03	1.62E+02				
	1500	1.00E+07	3.63E+04	3.72E+03	1.38E+03	5.89E+02	1.00E+02				
		Strain									
Haynes 230		0.003	0.004	0.005	0.0055	0.0065	0.007	0.008	0.01	0.015	0.02
	800	1.00E+06	4.47E+05	1.86E+05	1.20E+05	3.98E+04	2.88E+04	1.48E+04	7.59E+03	2.24E+03	1.00E+03
Temp F	1400	2.00E+05	7.59E+04	8.13E+03	6.46E+03	5.13E+03	3.16E+03	2.04E+03	8.51E+02	5.01E+02	1.58E+02

Kistler [35] pointed out that the strain cycles experienced by a solar receiver vary in magnitude. This is because the receiver power level varies each day, and each cloud passage is different. Considerable advantage can be gained by accounting for the smaller cycles using a "linear damage rule" relative to treating all cycles as full cycles. This can be accomplished by first establishing the number of cycles expected and their range over the receiver lifetime. This accounting has been performed based upon data taken at the Solar One pilot plant, by tabulating cycles in the direct-normal insolation measured at the ground. The accounting is complex because each cycle has both a high and a low value of insolation. The cycles reported in Kistler can, however, be grouped by their range, assuming that cycles of the same range are equally damaging, regardless of their mean. The number of cycles in ten range groupings is shown in Figure 7. The cumulative damage resulting from these cycles can be calculated from the linear damage rule:

$$\sum_{i=1}^{n} \frac{N_i}{N_{a,i}} = D_f \qquad (1)$$

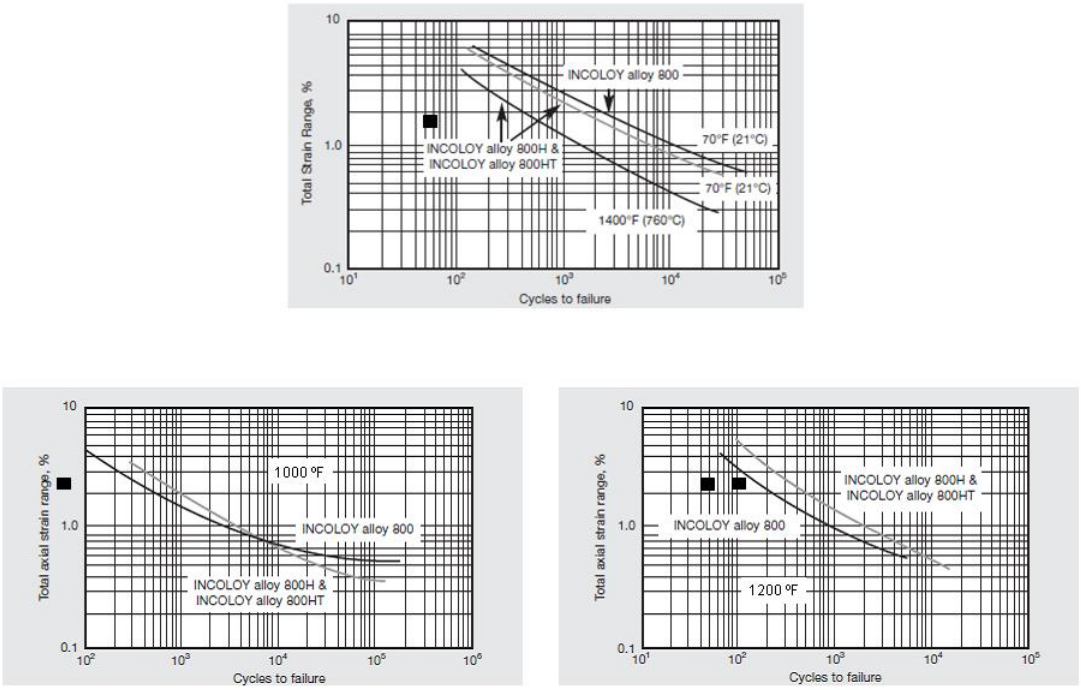

Figure 6. Low-cycle fatigue strength for I-800, I-800H, and I-800HT alloys at temperatures from 70 °F to 1400 °F [26]. Curves appear to have short hold times.[9] Black squares are data from four tests of I800 reported in Reference 33 given 5-hour hold times.

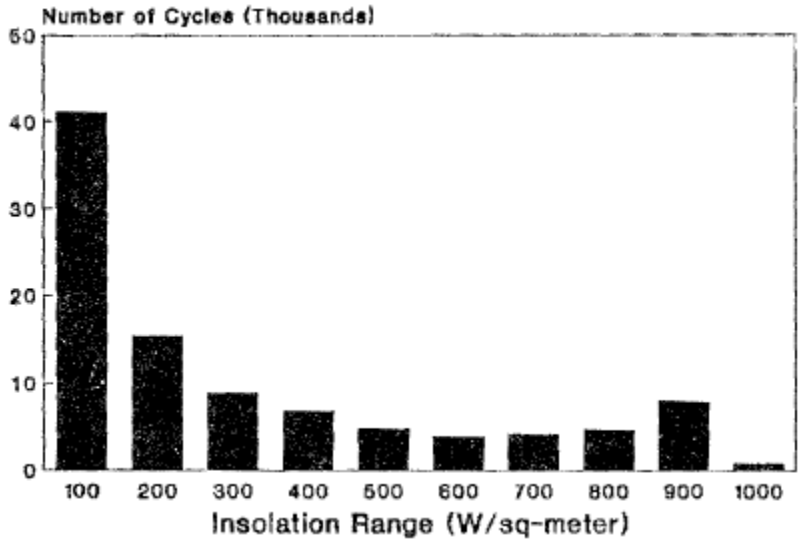

Figure 7. Number of strain cycles.

[9] According to an email sent from Lew Shoemaker (Special Metals) to G. Kolb (SNL) on December 2, 2009, the I-800 data is old and fatigue-cycle time is unknown. However, comparing the curve for I800 at 1200 °F with a similar curve found in Reference 32 suggests that the cycle time was ~10 seconds or less.

The allowable strain *e.* is defined as the full-range strain that results in a cumulative damage of 1 (failure) for the combination of cycles. An example of this calculation is presented in Table 5 for I-800H at a temperature of 1100 °F. In this example, the allowable strain range is found to be 0.00386. This strain corresponds to an allowable number of cycles of 12,800. For this case, the 98,900 cycles in the histogram are found to be equivalent to 12,800 full-range cycles. Similar calculations were performed for the range of tube temperatures anticipated in the operation of the receiver. An EXCEL spreadsheet was developed to perform the iterative calculations needed to determine the strain range that results in a cumulative damage of unity, for each temperature. The spreadsheet was also used to perform a linear interpolation of the cycles-to-failure values shown in Table 4. The resulting allowable strain-range curves for the three alloys are shown in Figure 8.

Table 5. Linear Damage Calculation for Incoloy 800H at 1100 ^{o}F (593 ^{o}C).

Design Strain 3.86e-03			**Allowable Cycles 12800**	
Cycle Range	**Strain Range**	**Number of Cycles**	**Allowable Cycles**	**Lifetime**
10%	3.86e-04	41100		
20%	7.72e-04	15300		
30%	1.16e-03	8900	1.18e+06	0.008
40%	1.54e-03	6900	7.02e+05	0.010
50%	1.93e-03	4900	2.24e+05	0.022
60%	2.32e-03	4000	1.00e+04	0.040
70%	2.70e-03	4200	5.41e+04	0.078
80%	3.09e-03	4800	1.81e+04	0.265
90%	3.47e-03	8000	1.55e+04	0.516
100%	3.86e-03	800	1.28e+04	0.062
	Total Cycles: 98900		Cumulative Damage: 1	

Given the allowable strain range, the next step in the absorber tube design process was to derive the allowable heat flux. The allowable heat flux is defined as that heat flux that results in the allowable strain range. Consider a receiver tube heated by solar radiation as shown in Figure 9. The heat flux can be assumed to be nearly entirely spectral. Given this, the heat flux normal to the surface of the tube will have a cosine distribution owing to the curvature of the tube.

$$q_n = q_o \cos(\phi) \tag{2}$$

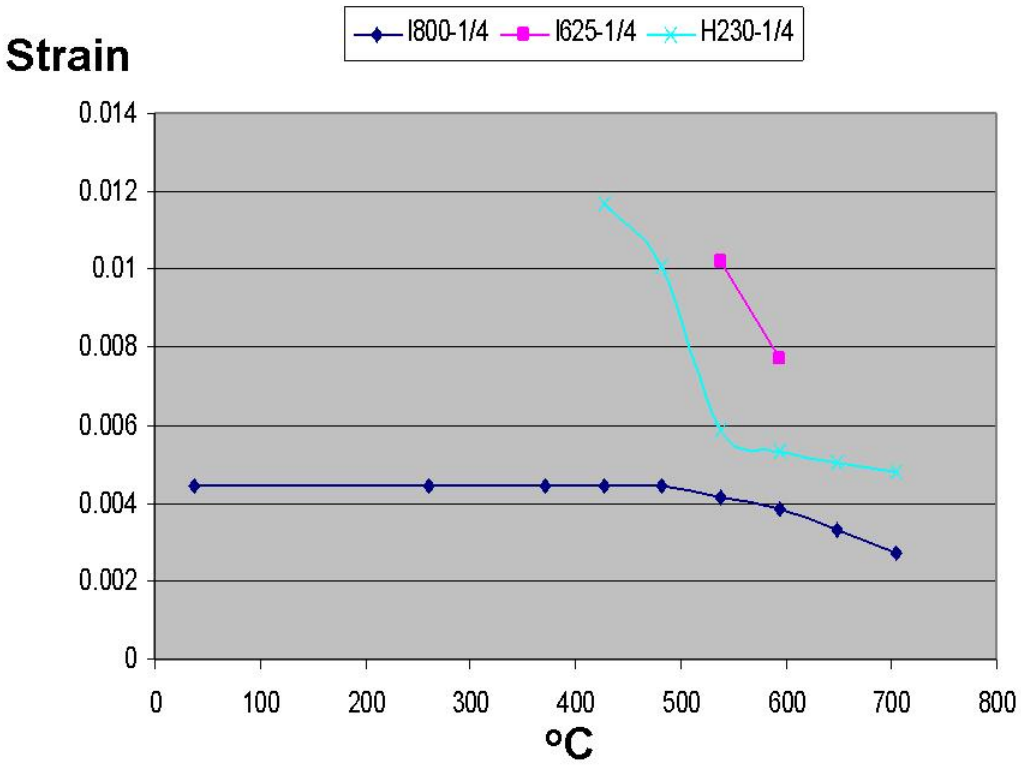

Figure 8. Allowable strain range.

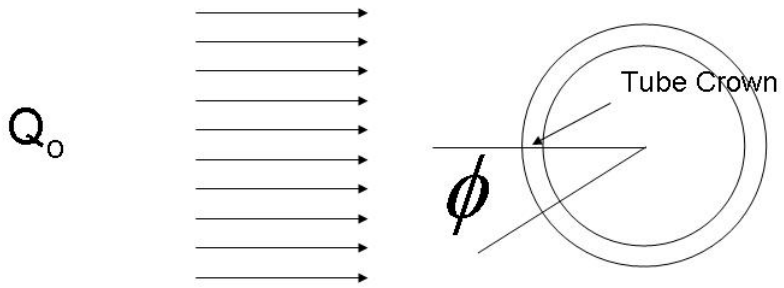

Figure 9. Receiver tube heated by uniform solar flux.

Because the tube wall is thin relative to the tube diameter, it can be assumed that the heat flux conducts one-dimensionally through a thin tube wall into the molten salt. The wall temperature will be governed in this case by the following formulas:

$$q_n = k\frac{(T_o - T_i)}{t} \tag{3}$$

$$q_n = h(T_i - T_s) \tag{4}$$

The convection heat transfer coefficient that is determined from the Gnielinski correlation for turbulent flow in tubes is:

$$Nu_D = \frac{(f/8)(\mathrm{Re}_D - 1000)\mathrm{Pr}}{1 + 12.7(f/8)^{1/2}(\mathrm{Pr}^{2/3} - 1)} \tag{5}$$

The highest metal temperature will occur on the tube crown at the outside surface of the tube. This location will develop the highest compressive thermal stress due to the heating. Assuming that the tube remains straight (a plane-strain assumption) the mechanical strain that results is approximately the sum of the strain due to the through-thickness temperature difference, and the front-to-back temperature difference. The resulting formula for strain is Reference 36 :

$$\varepsilon = \alpha\left[\left[\frac{[T_{oc} - T_{ic}]}{2(1-\nu)}\right] + \left[\frac{T_{oc} + T_{ic}}{2} - T_{ave}\right]\right] \tag{6}$$

where ε is the strain, α is the coefficient of thermal expansion, ν is Poisson's ratio, T_{oc} is the outer crown temperature, T_{ic} is the inner crown temperature, and T_{avg} is the average circumferential temperature.

The average temperature of the cross section can be found from the expression:

$$T_{ave} = \frac{\int_{-\pi/2}^{\pi/2}\left[\frac{T_o + T_i}{2}\right]d\phi + \pi T_s}{2\pi} \tag{7}$$

If Equations (2), (3), and (4), are substituted into Equation (7) to solve for T_{ave}, one gets:

$$T_{ave} = T_s + \frac{\left[\frac{(T_{oc} + T_{ic})}{2}\right] - T_s}{\pi} \tag{8}$$

Equation (6) can be employed to derive an equation for the allowable heat flux for a given tube diameter and tube-wall thickness. For every salt temperature, there exists a heat flux that results in a strain and temperature at the tube crown that intersects the allowable strain curve of Figure

8. Because the material properties depend on temperature, an iterative process is required to establish this flux limit.

The discussion thus far has focused on design of the receiver tubes to achieve a 30-year fatigue life. In addition to fatigue, the tube design should meet or exceed the requirements of the ASME Boiler and Pressure Vessel code [37], as well as be tolerant to the expected amount of salt-induced corrosion.

Section I of the ASME Code stipulates the method to determine minimum tube-wall thickness.[10] The thickness is a function of the operating pressure, temperature, and type of tube material. The relevant equations described in the code are

$$t = \frac{PD}{2S + P} + 0.005D \tag{9}$$

$$P = S\left[\frac{2t - 0.01D}{D - (t - 0.005D)}\right] \tag{10}$$

where P = maximum fluid pressure (psi), D = tube outside diameter (inches), S = maximum allowable stress of tube material obtained from ASME Section II tables in PG-23 that show allowable stress versus operating temperature (psi) for each of the three alloys, and t = minimum required tube-wall thickness (inches).

The maximum salt-fluid pressure (P) was selected to be 230 psi. The delta P across the Solar Two receiver was ~165 psi (60.4 m of head) and is also the approximate design delta P for commercial-scale receivers. The value of 230 was selected to add a 30% safety margin that might occur during abnormal events. (Pressures in this range are also similar to the operating pressure of the inlet salt tank located at the receiver inlet.)

The value for outside diameter (D) was calculated via an iterative procedure programmed within an EXCEL worksheet. The Darcy-Weisbach equation

$$h_f = f\frac{L}{D_{ID}}\frac{V^2}{2g} \tag{11}$$

was first used to estimate an overall friction factor (f) for the Solar Two receiver. Data acquisition records collected during operation on September 13, 1998, were examined. Solution of the Darcy equation to match the test data produced a 0.054 estimate for f. In addition,

[10] Section I of the code (Rules for Construction of Power Boilers) is primarily intended for water boilers. However, as explained in the introduction to Section I, "…. the rules of this Section are not intended to apply to thermal fluid heaters in which a fluid other than water is heated by the application of heat resulting from the combustion of solid, liquid, or gaseous fuel but in which no vaporization of the fluid takes place; however, such thermal fluid heaters may be constructed and stamped in accordance with this Section, provided all applicable requirements are met …." The molten-salt receivers designed in this report are "thermal fluid heaters" that meet the Section I criteria.

discussions with Rocketdyne regarding commercial-scale receiver parameters resulted in a 0.067 estimate for f, a value that is reasonably close to Solar Two. The latter value was selected for the analysis of the 1000-MW_t receivers studied here. The 1000-MW_t receivers characterized in Table 2 are assumed to consist of eight panels per flow path. Thus, the total flow length (L) is ~8*26.8m. The remaining parameters in the Darcy equation are known, except the tube inside diameter (D_{ID}).[11] The equation is solved to obtain an initial estimate of ~ 3 inches (76 mm). This initial estimate of the "tube inside diameter" is assumed to be equal to the "tube outside diameter" and Equation (9) is solved to determine the first estimate of the minimum tube wall thickness. For example, if the tube material is I-800-H operating at 600 ^oC, the minimum wall thickness is calculated to be 0.094 inches.

To maintain the minimum tube thickness required by the ASME code throughout its 30-year life requires the addition of some additional tube wall that is expected to be lost due to salt-induced corrosion. The data presented in Table 6 were used to estimate the amount lost. The data were provided by SNL's Robert Bradshaw [12] based on his many years of salt-corrosion-testing experience. It can be seen that corrosion rates are a function of the tube material, operating temperature, and the type of cover gas in the hot tank. Some data in the table are extrapolations of experimental data but many are based on his judgment.[13] How these data were used is best illustrated by example.

For the case of I-800H operating with a 600 ^oC outlet salt temperature, the receiver thermal model (described next) indicates that the salt film temperature in the outlet panel is 610 ^oC. The corrosion allowance is found to be 0.014 inches through interpolation of Table 6. To this corrosion allowance, 0.005 inches are added due to manufacturing tolerance. Thus, the total minimum thickness now becomes 0.094+0.014+0.005=0.113 inches (i.e., the 2.87-mm wall shown in Table 2).

A detailed receiver thermal model was developed to gain a better understanding of the tube and salt temperatures along the receiver flow path. The model was also used to calculate the tube strains (calculated with Equation (6)) to determine if they are acceptable relative to the limits defined in Figure 8. The model is a multi-node version of the SAM salt-receiver model; the standard SAM model [19] uses 1 node per panel, but the model used here employed 20 nodes per panel. The multi-node version is described within the master's thesis [14][14] that led to the SAM receiver model.

---

[11] Of course, the salt velocity (V) also depends on D_{ID} (via $Q= mdot*c*\Delta T=\rho V\pi D_{ID}^2/4*c*\Delta T$) and on the number of tubes per panel. The latter depends on the number of panels in the receiver and on the receiver diameter. These dependencies were programmed into the EXCEL spreadsheet that performed the iterative calculations.

[12] Retired from SNL in December 2010.

[13] Besides the three alloys investigated in this study, Bradshaw also provided estimates for I-617 since other solar researchers have proposed this material in advanced salt receivers [43] and because it also appears in the ASME code.

[14] The output of this model was compared with the output of another model [44] (now defunct) developed during the Solar Two project and found to give similar results.

Table 6. Salt Corrosion Estimates as a Function of Salt Temperature and Cover Gas.

	Mils of Total Corrosion after 10 yrs - With Air Blanket -			**Mils of Total Corrosion after 10 yrs - With Oxygen Blanket -**		
	600 °C	**625 °C**	**650 °C**	**600 °C**	**625 °C**	**650 °C**
I-625-LCF	3* a P	10	20 a P	3	6	10 b P
I-800H	3 d S	30 e f L	60 e L 10 c L	2	20	40
I-617	2	6	10 c L	2	4	7
Haynes 230	Slightly worse than I-625-LCF					

Extrapolations based on data are underlined. Other values are estimates.

1 Mil = 0.001 inch

Key:
P power law kinetics, time$^{0.7}$
L linear kinetics
S square-root (parabolic) kinetics, time$^{0.5}$
* thermal-cycling test, all others isothermal
a SAND2000-8240 [38]
b SAND2001-8758 [25]
c APC, *J. Metals*, 1985 [39]
d SAND82-8911, 600 °C loops report [40]
e SAND86-9009, 605-630 °C hot corrosion report [41]
f SAND82-8210, 630 °C loops report [42]

Assumptions:
1. 10 years of continuous corrosion is equivalent to 30 years of receiver operation because the receiver is assumed to be filled with salt 8 hours per day.
2. Isothermal data extrapolations are valid for thermally cycled receiver conditions.
3. Difference between air or oxygen blanket is negligible at 600 °C but significant at 650 °C.
4. I-617 corrodes no faster than I-625 because compositions of alloys are similar. I-617 is expected to corrode somewhat slower based on aluminum addition. Data in APC report for other test conditions support this assumption.
5. Molten-salt composition (oxide ion content) depends on T_{max} in hot-salt storage tank. Kinetics are too slow for chemical shift corresponding to tube film temperature during a single receiver pass.
6. Data for Alloy 800-standard grade apply to I-800H.
7. Compression of oxide scale on ID of tubes may be beneficial for scale adherence after substantial thickening.
8. For Haynes 230, Bradshaw's statement of "slightly worse" was assumed to be 20% worse.

The temperatures along the flow paths are shown in Figures 10 through 12. The bulk salt temperature continually increases from the entrance to the exit of the receiver, but the salt film temperatures and panel metal temperatures are the highest near the center of each of the eight panels since the incident solar flux is highest there. (A typical solar flux map is shown in Figure 13.) The I800H receivers show the highest surface temperatures due to the greater tube-wall thicknesses.

The normalized strains (i.e., Equation (6) divided by Figure 8) for the six case studies are displayed in Figure 14. The highest strains occur on the panels at the inlet of the receiver, which are exposed to the highest solar flux, limited to 1 MW/m^2 as described previously. It can be seen that I800H experiences the highest tube strains, primarily due to the thicker required wall. Use of this alloy with a 600 ^oC outlet temperature slightly exceeds the 30-year fatigue life. Haynes 230 exhibits acceptable strains, even when operating with a 650 ^oC salt outlet temperature. Inconel 625-LCF shows the lowest strain of the three alloys with a 565 ^oC outlet temperature. However, according to the ASME code this alloy is not recommended for use when metal temperatures exceed 600 ^oC; increased susceptibility to embrittlement failure appears to be the issue [27].

2.3 Salt Steam Generator Design

The U.S. Utility Studies [2] assumed that a steam generator built by Babcock and Wilcox (B&W) would be employed in commercial-scale plants. A system schematic of this "recirculating-drum" type system is found in Figure 15. Subcritical steam generators with thermal ratings of 260 MW_t and 520 MW_t were studied. This steam generator was recommended because a 3-MW_t scale model was successfully demonstrated at SNL in the 1980s [45]. Solar Two was built after completion of the Utility Studies. However, the Solar Two project did not adopt the recommendation of the Utility Study and built a 36-MW_t kettle-boiler-type steam generator that was similar to the type used in solar-trough plants. This was done to reduce capital costs. Significant problems related to salt freezing occurred and the system needed to be redesigned and retrofitted during the project [13]. Due to the bad experience at Solar Two, use of a steam generator that more closely resembles the B&W recirculating-drum design is again recommended for future subcritical-steam plants.

Since all case studies assume a solar multiple of 3, this fixes the thermal rating of the steam generator to be ~334 MW_t,[15] i.e., 1000 MW_t receiver thermal rating divided by 3. An EXCEL-based model developed by Kelly [16] was used to estimate the heat exchanger areas for the subcritical case study powered by 565 ^oC salt. The results of the analysis are shown in Figure 16. The steam conditions were determined by the GateCycle calculations described in Chapter 3.

[15] A value of 337 MW_t was actually used in the analysis.

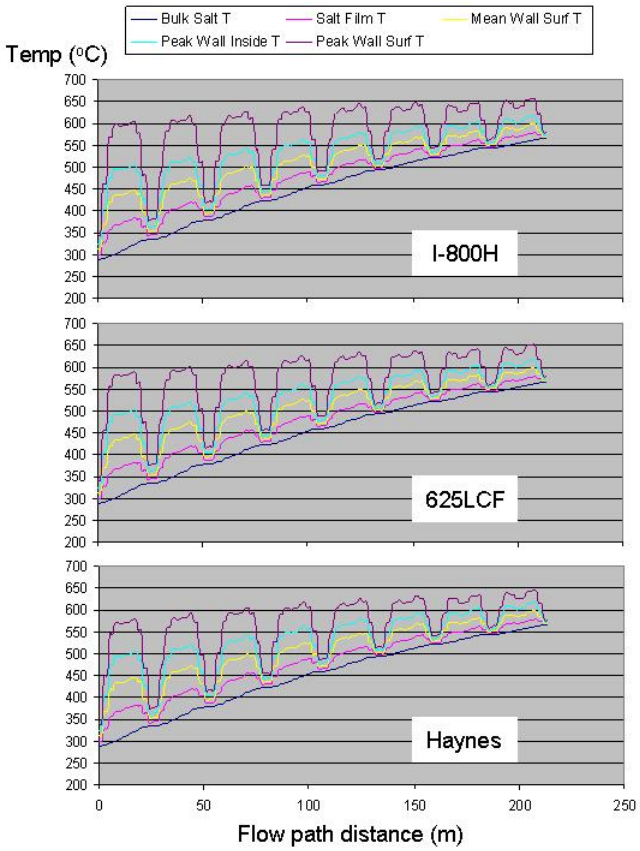

Figure 10. Receiver temperatures at equinox noon, 565 °C salt outlet temperature.

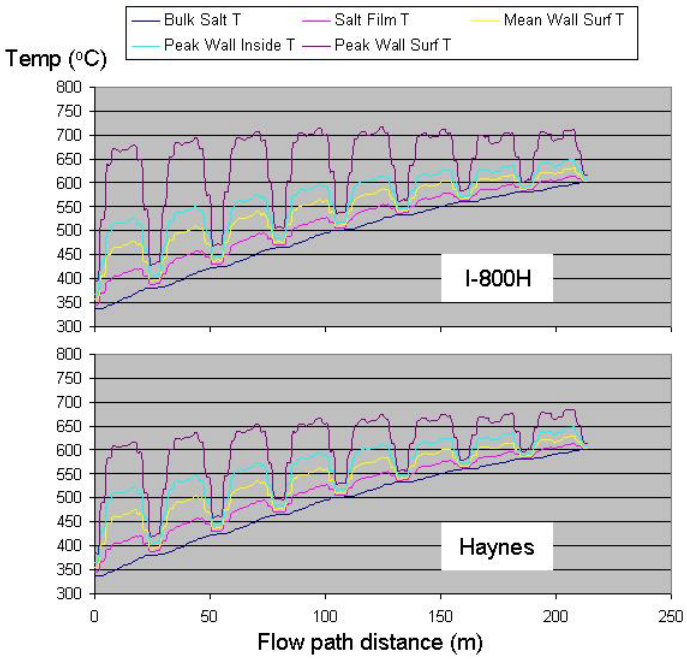

Figure 11. Receiver temperatures at equinox noon, 600 °C salt outlet temperature.

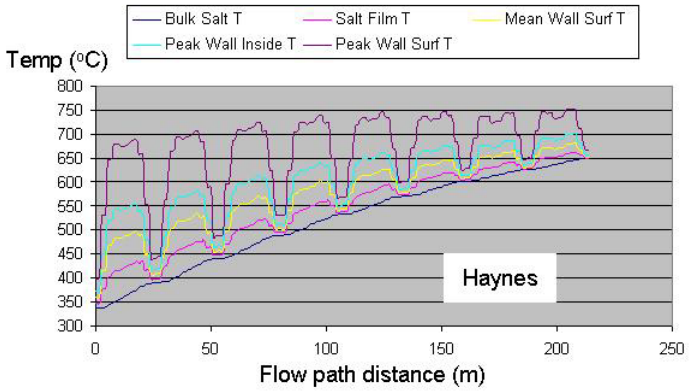

Figure 12. Receiver temperatures at equinox noon, 650 °C salt outlet temperature.

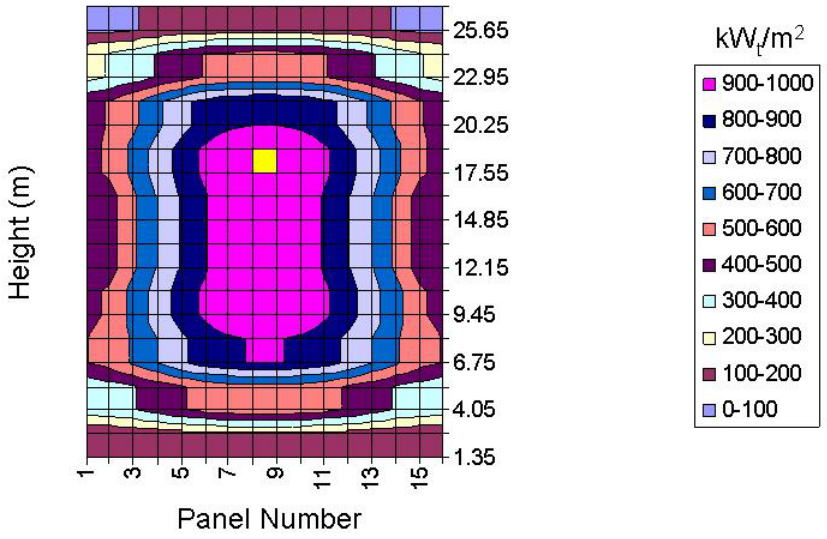

Figure 13. Solar flux on receiver panels at noon on equinox as predicted by DELSOL. There are two serpentine flow paths from salt inlet to outlet: 8,7,6,5,13,14,15,16 and 9,10,11,12,4,3,2,1. Panels 8 and 9 are facing north.

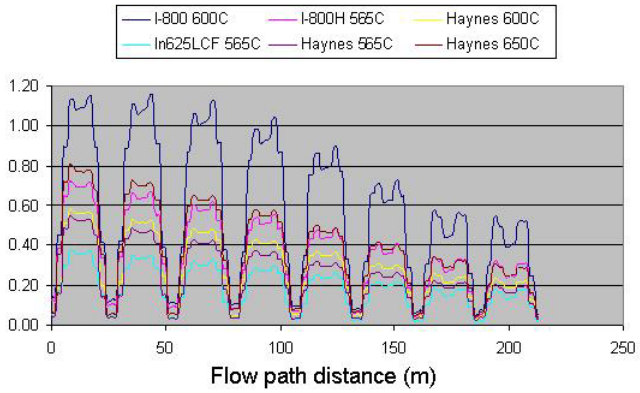

Figure 14. Normalized strain within receiver materials for the six case studies.

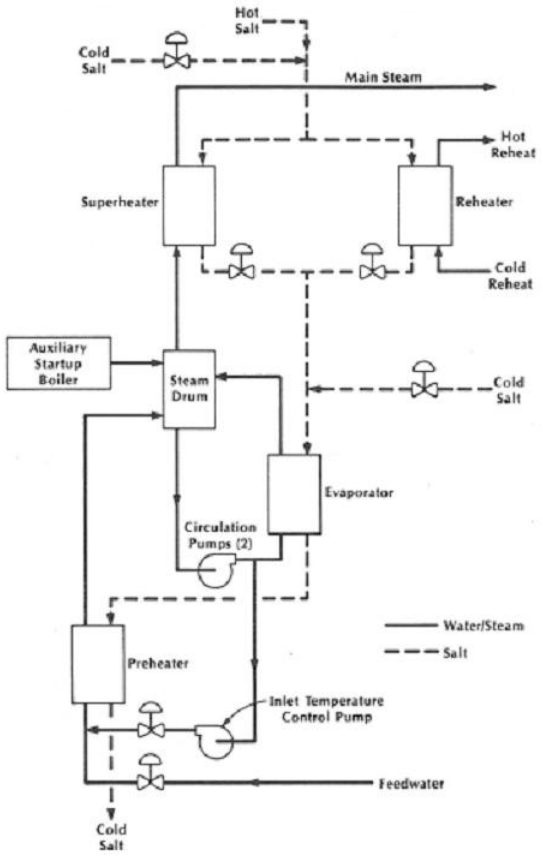

Figure 15. Steam generator system schematic proposed by Babcock and Wilcox [2].

No detailed designs currently exist for molten-salt steam generators that operate at supercritical and ultra-supercritical steam conditions. Kelly explored a concept [16], but much further work is required. Using Kelly's first-order model, heat exchanger areas were estimated for a supercritical steam generator powered by 600 ^{o}C salt. The results of the analysis are given in Figure 17. The system configuration is simpler than a subcritical steam generator because there is no steam boiling regime.

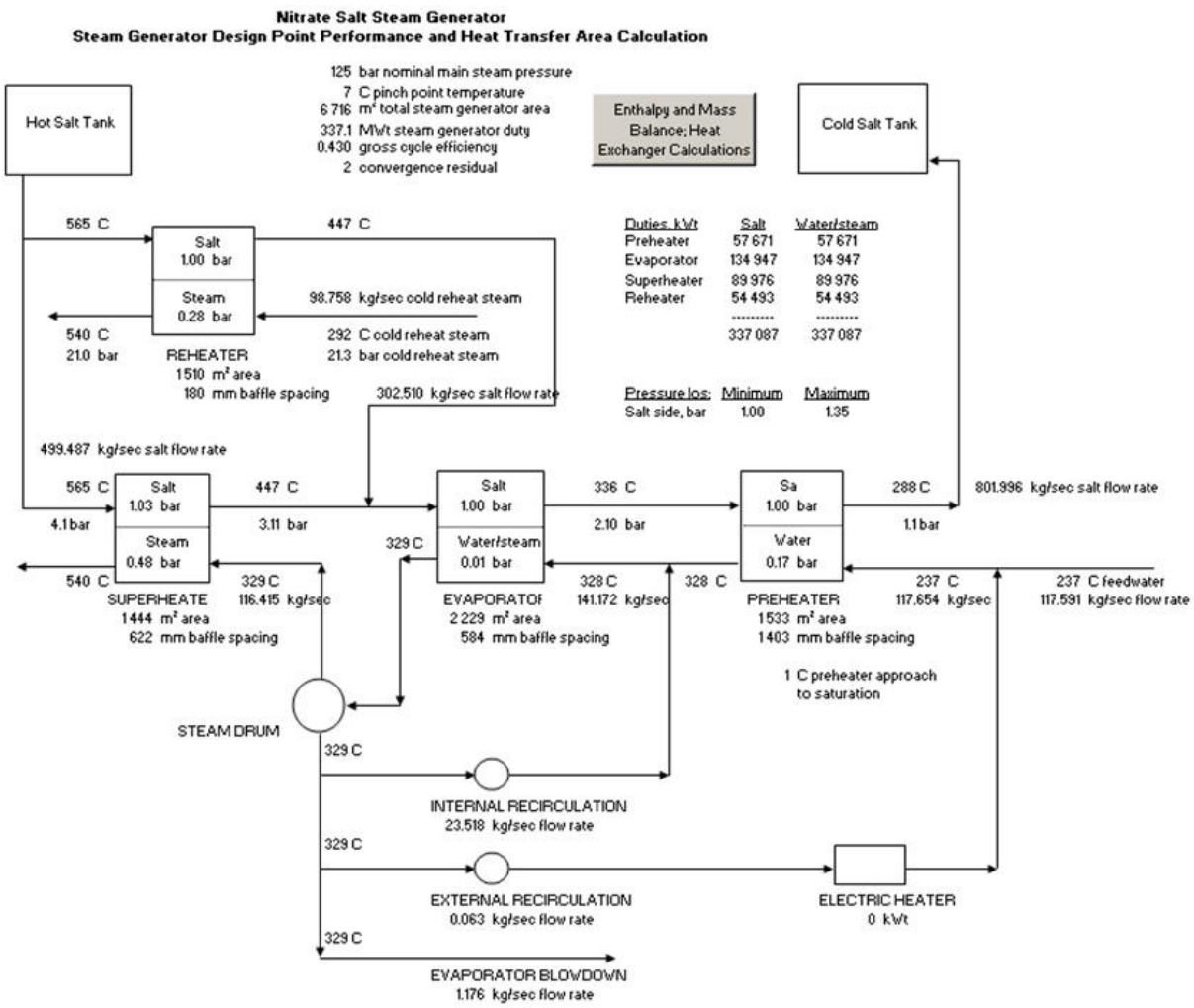

Figure 16. Subcritical molten-salt steam generator heat balance.

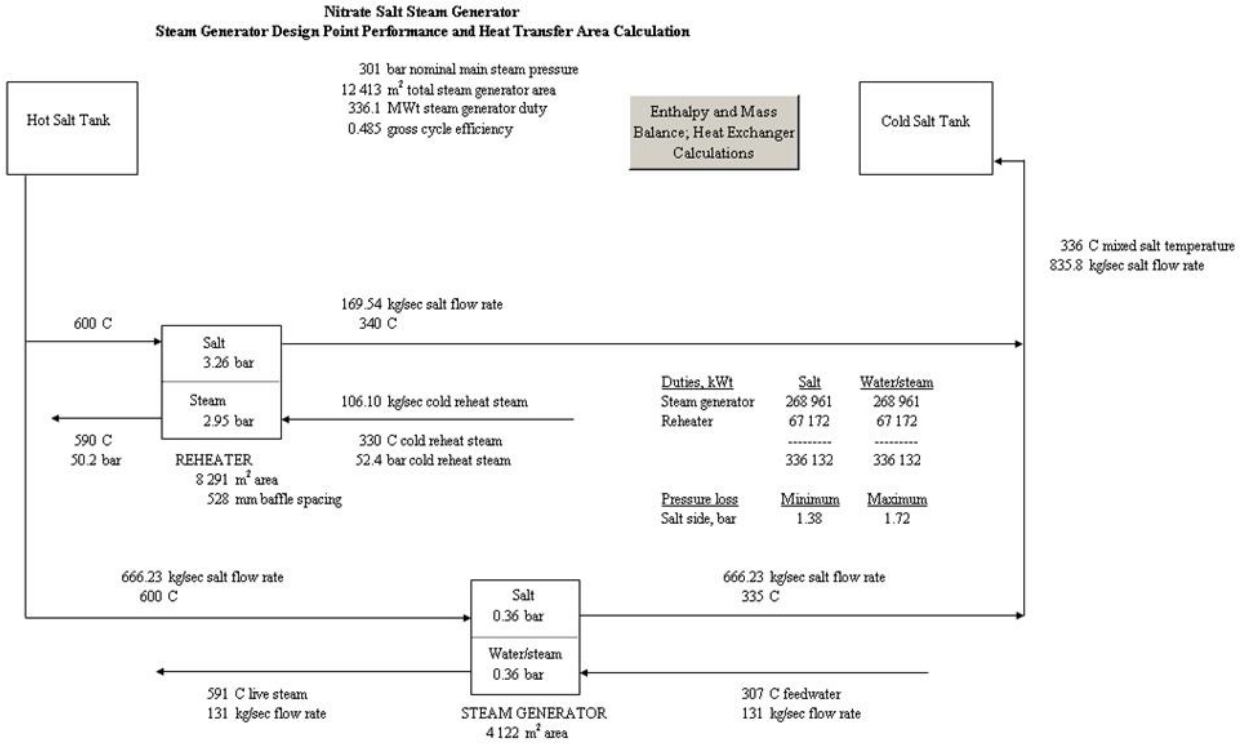

Figure 17. Supercritical molten-salt steam generator heat balance.

2.4 Balance of Plant

A two-tank thermal storage system, similar to that demonstrated at Solar Two, is assumed. The tank sizes given in Table 2 were determined using the SAM algorithm [19] given the assumed hot tank and cold tank temperatures for each case study. The tank dimensions necessary to achieve 15 hours of storage are nominally 21 m tall and 38.5 m in diameter. This is somewhat larger than the salt tanks currently operating at the Andasol trough plants.[16] The cold tank temperature for the 565 °C case is the same as at Solar Two, i.e., 288 °C. The cold tank temperature selected for the 600 and 650 °C cases are somewhat higher than Solar Two (336 °C) because the GateCycle analysis of the power cycle suggested that a higher-power conversion system efficiency can be achieved with this return temperature. As described next, supercritical plants have a higher feedwater temperature. This will result in a higher salt return temperature to the cold tank (compare the feedwater and salt return temperatures in Figure 16 and 17).

[16] The Andasol solar trough plants are using the largest molten-salt tanks currently in existence. They are 14 m tall by 38.5 m in diameter. The cold tank temperature is the same as analyzed here, but the hot tank is only 390 °C.

The steam turbine system designs are assumed to be similar to subcritical and supercritical designs found in today's coal-fired power plants. As shown in Table 2, gross turbine system output is different for each case study given an identical 337 MW_t thermal input from the steam generator. The different electrical outputs (from 139 to 167 MW_e) are caused by variations in thermal-to-electric conversion efficiency. With supercritical pressures, because of the greater steam pressure range in the turbine from inlet through to the condenser, there is greater scope for including an extra stage or stages of feedwater heating; for example, the subcritical cycles depicted in Figures 18 and 19 incorporate 5 closed and 1 open heater and the supercritical cycles shown in Figures 20 through 23 have 7 closed and 1 open heater. This enables an even higher feedwater temperature to be achieved in supercritical cycles and thereby provide a further increase in cycle efficiency. Typical feedwater temperatures are ~300 °C compared to ~240 °C for sub-critical plants.

Subcritical coal-fired plants currently exist in the 150-MW_e power range. However, the smallest supercritical plants are greater than 400 MW_e[17]. Thus, it is assumed that supercritical technology can be successfully scaled down to the 150-MW_e power range. It is also assumed that it is not practical to thermally cycle a supercritical-power block on a daily basis; it will need to operate nearly 24/7, much like it does in a coal plant. The much higher steam pressures (≥300 bar supercritical versus 125 bar subcritical) will result in very thick pipe walls and turbine casings, which should greatly increase startup time relative to a subcritical plant.

Future solar power plants will likely require the use of dry-cooled condensers to reduce water consumption. Dry-cooling technology similar to that offered by SPX Cooling Technologies is assumed in the analysis. According to SPX design specifications [8], the air-side delta P across the cooling coils can be estimated to be ~1.5 mbar and the fan power required by each bay is ~200 hp. These parameters, along with the amount of rejected heat calculated by GateCycle, were used to determine the number of cooling bays. The design condition was the hottest time of the year (42.8 ^oC), a condenser design pressure of 0.17 bar (versus a typical value of 0.087 bar for wet-cooled plants), and a design initial-temperature difference (ITD) of 14 ^oC.[18] these assumptions were found to optimize the annual performance of dry-cooled solar trough plants [9].

[17] Ansaldo is offering a 200 MW supercritical steam turbine but detailed information about it could not be found. See www.ansaldoenergia.com.

[18] ITD is defined as condenser temperature minus ambient temperature.

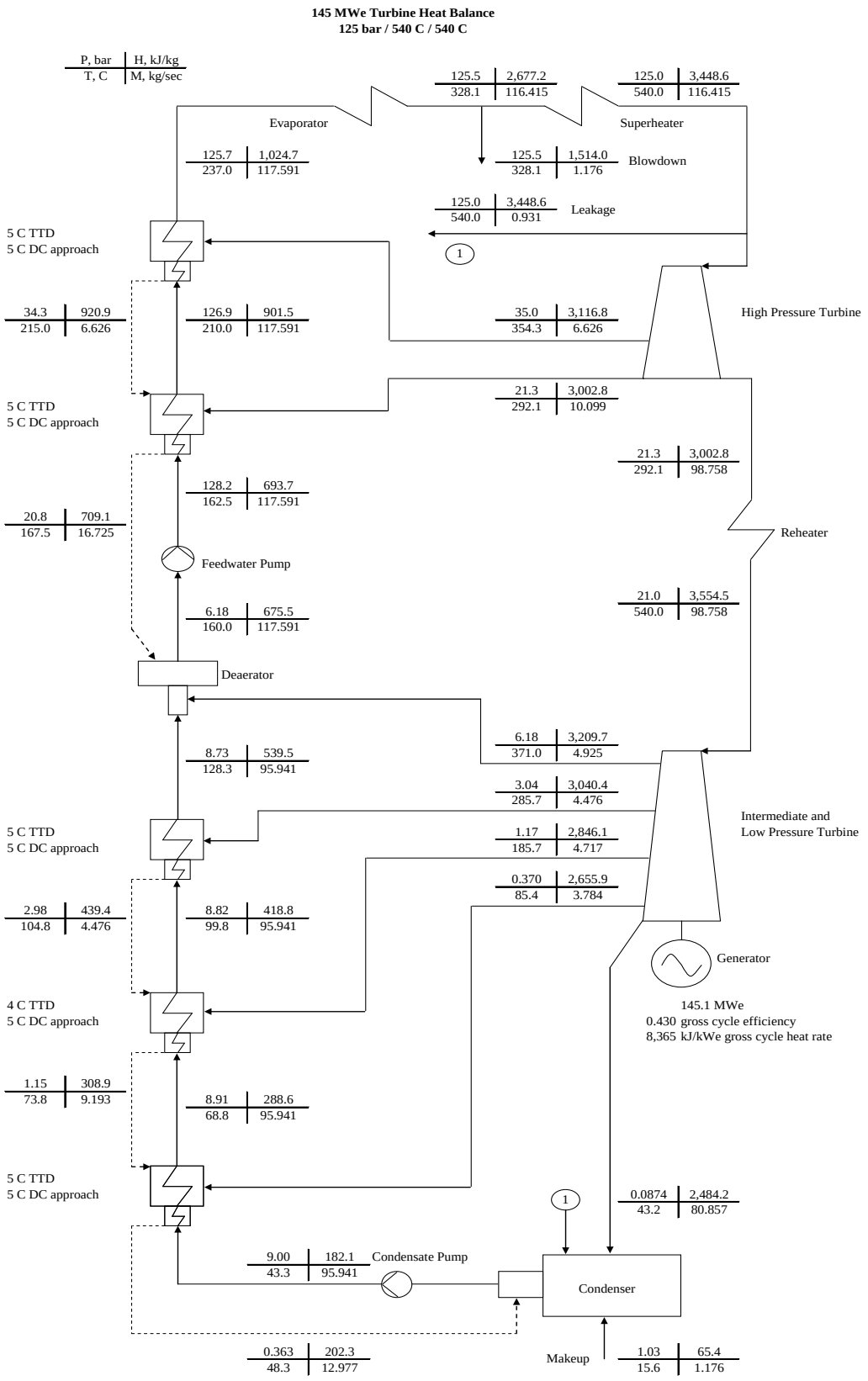

Figure 18. Heat balance for subcritical Rankine plant with wet condenser cooling.

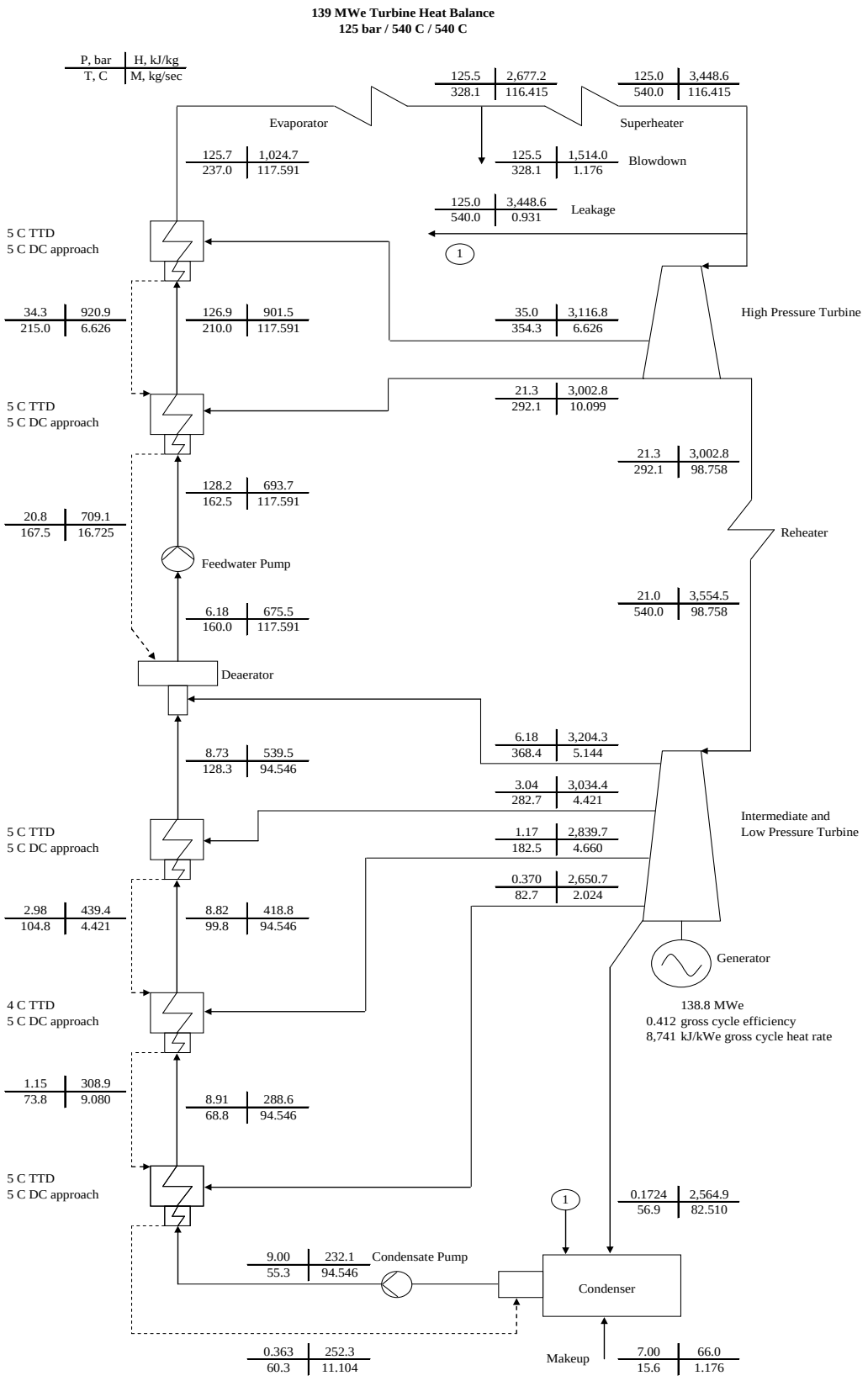

Figure 19. Heat balance for subcritical Rankine plant with dry condenser cooling.

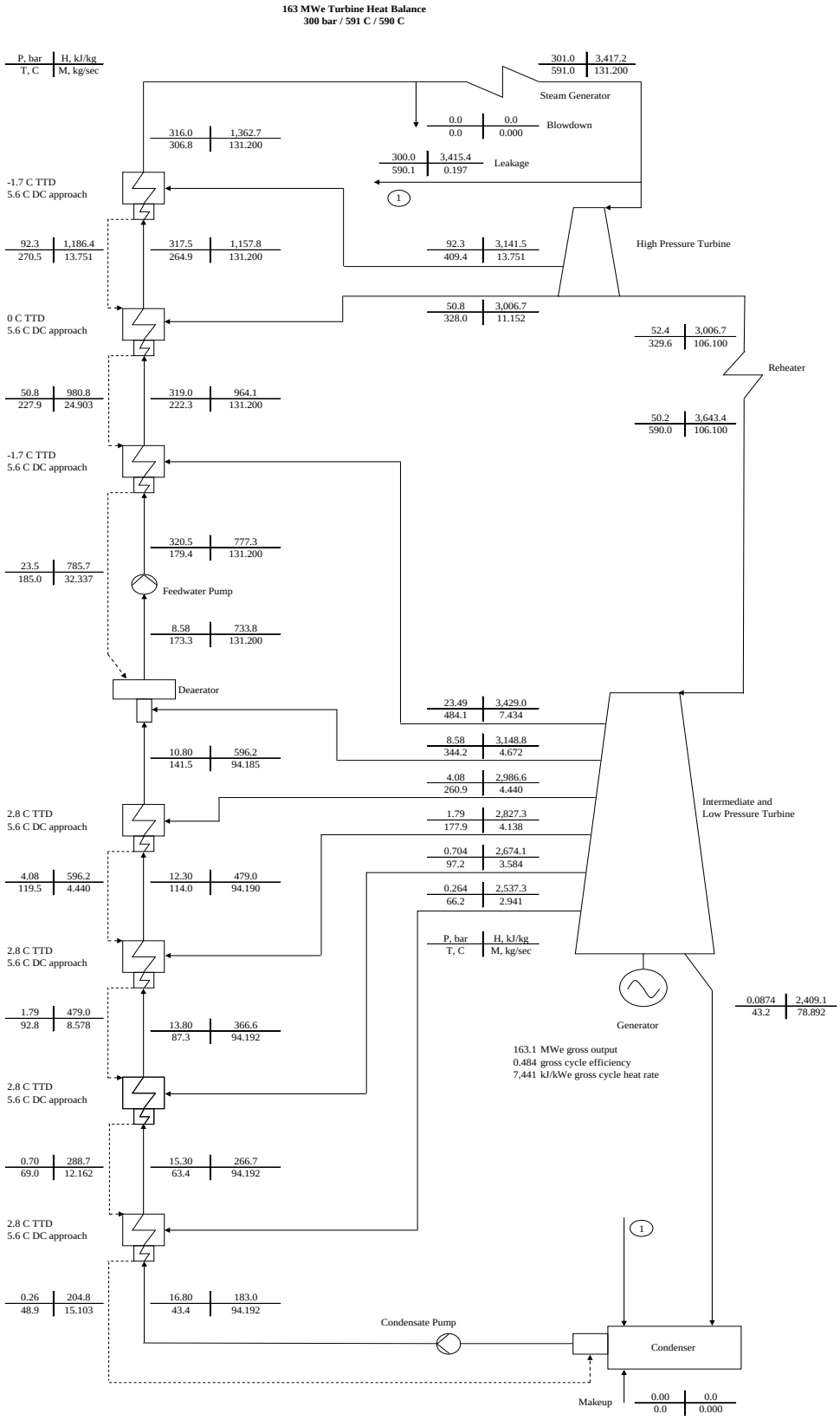

Figure 20. Heat balance for supercritical Rankine plant with wet condenser cooling.

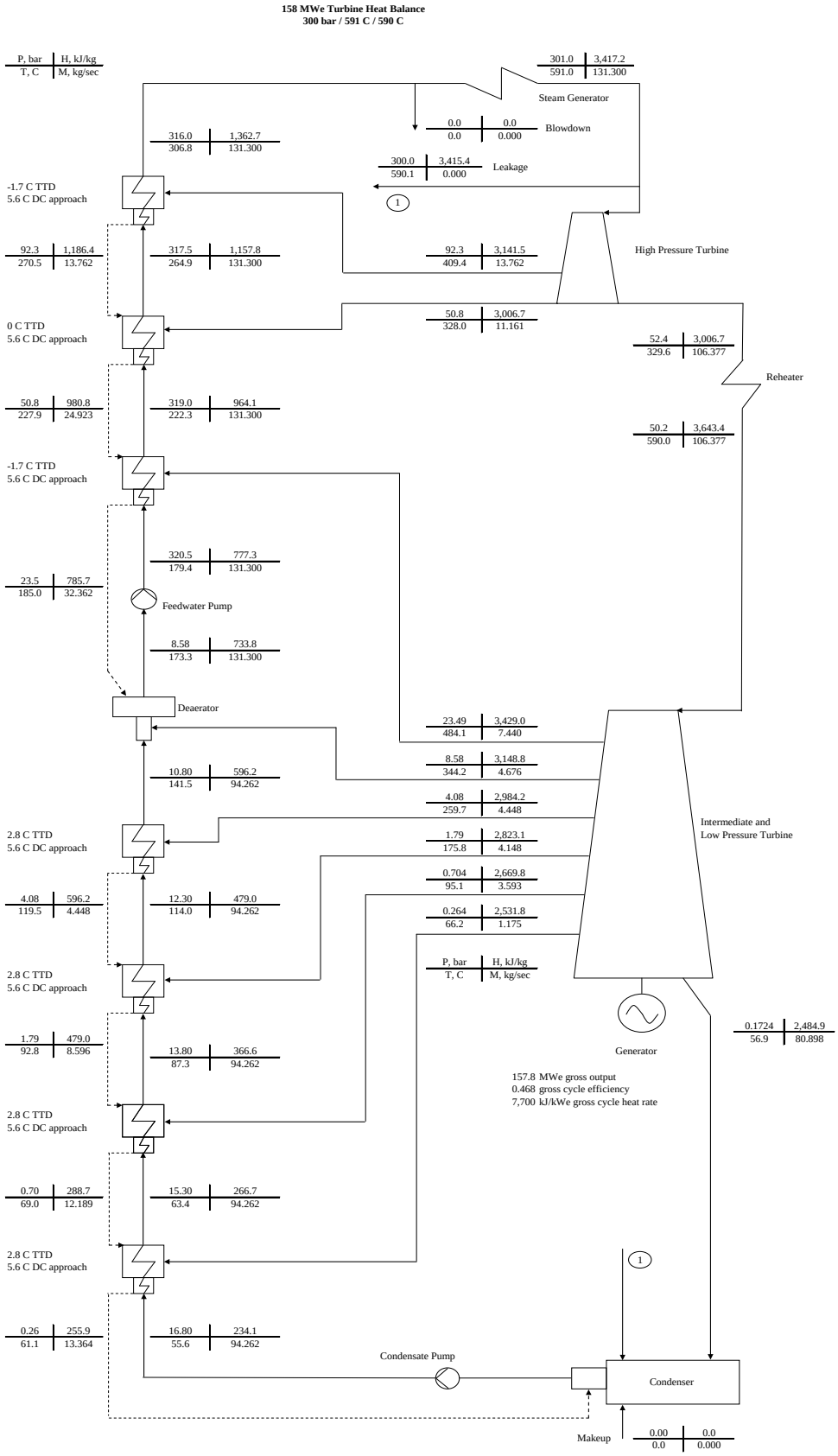

Figure 21. Heat balance for supercritical Rankine plant with dry condenser cooling.

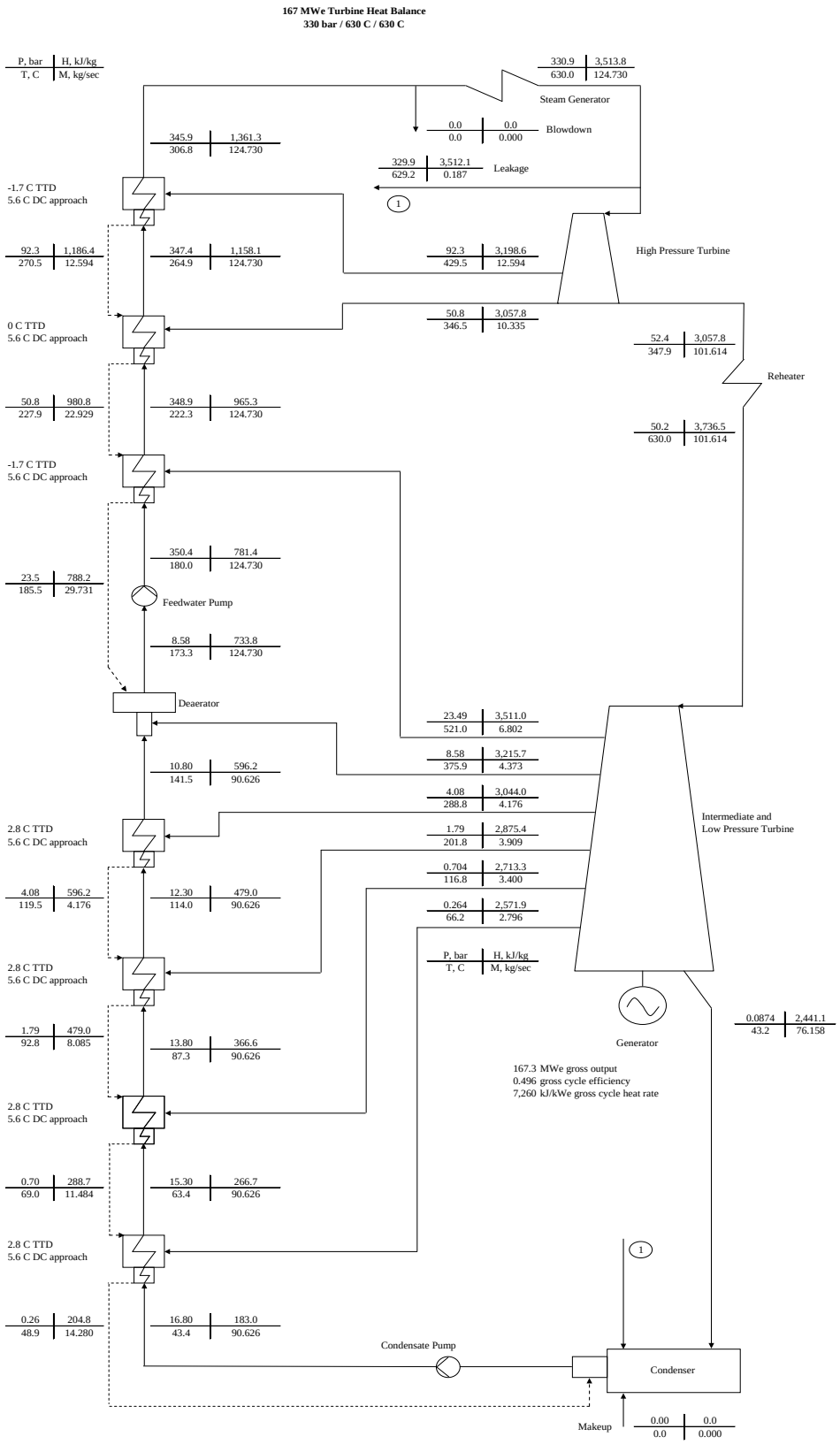

Figure 22. Heat balance for ultrasupercritical Rankine plant with wet condenser cooling.

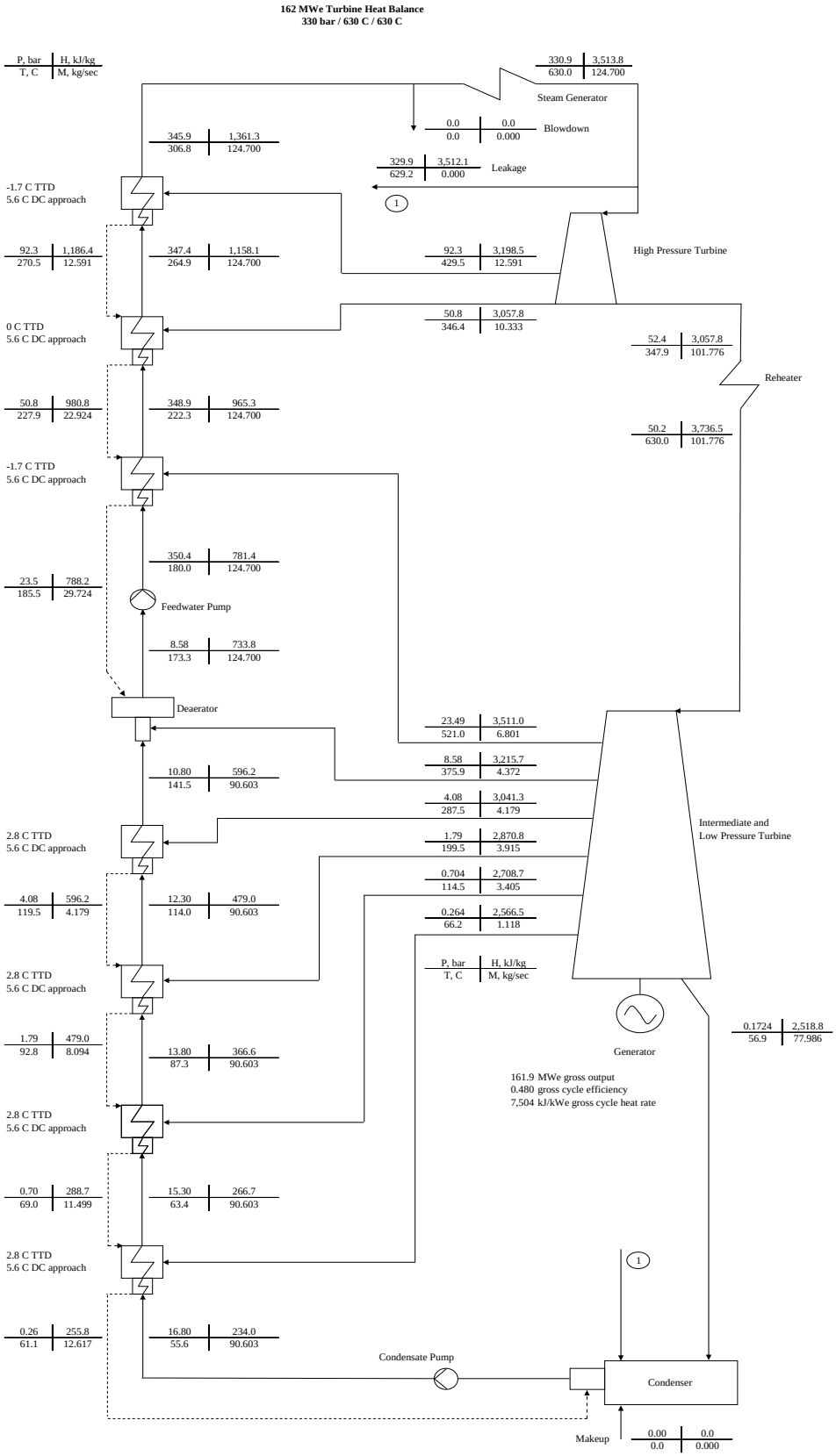

Figure 23. Heat balance for ultrasupercritical Rankine plant with dry condenser cooling.

Chapter 3
Performance Analysis

This chapter begins by describing the computer code used to estimate the annual energy of the plant designs described in Chapter 2. This is followed, in subsequent sections, by discussions of the development of the input parameters to the code and the results of the analysis.

3.1 Overview of the SOLERGY Computer Code

The SOLERGY computer code [46] was used to predict the annual energy production of the power plant designs. This code was selected because it was shown to give a realistic estimate of the actual energy produced by the Solar One and Solar Two plants [12, 13].

SOLERGY simulates the operation of a solar central receiver power plant using an insolation record recorded at 15-minute intervals. The relatively short intervals are needed to model plant startup and the effects of cloud transients. The code has subroutines for each major plant system, i.e., heliostat field, receiver, thermal-energy storage, and turbine/generator. A program flow diagram is shown in Figure 24. For each 15-minute time step, SOLERGY determines the plant's operational state (shutdown, starting up, etc.) and calculates steady-state power flows through each plant system. Annual plant performance is found by summing the performance at every 15-minute time step.

SOLERGY's computational algorithms are based on simple conservation of energy. There are no detailed thermodynamic calculations—no tracking of pressures and temperatures throughout the plant. Detailed calculations are necessary for the design and analysis of the performance over short periods but are not practical for an analysis of annual energy performance. Such calculations, however, are an important source of the data used as input to SOLERGY.

In SOLERGY, user-specified plant operational parameters are used to determine the plant's operation and performance during each time step. Examples of these parameters are (1) the time or energy required to start up and operate a system, (2) the parasitic load of major components and/or systems, and (3) the performance of individual components (e.g., receiver thermal losses or turbine efficiency). Parameters are typically estimated from hand-done calculations or obtained by running complex computer codes outside of SOLERGY. In some cases, data from tests performed at SNL or Solar One/Two can be used to estimate the code input parameters.

The versions of SOLERGY used in this study are somewhat different than the original version documented in Reference 46. Improvements in the modeling of parasitic power consumption, system behavior during short-term cloud transients, and dry-condenser cooling constitute the most important differences. These improvements are described later in this chapter.

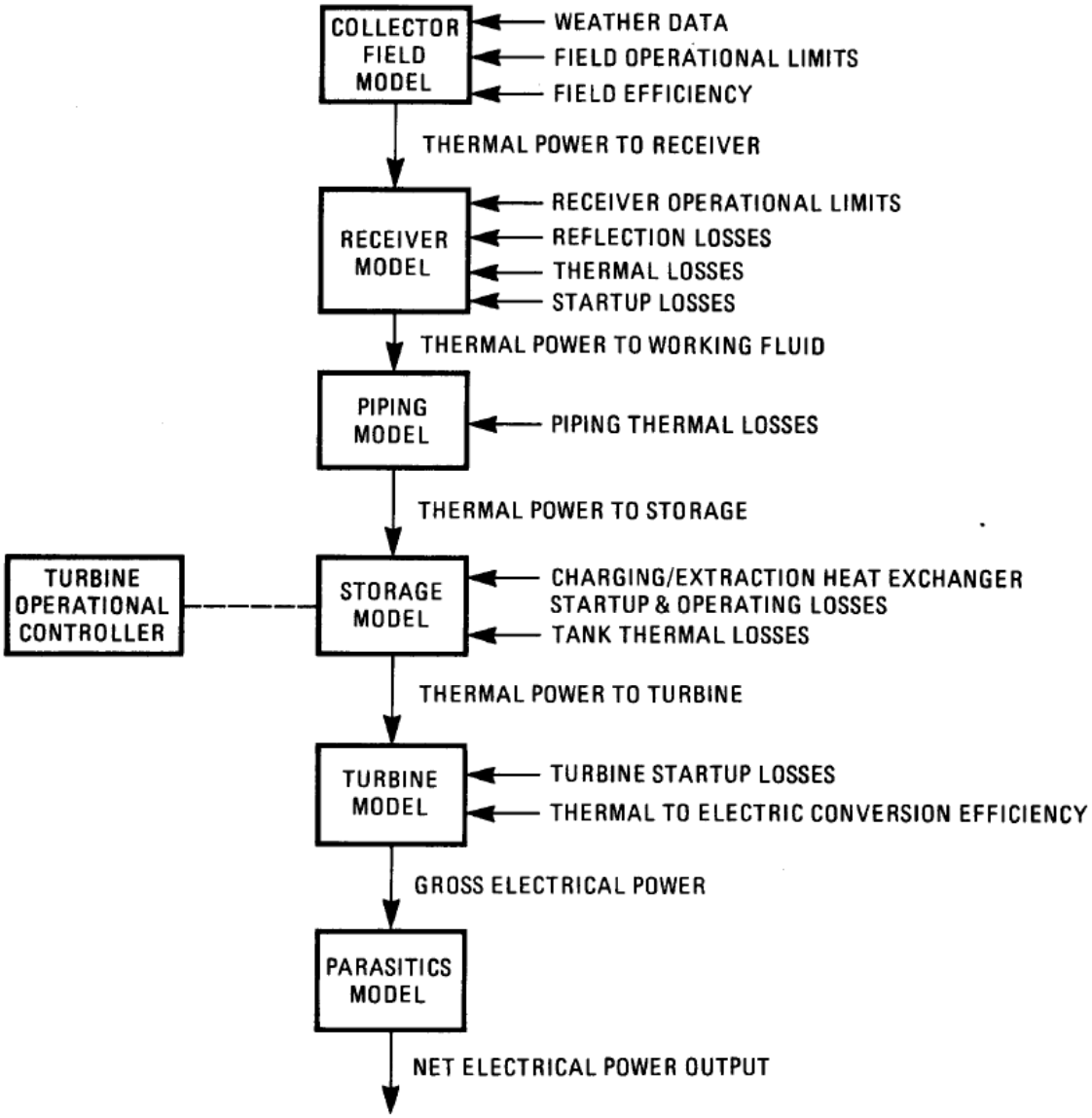

Figure 24. Program flow diagram for the SOLERGY computer code.

3.2 Development of SOLERGY Input Parameters

Simulation of a particular central receiver design requires the user of the code to input design-specific values for each of the plant's subsystems. In addition, information related to the location of the site and an insolation/weather file must be provided. The SOLERGY parameters presented in Table 7 are categorized into eight groups and the values assigned to each are described in the subsections that follow. For a detailed discussion of the definitions of these parameters, the reader is referred to the SOLERGY user's manual [46].

Site Parameters

The power plants are assumed to be located near the Solar One/Two site in Barstow, California. This site was selected because it has good insolation characteristics and an abundance of weather data exist. For example, the 30-year average value of direct-normal insolation in Barstow (Daggett) was estimated to be 2.74 MWhr/m^2/yr [47]. The 15-minute weather file used in this study was measured in 1977 at Barstow by Aerospace Corporation; total annual direct normal irradiation (DNI) was 2.71 MWhr/m^2/yr [48].

Parameters for the Heliostat Field

This group addresses the availability and performance of the heliostats in the collector field.

As described in Chapter 2, the field sizes for the subcritical, supercritical, and ultra-supercritical plants were calculated by the DELSOL3 computer code [10]. DELSOL3 was also used to determine field efficiency as a function of sun position. The results of these DELSOL calculations are presented in Tables 8 through 10. These efficiencies include optical losses due to heliostat reflectance, cosine effects, heliostat shading and blocking, atmospheric transmission, receiver interception, and receiver absorptance.

When running DELSOL a flux constrained aiming strategy for the heliostats was employed such that peak flux on the receiver was limited to ~1 MW/m^2 (1000 suns). This value is somewhat larger than the 800-sun limit adopted at Solar Two but is predicted to be acceptable using advanced receiver materials (see discussion in Section 2.2).

As described in Chapter 2, all plants are assumed to use glass/metal heliostats similar to the 95 m^2 Generation-3 version made by ATS in the 1980s (see Figure 4). The clean reflectance for this type of heliostat was measured to be 94% when new [49] and has not degraded significantly in more than 20 years of outdoor, face-up exposure at the National Solar Thermal Test Facility (NSTTF). The reflectivity values presented in Table 7 are the product of the clean reflectance and a cleanliness factor of 95%. The latter value was obtained from experience at trough power plants that suggests that regular mirror washing can achieve an annual-average cleanliness of 95% [50].

Table 7. SOLERGY Input Parameters for Subcritical (Sub), Supercritical (SC), and Ultra-Supercritical (USC) Rankine Plants.

Parameter	Description	Sub	SC	USC
Site Parameters				
SOLWEA	Insolation/weather file	1977 Barstow, 2.707 MWh/m^2		
ALAT	Local latitude (degrees)	34.9	34.9	34.9
ALONG	Local longitude (degrees)	117.0	117.0	117.0
ZONE	Local international time zone	Pacific	Pacific	Pacific
Parameters for Heliostat Field				
FS	Heliostat field reflective area (m^2)	1901157	1926548	1948216
ELIM	Minimum sun elevation angle for heliostat field operation (degrees)			
RFLCTY	Heliostat reflectivity (included in Tables 8 to 10)	0.893	0.893	0.893
	Heliostat availability	0.99	0.99	0.99
FR	Field efficiency matrix	Tab 8	Tab 9	Tab 10
WSLIM	Wind stow speed (m/s)	17.9	17.9	17.9
Parameters for Receiver System				
EPS	Receiver absorptance (included in Tables 8 to 10)	0.94	0.94	0.94
RS	Receiver thermal rating (MW_t)	1000.0	1000.0	1000.0
ALPHAR	Receiver cooldown parameter (hrs^{-1})	0.2	0.2	0.2
TREQD	Time delay for receiver startup (hrs)	0.75	0.75	0.75
RMF	Receiver minimum flow fraction	0.16	0.16	0.16
PLXLR	Receiver thermal losses, hot (MW_t) vs. wind speed	55.5	66.6	74.9
PA(26)	Receiver thermal losses, standby (MW_t)	16.7	16.7	16.7
EXFAC	Fraction of clear-sky insolation that is unusable (if=0, all DNI is usable)	0	0	0
Parameters for Thermal Storage System				
PTSMAX	Maximum charging rate (MW_t)	1000.0	1000.0	1000.0
PFSMAX	Maximum discharge rate (MW_t)	337.5	337.5	337.5
EMAX	Maximum value of storage (MW_thr)	5000.0	5000.0	5000.0
EMIN	Minimum value of storage (MW_thr)	0	0	0
TNKLF	Heat loss from storage system (MW_t)	1.0	1.05	1.05
DLF	Heat loss from steam generator (MW_t)	1.0	1.0	1.0
Parameters for Steam Turbine System				
TBHWS	Time between hot and warm start (hr)	12	12	12
TBHWS	Time between warm and cold start (hr)	60	60	69
SDH	Hot turbine sync delay (hr)	0.25	0.25	0.25

Table 7. SOLERGY Input Parameters for Subcritical (Sub), Supercritical (SC), and Ultra-Supercritical (USC) Rankine Plants

Parameter	Description	Sub	SC	USC
SDW	Warm turbine sync delay (hr)	1.0	1.0	1.0
SDC	Cold turbine sync delay (hr)	1.8	1.8	1.8
RDH	Hot turbine ramp delay (hr)	0.4	0.4	0.4
RDW	Warm turbine ramp delay (hr)	1.7	1.7	1.7
RDC	Cold turbine ramp delay (hr)	2.7	2.7	2.7
TPFSL	Thermal power for rated turbine operation (MW_t)	337.5	337.5	337.5
TMFS	Minimum turbine flow fraction	0.3	0.3	0.3
ESMIN1	Minimum storage level for turbine start, receiver operating (MW_thr)	200.0	200.0	200.0
ESMIN2	Minimum storage level for turbine start, receiver not operating (MW_thr)	337.5	337.5	337.5
ESMAX1	Storage level at which turbine must be started, receiver operating (MW_thr)	200.0	200.0	200.0
TSTDR	Time to startup steam generator (hr) (included startup in TMFS and SDX)	0.	0.	0.
FEPSS	Turbine thermal-to-electric efficiency	Tab 11	Tab 12	Tab 13
REPSS	vs. fraction of rated power			
CEPSS	vs. temperature (^oF)			
Piping Parameters				
YXLP	Piping loss coefficients			
TXLP	vs. ambient temperature (/^oF)	3.4e-4/-4.	Same	
		3.2e-4/32.		
		3.2e-4/50.		
		3.0e-4/86.		
		2.8e-4/122.		
Parameters for Steam Generator				
DLF	Steam generator heat losses (MW_t)	1.0	1.0	1.0
REFPC	Reference power for steam generator thermal losses (MW_t)	337.5	337.5	337.5
PWARMD	Maximum heat to steam generator during startup (MW_t)	30.0	30.0	30.0
Parameters for Electrical Parasitics				
PA(1)	Power to run heliostat field (MW_e/m^2)	5.22e-7	5.22e-7	5.22e-7
PA(2)	Power to stow/unstow heliostat field during 0.25 hr interval (MW_e /m^2)			
PA(3)-PA(5)	Cold salt pump curve-fit parameters	Fig 26	Fig 26	Fig 26
PA(7)-PA(8)	Turbine plant curve-fit parameters	Tab 11	Tab 12	Tab 13

Table 7. SOLERGY Input Parameters for Subcritical (Sub), Supercritical (SC), and Ultra-Supercritical (USC) Rankine Plants

Parameter	Description	Sub	SC	USC
PA(10)-PA(12)	Hot salt pump power (MW_e)	0.85	0.85	0.85
PA(13)-PA(25)	PG&E condenser cooler (not used)	0	0	0
PA(26)	Receiver thermal loss in standby (MW_t)			
PA(27)	# of time steps allowed for receiver standby before shutdown of receiver	3	3	3
PA(28)-PA(29)	Baseline parasitics (MW_e)	0.7	0.7	0.7
PA(31)	Turbine plant curve fit parameter	Tab 11	Tab 12	Tab 13

Table 8. DELSOL Field and Receiver Interception Efficiency as a Function of Sun Location for 1000-MW_t Receiver With 565 ^oC Outlet Temperature. (Values include 0.893 heliostat reflectance and 0.94 receiver absorptance.)

		Elevation Angle						
		0.	**5.**	**15.**	**25.**	**45.**	**65.**	**89.5**
	0.	0.0	0.237	0.421	0.518	0.577	0.590	0.600
	30.	0.0	0.235	0.418	0.514	0.575	0.588	0.600
	60.	0.0	0.230	0.410	0.505	0.568	0.585	0.600
Azimuth	75.	0.0	0.276	0.413	0.503	0.564	0.582	0.600
Angle	90.	0.0	0.220	0.398	0.494	0.560	0.580	0.600
	110.	0.0	0.257	0.399	0.488	0.554	0.577	0.600
	130.	0.0	0.269	0.396	0.483	0.549	0.574	0.600

Table 9. DELSOL Field and Receiver Interception Efficiency as a Function of Sun Location for 1000-MW_t Receiver With 600 ^oC Outlet Temperature. (Values include 0.893 heliostat reflectance and 0.94 receiver absorptance.)

		Elevation Angle						
		0.	**5.**	**15.**	**25.**	**45.**	**65.**	**89.5**
	0.	0.0	0.235	0.419	0.515	0.576	0.588	0.599
	30.	0.0	0.236	0.417	0.512	0.573	0.587	0.599
	60.	0.0	0.231	0.410	0.504	0.567	0.584	0.599
Azimuth	75.	0.0	0.275	0.412	0.502	0.562	0.581	0.599
Angle	90.	0.0	0.219	0.397	0.492	0.558	0.579	0.599
	110.	0.0	0.257	0.399	0.488	0.553	0.576	0.599
	130.	0.0	0.268	0.396	0.483	0.548	0.573	0.599

Table 10. DELSOL Field and Receiver Interception Efficiency as a Function of Sun Location for 1000-MW_t Receiver With 650 ^oC Outlet Temperature. (Values include 0.893 heliostat reflectance and 0.94 receiver absorptance.)

		Elevation Angle						
		0.	**5.**	**15.**	**25.**	**45.**	**65.**	**89.5**
	0.	0.0	0.235	0.417	0.513	0.573	0.587	0.599
	30.	0.0	0.236	0.415	0.510	0.571	0.586	0.599
	60.	0.0	0.230	0.408	0.503	0.565	0.583	0.599
Azimuth	75.	0.0	0.275	0.412	0.501	0.561	0.580	0.598
Angle	90.	0.0	0.222	0.398	0.493	0.558	0.578	0.598
	110.	0.0	0.259	0.400	0.489	0.553	0.575	0.598
	130.	0.0	0.268	0.397	0.484	0.549	0.573	0.598

The value for heliostat availability was selected to be 99%. This value is supported by reliability data collected for the Solar One heliostat field [51]. The collector field startup angle is also supported by experience at Solar One/Two; the heliostats were typically tracking the receiver at sunrise.

Parameters for the Receiver System

This group of parameters addresses the performance of the receiver during startup, shutdown, and steady-state operation.

The receiver thermal ratings are assumed to be 1000 MW_t. The Utility Studies [2] investigated salt receivers with thermal ratings of ~500 MW_t[19] and ~1000 MW_t and a solar plant using the larger receiver was predicted to result in a lower LCOE. Another reason for selecting 1000 MW is due to the belief by SNL that supercritical Rankine plants will likely need to provide Baseload energy with power ratings of ~160 MW_e (as described in Section 2.4). Given a conversion efficiency of 48%, this Rankine plant would require 160/0.48 = 333 MW of thermal energy. Studies have shown (e.g., see Reference 6) that a molten-salt plant with a solar multiple of 3 combined with 15 hours of thermal storage yields the lowest LCOE for a given turbine size and achieves a solar-only capacity factor of 70 to 75%[20] for a plant installed in the Southwestern deserts. Thus, the receiver should be 3*333 or ~1000 MW_t.

Receiver absorptance was estimated by taking the average of possible best-case and worst-case values. The best case would be the value achieved at Solar One, i.e., 95%. This value was maintained during the final 2.5 years of its operation. The average absorptance for a molten-salt receiver could be somewhat lower than the receiver at Solar One, even though the tubes of both receivers are coated with the same Pyromark paint. This is because the paint on a salt receiver is exposed to a harsher environment; solar flux and temperatures are higher and any salt leakage

[19] The salt receiver currently being promoted by SolarReserve is ~500 MW_t.

[20] If capacity factors greater than 70% are required, a small amount of fossil backup might be used to achieve a typical baseload capacity factor of >80%.

will rapidly degrade the paint near the hole in the tube. It was therefore judged that in the worst case the average absorptance could be 93%, even with regular repainting of the receiver every few years.

The minimum flow at which the receiver can operate, 16%, was measured during testing of a 5-MW_t salt receiver at SNL during 1988 [23]; values between 15 and 20% were also demonstrated at Solar Two [13].

Thermal losses from the Solar Two receiver were measured to be between 2.7 and 3 MW_t over a range of wind speeds [15]. Since the absorber surface area was 99 m^2, the loss was ~30 kW_t/m^2. This value was used to estimate the thermal losses for the receiver in the subcritical plant with the same 285/565 ^oC salt inlet/exit temperatures as Solar Two. For the higher-temperature receivers in the supercritical plants, the receiver thermal model described in Section 2.2 was calibrated with the Solar Two data and used to calculate the increased thermal losses given a 600 or 650 ^oC outlet temperature, estimated to be 36 and 40 kW_t/m^2, respectively. When the receiver is in standby with no sun on it, the outlet temperature will drop to a few degrees below the inlet temperature. The receiver model predicts ~9 kW_t/m^2 with the receiver in standby. Standby can occur during startup of the receiver and while waiting for cloudy weather to clear. It was assumed the operators would maintain the receiver in cloud standby for 0.75 hours before shutting it down and draining it.

Receiver startup in the morning and restart following cloud-induced shutdowns is simulated by selecting proper values for the SOLERGY parameters TREQD and ALPHAR. Experimentation with SOLERGY found the values listed in Table 7 to produce reasonable results; the salt receiver completed start up 1.25 hours after sunrise and returned to rated conditions 0.25 hours after a cloud shutdown. This matches experimental data recorded during the test of the 5-MW_t salt receiver at SNL [23] and at Solar Two. (Typically, 0.5 hours is required to achieve minimum flow, followed by 0.75 hours of startup for a total of 1.25 hours to rated condition after sunrise.)

When SOLERGY was validated with Solar One data it was found that use of 15-minute-average insolation data, rather than more frequent 3-minute data, led to an overprediciton of plant performance on days when large and frequent opaque clouds were passing over the heliostat field [12]. Since Solar One used a steam receiver that was powered by a relatively small heliostat field, this type of weather quickly caused the steam conditions in the receiver to degrade below the trip setpoint of the turbine. When the sun returned there was a significant amount of time when solar energy was not converted to electricity while the operators restarted the receiver and turbine. These short-term transients and corresponding energy losses were not captured by SOLERGY with 15-minute insolation data; however, they were captured when 3-minute data were used. Typical insolation data files have time steps of 15-minute or longer. SOLERGY was therefore improved to model the concept of "useful insolation." The amount that is "useful" is a function of the time constant and trip setpoints of the solar plant, as well as the DNI time-step. The parameter EXFAC is used to capture these features associated with the plant design, as well as the weather file. The new SOLERGY model compares the DNI for a particular time step in the weather file with a value that would occur if the sky was totally clear and calculates a ratio of the 2 values. If the actual DNI is less than X% of clear sky value, SOLERGY will trip the receiver and force a restart at a later time step when the clouds clear the field. For example, it

was found that a value of 60% greatly improved the SOLERGY prediction of Solar One performance on partly cloudy days when 15-minute DNI data were used. All this being said, the value of EXFAC chosen for a molten-salt plant was set to zero, implying that all DNI in the 15-minute weather file is considered useful. Experience at Solar Two indicated that, unlike Solar One, the receiver and turbine could continue to operate through partly cloudy weather; since there was a storage tank between the turbine and receiver, clouds did not quickly lead to turbine trip.

Parameters for the Thermal Storage System

The maximum charging rate of the salt-storage system (PTSMAX) was set equal to the maximum power of the receiver, and the maximum discharge rate (PFSMAX) was set equal to the thermal power demands of the steam-generator system.

A sun-following dispatch strategy of stored energy within the tanks was chosen.[21] This minimizes the size of the tanks because the stored energy is held for the minimum amount of time before being discharged to the steam generator. The size of the storage tanks was chosen to operate the turbine for 15 hours. Given a solar multiple of 3, approximately 15 hours of storage has been shown to result in the lowest LCOE [6]. Since the receiver is 1000 MW_t, a solar multiple of 3 results in a steam generator with a 333-MW_t rating.[22] Fifteen hours of storage is thus 15 * 333 ~ 5000 MWh_t. This size is the value for EMAX in Table 7.

The heat loss from the hot and cold tanks for the 5000-MWh system was based on a heat loss calculation performed by Chicago Bridge and Iron for a hypothetical commercial-scale system [53]. In that study, the heat loss for the hot tank within a 1560-MWh system was estimated to be 244 kW. Thermal losses from the cold tank were not given, but can be estimated by assuming the same overall heat transfer coefficient (UA). Assuming an ambient temperature of 25 ^oC, the value for the hot tank is estimated from $UA = Q/\Delta T = (244/(565-25)) = 0.45$ kW/^oC. The cold tank losses would therefore be $Q = 0.45*(288-25) = 118$ kW_t. Total hot and cold tank thermal losses are therefore 362 kW_t for the 1560-MWh system. Since the 5000 MWh is roughly three times larger, the total thermal losses are also assumed to be 3 times larger, or ~1 MW_t.

Parameters for the Steam-Turbine System

This group of parameters addresses the performance of the turbine generators during startup and steady-state operation.

The startup parameters were taken from the SOLERGY model developed by Bechtel National, Inc., for the US Utility Study [2]. This subcritical turbine was made by General Electric (GE) and was first proposed for use in the Solar 100 study [54]. The parameters were assumed to be the same for the supercritical turbines.

[21] SOLERGY can also be run to maximize revenue according to a "time-of-day" electricity pricing schedule. The optimum amount of storage given time-of-day pricing would be different than a "sun-following" dispatch strategy. See References 46 and 52.

[22] The analysis was actually based on a value of 337 MWt.

The ESXXXX parameters listed in Table 7 start the turbine at a particular storage level. These values were chosen to emulate the sun-following-dispatch strategy.

The thermal-to-electric conversion efficiencies (input to SOLERGY via lookup tables) for the subcritical, supercritical, and ultra-supercritical steam-Rankine cycles were calculated using Gatecycle software [7]. The efficiency of each cycle is a function of the condenser cooling method (wet or dry) and power level. Wet-cooled subcritical and supercritical models developed for the analysis of larger power tower systems [16] were scaled down from a plant size of >400 MW_e to a sizes in the range of 139 to 167 MW_e and extended to include cases that apply to dry condenser cooling and ultra-supercritical steam conditions. The design-point heat balances for the 6 case studies are depicted in Figures 18 through 23 and the corresponding efficiencies in Tables 11 through 13. The solar-thermal input to the steam is the same for all six cases (337 MW_t). However, since the thermal-to-electric conversion efficiency is increased if wet (rather than dry) cooling is used and is also increased if a supercritical (rather than subcritical) steam cycles is used, the gross turbine output ranges from 139 to 167 MW_e at the design point condition of 43 ^oC dry bulb and 22 ^oC wet bulb.[23]

The key Rankine system design parameters from the Gatecycle analysis are shown in Table 14.

Parameters for the Steam Generator

A few parameters address the startup of the steam generator. During the SOLERGY modeling of the Solar Two steam generator is was found that it is easier to include startup of the molten-salt steam generator within startup of the turbine generator system. This is accomplished by setting TSTDR to zero and selecting turbine parameters SDX, TMFS, and RDX that match the thermal energy needed to heat up the steam generator/turbine before syncing to the grid. The data from Solar Two indicated that an optimized startup required ~10 MWh_t for the 35 MW_t steam generator following an overnight shutdown [13].

The steam generator assumed in the current analysis (337 MW_t) is ~10 times larger than the steam generator at Solar Two. Given overnight shutdown, the startup energy is assumed to be 5 times larger (~50 MWh), thus assuming some economy of scale. Given an extended shutdown, the assumed startup energy is ~125 MWh_t. The parameter values shown in Table 7 produced these startup energy losses.

The steam generator will also incur thermal losses from the vessels and piping when it is operating. These losses (DLF) are assumed to similar to the thermal storage tank losses.

[23] These design point conditions were found to be optimal for a CSP plant near Las Vegas, NV [9].

Table 11. GateCycle Prediction of Gross Rankine Cycle Efficiency and Parasitics for Subcritical Steam Plants. (Designed at 43 °C (109 °F) Dry Bulb, 22 °C (72 °F) Wet Bulb.)

Wet-Cooled Condenser (43.0% η @DP)

Wet Bulb	Power		
	50%	70%	100%
20 °F	42.7% η 585 FWP 78 CP 1142 CTF 744 CWP 2549 kW Total	43.1% η 1015 FWP 90 CP 1106 CTF 744 CWP 2955 kW Total	43.6% η 2140 FWP 116 CP 1058 CTF 745 CWP 4058 kW Total
40 °F	42.7% η	43.1% η	43.6% η
60 °F	42.2% η	42.8% η	43.4% η
80 °F	40.6% η 585 FWP 78 CP 1095 CTF 747 CWP 2506 kW Total	41.8% η 1015 FWP 90 CP 1075 CTF 747 CWP 2927 kW Total	42.6% η 2140 FWP 116 CP 1045 CTF 748 CWP 4048 kW Total

Dry-Cooled Condenser (41.2% η @DP)

Dry Bulb	Power		
	50%	70%	100%
30 °F	41.1% η 585 FWP 78 CP 1229 CTF 1892 kW Total	41.5% η 1015 FWP 90 CP 1229 CTF 2333 kW Total	41.7% η 2140 FWP 114 CP 1229 CTF 3483 kW Total
60 °F	40.9% η 585 FWP 78 CP 1555 CTF 2218 kW Total	41.3% η 1015 FWP 90 CP 1555 CTF 2660 kW Total	41.9% η 2140 FWP 114 CP 1944 CTF 4198 kW Total
90 °F	40.3% η 585 FWP 78 CP 2584 CTF 3247 kW Total	41.0% η 1015 FWP 89 CP 2584 CTF 3688 kW Total	41.7% η 2140 FWP 114 CP 2953 CTF 5207 kW Total
120 °F	37.5% η 585 FWP 78 CP 3147 CTF 3810 kW Total	39.0% η 1015 FWP 89 CP 3497 CTF 4600 kW Total	40.2% η 2140 FWP 113 CP 3497 CTF 5750 kW Total

FWP (Feed Pump), CP (Condensate Pump), CTF (Tower Fans), CWP (Circ Water Pump)

Table 12. GateCycle Prediction of Gross Rankine Cycle Efficiency and Parasitics for Supercritical Steam Plants. (Designed at 43 °C (109 °F) Dry Bulb, 22 °C (72 °F) Wet Bulb.)

Wet-Cooled Condenser (48.4% η @DP)

Wet Bulb	Power		
	50%	**70%**	**100%**
20 °F	47.1% η	48.0% η	49.1% η
40 °F	47.1% η	48.0% η	49.0% η
60 °F	46.6% η 2441 FWP 99 CP 1232 CTF 773 CWP 4545 kW Total	47.6% η 3620 FWP 138 CP 1208 CTF 773 CWP 5739 kW Total	48.8% η 5705 FWP 198 CP 1174 CTF 774 CWP 7851 kW Total
80 °F	44.9% η	46.4% η	47.9% η

Dry-Cooled Condenser (46.7% η @DP)

Dry Bulb	Power		
	50%	**70%**	**100%**
30 °F	45.7% η 2441 FWP 98 CP 968 CTF 3507 kW Total	46.6% η 3620 FWP 138 CP 1161 CTF 4918 kW Total	47.6% η 5709 FWP 198 CP 1355 CTF 7262 kW Total
60 °F	45.6% η 2441 FWP 98 CP 1467 CTF 4006 kW Total	46.5% η 3619 FWP 138 CP 1650 CTF 5407 kW Total	47.6% η 5710 FWP 199 CP 1833 CTF 7741 kW Total
90 °F	44.8% η 2441 FWP 99 CP 2426 CTF 4966 kW Total	46.2% η 3619 FWP 138 CP 2773 CTF 6530 kW Total	47.5% η 5710 FWP 199 CP 3120 CTF 9028 kW Total
120 °F	42.0% η 2441 FWP 99 CP 3253 CTF 5792 kW Total	43.9% η 3620 FWP 138 CP 3253 CTF 7010 kW Total	45.8% η 5709 FWP 199 CP 3253 CTF 9161 kW Total

FWP (Feed Pump), CP (Condensate Pump), CTF (Tower Fans), CWP (Circ Water Pump)

Table 13. GateCycle Prediction of Gross Rankine Cycle Efficiency and Parasitics for Ultra-supercritical Steam Plants. (Designed at 43 °C (109 °F) Dry Bulb, 22 °C (72 °F) Wet Bulb.)

Wet-Cooled Condenser (49.6% η @DP)

Wet Bulb	Power		
	50%	**70%**	**100%**
20 °F	48.3% η	49.2% η	50.2% η
40 °F	48.3% η	49.2% η	50.2% η
60 °F	47.8% η 2544 FWP 94 CP 1207 CTF 757 CWP 4604 kW Total	48.9% η 3789 FWP 133 CP 1183 CTF 757 CWP 5862 kW Total	50.0% η 5934 FWP 191 CP 1149 CTF 758 CWP 8032 kW Total
80 °F	46.2% η	47.7% η	49.1% η

Dry-Cooled Condenser (48.0% η @DP)

Dry Bulb	Power		
	50%	**70%**	**100%**
30 °F	47.0% η 2545 FWP 94 CP 947 CTF 3587 kW Total	47.9% η 3789 FWP 133 CP 1136 CTF 5058 kW Total	48.9% η 5932 FWP 191 CP 1325 CTF 7449 kW Total
60 °F	46.9% η 2545 FWP 94 CP 1435 CTF 4075 kW Total	47.8% η 3789 FWP 133 CP 1615 CTF 5536 kW Total	48.9% η 5933 FWP 191 CP 1794 CTF 7918 kW Total
90 °F	46.1% η 2545 FWP 94 CP 2375 CTF 5015 kW Total	47.5% η 3789 FWP 133 CP 2714 CTF 6636 kW Total	48.8% η 5933 FWP 191 CP 3053 CTF 9177 kW Total
120 °F	43.3% η 2545 FWP 94 CP 3184 CTF 5823 kW Total	45.2% η 3789 FWP 133 CP 3184 CTF 7105 kW Total	47.0% η 5933 FWP 191 CP 3184 CTF 9307 kW Total

FWP (Feed Pump), CP (Condensate Pump), CTF (Tower Fans), CWP (Circ Water Pump)

Table 14. GateCycle Rankine Plant Design Parameters.

	SUB		SC		USC	
	Wet	**Dry**	**Wet**	**Dry**	**Wet**	**Dry**
LP turbine exhaust area (m^2)	3.3	1.9	3.2	1.9	3.1	1.9
FW heater areas (m^2)	296	296	624	624	550	550
(top to bottom on heat balance diagram)	432	432	682	682	603	603
	217	215	532	532	476	476
	276	274	256	256	235	235
	260	178	287	288	265	266
			299	299	284	285
			275	162	264	156
Steam generator duties (MW_t)						
Preheater	58	58				
Evaporator	135	135	269	269	268	268
Superheater	90	90				
Reheater	54	54	68	68	69	69
Total	337	337	337	337	337	337
Steam generator areas (m^2)[24]						
Preheater	1533	1533				
Evaporator	2229	2229				
Superheater	1444	1444				
Reheater	1510	1510				
Condenser saturation pressure (bar)	0.087	0.17	0.087	0.17	0.087	0.17
Condenser cooling system						
Cooling tower air-side ΔP (mbar)	2.1	1.5	2.1	1.5	2.1	1.5
Number of dry-cooling bays		24		22		22
Initial Temperature Difference (^oC)		14		14		14
OD surface area ($x10^3$ m^2)		20		18.7		18.4
OD+Fin surface area ($x10^3$ m^2)		592		552		542

[24] The molten salt heat transfer areas were estimated by software developed by Abengoa Solar [16]. See Chapter 2.

Piping Parameters

The piping model parameters in SOLERGY define the energy lost from the receiver riser and downwcomer as a function of ambient temperature. The values presented in the table are the SOLERGY defaults. The model predicts ~0.3 MW_t of thermal loss during times when the receiver is operating.

Parameters for Electrical Parasitics

This group of parameters addresses the electrical power used by plant auxiliaries (pumps, fans, trace heaters, etc.) during various modes of plant operation and shutdown. This electrical energy is subtracted from the gross electricity produced by the turbine generator during the calendar year to yield the net electrical output of the plant.

The electric power to track and stow the heliostats was estimated by the manufacturer ATS [55], and checked with experience at Solar One [12].

Like Solar Two, variable speed pumps are used to pump the salt up the tower and through the receiver. The receivers were designed to have the same delta P as Solar Two (165 psi at full flow) with the inlet tank set to 250 psi.[25] The total head requirements for the cold salt pumps are expressed by the following equation [56]:

$$H_{total} = H_{static} + H_{full} (W_{x\%}/W_{full})^2 \quad (12)$$

where

H_{total} = Total head (ft),[26]
H_{static} = Static head (ft) = tower height + receiver height,
H_{full} = Friction head loss across the receiver at full pump flow (ft), and
$(W_{x\%}/W_{full})$ = Fraction of full flow.

The power consumed by the pumps can be estimated from the traditional fluid mechanics: $P = W * H/\eta$. Given operation of a single 100% capacity pump (with the redundant pump idle), the specific equation used was

$$EP = [W_{1pump} * H_{total}]/[\eta pump * \eta motor * \eta varsp * fac] \quad (13)$$

[25] The receiver inlet tank contains a pressurized inventory of salt that passively discharges to protect the receiver during a station blackout. The inventory cools the receiver for 1 to 2 minutes while the diesel generator starts to repower the cold salt pumps.

[26] For molten salt at 288 ^oC (550 ^oF), the conversion factor from pressure to head is 0.833 psi per foot.

where

EP = electric power for one 100% capacity pump (kW),
W_{1pump} = flow rate of 1 pump (lb/sec),
ηpump = pump efficiency as a function of flow rate and head (Figure 25),
ηmotor = pump motor efficiency (0.95),
ηvarsp = efficiency of variable speed coupler (0.95), and
fac= =units conversion factor (737.) to yield kW when pump flow is in lb/sec and head is in ft.

Plots of Equation (13) for the cold-salt pumps are presented in Figure 26, along with the curve fit equations.

The turbine-plant parasitics for the three salt plants were calculated by GateCycle. By studying the results in Tables 11 through 13, the following conclusions can be drawn:

- Parasitics for the supercritical plants are higher than the subcritical plant primarily because of the higher feedwater pump parasitic; this is caused by the much higher feedwater pressure in the supercritical plants (125 bar subcritical and >300 bar for supercritical).
- Parasitics of plants with wet-cooled condensers are a weak function of wet-bulb temperature (compare 20 ^{o}F and 80 ^{o}F entries in Table 11); this dependence can be ignored. Parasitics of plants with dry-cooled condensers are a strong function of dry-bulb temperature, due to the operation of more fan bays at higher temperature.
- There is a significant variation in parasitics as a function of load.[27]

The parasitic results shown in Tables 11 through 13 are input to SOLERGY via curve fit relationships. The numbers in the equations are input to SOLERGY via PA(7), PA(8), and PA(31).

Subcritical Wet: P = 1.0 + 3.0 * Power Level
Subcritical Dry: P = 3.6395 * Power Level + 0.02645 * Dry Bulb T – 1.0404
Supercritical Wet: P = 1.2 + 6.67 * Power Level
Supercritical Dry: P = 7.033 * Power Level + 0.02756 * Dry Bulb T – 0.8767
Ultrasupercritical Wet = 1.42 + 6.63 * Power Level
Ultrasupercritical Dry = 7.2406 * Power Level + 0.02711 * Dry Bulb T – 0.8861

Power for the hot-salt pumps was taken from calculations performed by Babcock and Wilcox during the US Utility Study to supply salt to a U-tube, U-shell subcritical steam generator with a power rating of 260 MW_t [2]. Two pumps consumed 660 kW_e. Thus, for the 337 MW_t steam generators analyzed here it is assumed that hot pump parasitics are (337/260)*660 = 855 kW_e.

[27] However, since the steam generator/turbine is operating from storage, it runs at 100% power most of the time. Thus, part load characteristics have a second order effect on the results.

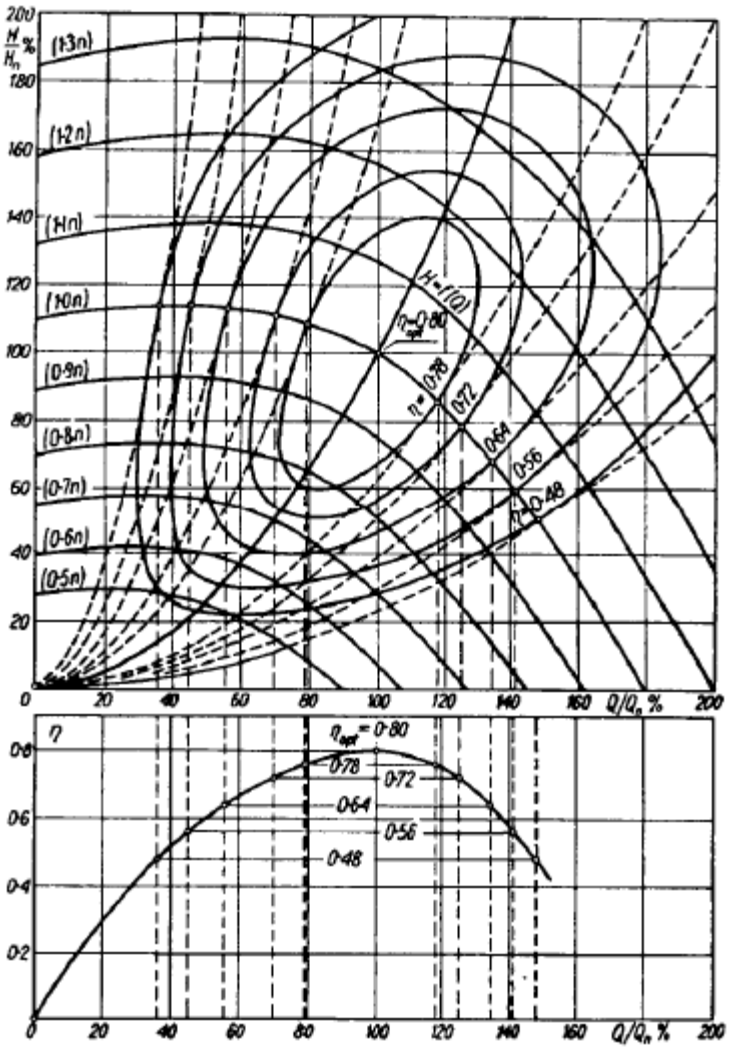

Figure 25. Complete characterization for a centrifugal pump, including iso-efficiency curves, in a two-dimensional system [56].

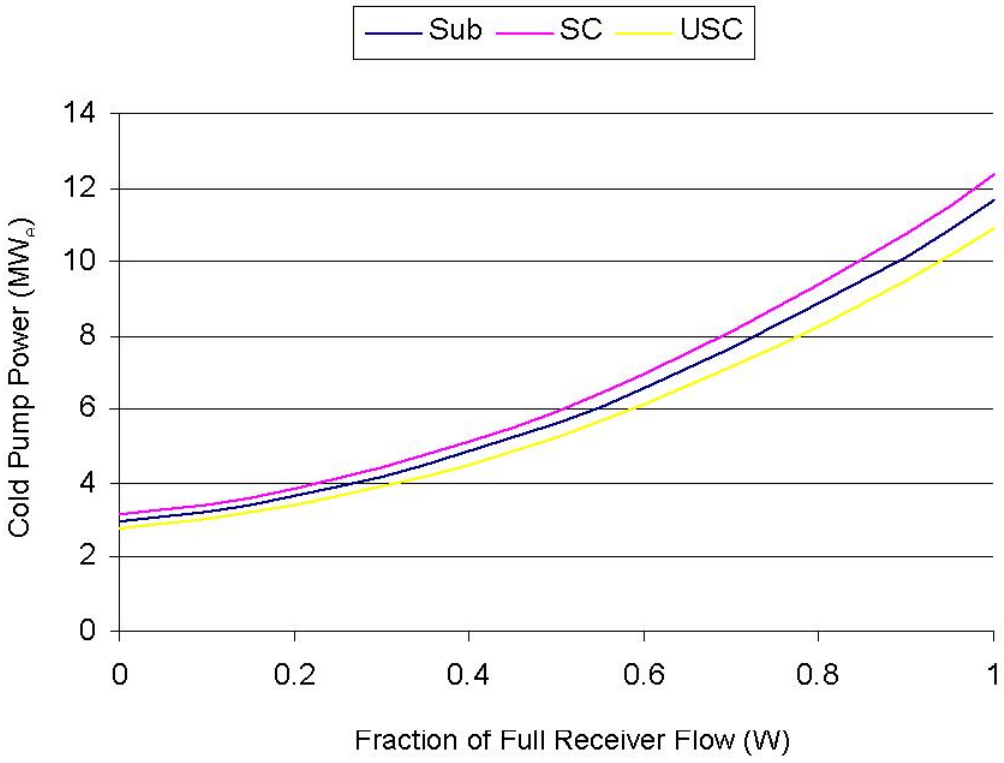

Figure 26. Parasitics for the cold-salt pump as a function of flow rate. Second-order curve-fit parameters [const,W,W^2] for SOLERGY are: Sub [2.9675, 2.058, 6.6], SC [3.153, 2.09, 7.08], USC [2.785, 1.848, 6.24].

The baseline parasitics for the plants are presented in Table 15. These parasitics are assumed to occur during every hour of the year. The values were taken from Appendix B of the PG&E Utility Study [2] with a few modifications: (1) transformer losses and storage foundation cooling were added because of an apparent omission in the Utility Study and (2) plant lighting and HVAC were set to values that are consistent with the Solar One experience [12].

Table 15. Baseline Parasitics (MW_e)

Load	Sub	SC	USC
Turbine-Gen auxiliaries Lube oil pump Lube oil vapor extractor	 36 3	Same	
Collector system	8		
Aux service water system	1		
Storage foundation cooling	28		
Secondary cooling water pump	1		
Water treatment	56		
Plant control system	30		
Fire water jockey pump	3		
Air compressor	10		
Steam generator heaters	24		
Small nitrate salt pipe trace heaters	183		
Plant lighting	50		
HVAC	100		
Unidentified and overnight plant maintenance	100		
Transformer losses	54		
Total Baseline Parasitics	**687**	**687**	**687**

3.3 SOLERGY Analysis Results

Figures 27 through 32 compare the annual energy flows calculated by SOLERGY for the six case studies. The left side of each diagram shows the calculated efficiencies for each of several categories. On the right side are the absolute values of the energy losses associated with each category. It can be noted that these calculations assumed 100% plant availability. Plant availability is calculated in Chapter 4.

The category "REDIRECTED ENERGY" includes losses represented within the field-efficiency matrices (Tables 8 through 10 includes heliostat cosine, shading, blocking, reflectance, receiver interception, atmospheric transmission, and receiver absorptance), as well as heliostat unavailability and times in the weather file when field operation limits are exceeded (in this case, when high winds cause the shutdown of the heliostat field). Comparing the six case studies reveals that field efficiency is slightly worse for the supercritical plants; since receiver thermal losses are higher for the supercritical plants, additional heliostats were added by DELSOL to the southern portion of the field to compensate for this additional thermal loss and heliostats in the south field have the lowest cosine efficiency.

The category "RCVR INCIDENT ENERGY" represents losses caused by defocussing of a portion of the heliostat field when the storage system is full. The efficiency of this category is nearly the same for all six case studies.

The category "RECEIVER ABSORBED ENERGY" includes losses in the receiver incurred during startup and steady-state operation. The annual efficiencies for the receivers within the subcritical, supercritical, and ultrasupercritical plants are calculated to be 85.8%, 84.3%, and 83.3%, respectively. The subcritical receiver has the highest efficiency because it operates at the lowest temperature and incurs the lowest thermal losses.

The category "ENERGY TO STORAGE" represents losses in the piping between the receiver and the storage system (i.e., the riser and downcomer). These losses are insignificant.

The category "ENERGY TO TURBINE" includes the thermal losses from the hot and cold storage tanks as well as operation of the steam generator. The efficiency of this category is nearly the same for all six case studies.

```
 PLANT SUMMARY - DAYS 1 TO 365 YEAR 1985

EFFICIENCY        (MWHRS)           ENERGY LOSSES
        I------------------------I   (MWHRS)
        I     TOTAL INSOLATION    I
        I       5146424.00        I
        I------------------------I
                     V
        I------------------------I OUTAGE LOSSES
  1.000 I     AVAILABLE ENERGY    I        .00 (YEOUTAGE)
        I       5146424.00        I
        I------------------------I
                     V
        I------------------------I FIELD LOSSES
   .990 I    REDIRECTED ENERGY    I   51464.19 HELIOSTAT UNAVAILABILITY LOSS
   .525 I       2674830.00        I 2420130.00 REFLECTANCE, COSINE,SHADOWING, BLOCKING,
        I------------------------I           SPILLAGE,TRANSMISION (OPERATION LIMITS=2051.30)
                     V
        I------------------------I STORAGE FULL
   .951 I  RCVR INCIDENT ENERGY   I  131497.60 DEFOCUS HELIOSTATS (YSUPTR)
        I       2543332.00        I
        I------------------------I
                     V
        I------------------------I RECEIVER LOSSES
        I        RECEIVER         I   59211.55 RCVR MIN FLOW (YPLRMF)
        I     ABSORBED ENERGY     I   12025.50 SURPLUS ENERGY TO  RCVR DEFOCUS HELIOSTATS (YSPTR)
   .858 I                         I        .00 ABSORPTANCE (INCLUDED IN FIELD)
        I       2181052.00        I  177140.40 THERMAL LOSS (RADIATION AND CONVECTION)
        I------------------------I  113902.80 RCVR STARTUP (YRSTRT)
                     V
        I------------------------I PIPING LOSSES
  1.000 I    ENERGY TO STORAGE    I     910.25
        I       2180141.00        I
        I------------------------I
                     V
        I------------------------I STORAGE LOSSES
        I                        I
        I        ENERGY TO       I
   .993 I         TURBINE*       I    8760.00 TANK LOSS (YTNKLOS)
        I       2164816.00       I        .00 STEAM GENERATOR STARTUP (INCLUDED IN TURBINE SYNC)
        I------------------------I    6586.75 LOSS FROM STEAM GEN (YTPLDD)
                     V               *  -21.75 MWHRS IN STORAGE AT END OF DAY 365
                     V
        I------------------------I EPGS LOSSES
   .431 I      GROSS ENERGY       I   15778.12 TURBINE SYNC LOSS (YTSTRT)
        I        933282.20        I 1215754.00 RANKINE LOSS (APPROX)
        I------------------------I
                     V
        I------------------------I AUXILIARY ENERGY
        I       NET ENERGY       I
   .922 I         OUTPUT          I   31516.38 TURBINE PLANT      (YTPPAR)
        I                        I   34949.82 SOLAR PLANT        (YSPPAR)
        I        860797.70 MWHe  I    6018.10 BASELINE           (YPMPAR)
        I------------------------I
   .167                           (  72484.34 TOTAL AUX ENERGY (YPARN))

   .167 OVERALL PLANT EFFICIENCY (TOTAL NET ELECTRICITY/ TOTAL DNI ON FIELD)
```

Figure 27. Annual energy flows within the subcritical plant with wet cooling as predicted by SOLERGY.

```
 EFFICIENCY        (MWHRS)           ENERGY LOSSES
      I-------------------------I   (MWHRS)
      I     TOTAL INSOLATION    I
      I       5146423.50        I
      I-------------------------I
                  V
      I-------------------------I OUTAGE LOSSES
1.000 I     AVAILABLE ENERGY    I       0.00 (YEOUTAGE)
      I       5146423.50        I
      I-------------------------I
                  V
      I-------------------------I FIELD LOSSES
0.990 I    REDIRECTED ENERGY    I   51464.19 HELIOSTAT UNAVAILABILITY LOSS
0.525 I       2674829.50        I 2420129.75 REFLECTANCE, COSINE, SHADOWING, BLOCKING,
      I-------------------------I              SPILLAGE, TRANSMISION (OPERATION LIMITS=2051.30)
                  V
      I-------------------------I STORAGE FULL
0.951 I  RCVR INCIDENT ENERGY   I  131497.92 DEFOCUS HELIOSTATS (YSUPTR)
      I       2543331.50        I
      I-------------------------I
                  V
      I-------------------------I RECEIVER LOSSES
      I        RECEIVER         I   58937.30 RCVR MIN FLOW (YPLRMF)
      I     ABSORBED ENERGY     I   12025.51 SURPLUS ENERGY TO  RCVR DEFOCUS HELIOSTATS (YSPTR)
0.858 I                         I       0.00 ABSORPTANCE(INCLUDED IN FIELD)
      I       2181221.00        I  177185.28 THERMAL LOSS (RADIATION AND CONVECTION)
      I-------------------------I  113962.23 RCVR STARTUP (YRSTRT)
                  V
      I-------------------------I PIPING LOSSES
1.000 I    ENERGY TO STORAGE    I     910.50
      I       2180310.50        I
      I-------------------------I
                  V
      I-------------------------I STORAGE LOSSES
      I                         I
      I        ENERGY TO        I
0.993 I         TURBINE*        I    8760.00 TANK LOSS (YTNKLOS)
      I       2164984.25        I       0.00 STEAM GENERATOR STARTUP (INCLUDED IN TURBINE SYNC)
      I-------------------------I    6587.25 LOSS FROM STEAM GEN (YTPLDD)
                  V               *  -21.75 MWHRS IN STORAGE AT END OF DAY 365
                  V
      I-------------------------I EPGS LOSSES
0.415 I      GROSS ENERGY       I   15778.12 TURBINE SYNC LOSS (YTSTRT)
      I        897816.31        I 1251389.75 RANKINE LOSS (APPROX)
      I-------------------------I
                  V
      I-------------------------I AUXILIARY ENERGY
      I       NET ENERGY        I
0.915 I         OUTPUT          I   34894.80 TURBINE PLANT (YTPPAR)
      I                         I   34955.34 SOLAR PLANT (YSPPAR)
      I        821948.31 MWHe   I    6018.10 BASELINE  (YPMPAR)
      I-------------------------I
0.160                          (  75868.24 TOTAL AUX ENERGY (YPARN))

0.160 OVERALL PLANT EFFICIENCY (TOTAL NET ELECTRICITY/TOTAL DNI ON FIELD)
```

Figure 28. Annual energy flows within the subcritical plant with dry cooling as predicted by SOLERGY.

```
 EFFICIENCY        (MWHRS)           ENERGY LOSSES
      I------------------------I   (MWHRS)
      I     TOTAL INSOLATION    I
      I       5215156.00        I
      I------------------------I
                  V
      I------------------------I OUTAGE LOSSES
1.000 I     AVAILABLE ENERGY    I        .00 (YEOUTAGE)
      I       5215156.00        I
      I------------------------I
                  V
      I------------------------I FIELD LOSSES
 .990 I    REDIRECTED ENERGY    I   52151.50 HELIOSTAT UNAVAILABILITY LOSS
 .524 I       2703542.00        I 2459462.00 REFLECTANCE, COSINE, SHADOWING, BLOCKING,
      I------------------------I              SPILLAGE, TRANSMISION (OPERATION LIMITS=2072.19)
                  V
      I------------------------I STORAGE FULL
 .953 I  RCVR INCIDENT ENERGY   I  127872.90 DEFOCUS HELIOSTATS (YSUPTR)
      I       2575669.00        I
      I------------------------I
                  V
      I------------------------I RECEIVER LOSSES
      I        RECEIVER         I   63955.45 RCVR MIN FLOW      (YPLRMF)
      I     ABSORBED ENERGY     I   12318.18 SURPLUS ENERGY TO  RCVR DEFOCUS HELIOSTATS (YSPTR)
 .843 I                         I        .00 ABSORPTANCE(INCLUDED IN FIELD)
      I       2172497.00        I  211255.30 THERMAL LOSS        (RADIATION AND CONVECTION)
      I------------------------I  115642.70 RCVR STARTUP       (YRSTRT)
                  V
      I------------------------I PIPING LOSSES
1.000 I    ENERGY TO STORAGE    I     905.50
      I       2171592.00        I
      I------------------------I
                  V
      I------------------------I STORAGE LOSSES
      I                        I
      I        ENERGY TO       I
 .993 I         TURBINE*       I    9198.04 TANK LOSS          (YTNKLOS)
      I       2155858.00        I       .00 STEAM GENERATOR STARTUP (INCLUDED IN TURBINE SYNC)
      I------------------------I    6559.00 LOSS FROM STEAM    GEN (YTPLDD)
                  V               *  -23.10 MWHRS IN STORAGE AT END OF DAY 365
                  V
      I------------------------I EPGS LOSSES
 .484 I      GROSS ENERGY       I   15778.12 TURBINE SYNC LOSS (YTSTRT)
      I       1044489.00        I 1095590.00 RANKINE LOSS        (APPROX)
      I------------------------I
                  V
      I------------------------I AUXILIARY ENERGY
      I       NET ENERGY       I
 .905 I         OUTPUT          I   56270.31 TURBINE PLANT      (YTPPAR)
      I                        I   36588.38 SOLAR PLANT        (YSPPAR)
      I        945611.70 MWHe  I    6018.10 BASELINE           (YPMPAR)
      I------------------------I
 .181                          (  98876.80 TOTAL AUX ENERGY (YPARN))

 .181 OVERALL PLANT EFFICIENCY (TOTAL NET ELECTRICITY/ TOTAL DNI ON FIELD)
```

Figure 29. Annual energy flows within the supercritical plant with wet cooling as predicted by SOLERGY.

```
 EFFICIENCY        (MWHRS)           ENERGY LOSSES
      I-------------------------I   (MWHRS)
      I     TOTAL INSOLATION    I
      I       5215155.50        I
      I-------------------------I
                  V
      I-------------------------I OUTAGE LOSSES
1.000 I     AVAILABLE ENERGY    I       0.00 (YEOUTAGE)
      I       5215155.50        I
      I-------------------------I
                  V
      I-------------------------I FIELD LOSSES
0.990 I    REDIRECTED ENERGY    I   52151.50 HELIOSTAT UNAVAILABILITY LOSS
0.524 I       2703541.75        I 2459462.25 REFLECTANCE, COSINE, SHADOWING, BLOCKING,
      I-------------------------I              SPILLAGE, TRANSMISION (OPERATION LIMITS=2072.19)
                  V
      I-------------------------I STORAGE FULL
0.953 I  RCVR INCIDENT ENERGY   I  127867.69 DEFOCUS HELIOSTATS (YSUPTR)
      I       2575674.00        I
      I-------------------------I
                  V
      I-------------------------I RECEIVER LOSSES
      I        RECEIVER         I   63677.57 RCVR MIN FLOW (YPLRMF)
      I     ABSORBED ENERGY     I   12318.18 SURPLUS ENERGY TO  RCVR DEFOCUS HELIOSTATS (YSPTR)
0.844 I                         I       0.00 ABSORPTANCE(INCLUDED IN FIELD)
      I       2172666.50        I  211309.64 THERMAL LOSS (RADIATION AND CONVECTION)
      I-------------------------I  115702.11 RCVR STARTUP (YRSTRT)
                  V
      I-------------------------I PIPING LOSSES
1.000 I    ENERGY TO STORAGE    I     905.75
      I       2171760.75        I
      I-------------------------I
                  V
      I-------------------------I STORAGE LOSSES
      I                         I
      I        ENERGY TO        I
0.993 I         TURBINE*        I    9198.04 TANK LOSS (YTNKLOS)
      I       2156026.50        I       0.00 STEAM GENERATOR STARTUP (INCLUDED IN TURBINE SYNC)
      I-------------------------I    6559.50 LOSS FROM STEAM GEN (YTPLDD)
                  V               *  -23.10 MWHRS IN STORAGE AT END OF DAY 365
                  V
      I-------------------------I EPGS LOSSES
0.471 I      GROSS ENERGY       I   15778.12 TURBINE SYNC LOSS (YTSTRT)
      I       1015313.37        I 1124934.50 RANKINE LOSS (APPROX)
      I-------------------------I
                  V
      I-------------------------I AUXILIARY ENERGY
      I       NET ENERGY        I
0.900 I         OUTPUT          I   58762.46 TURBINE PLANT (YTPPAR)
      I                         I   36594.18 SOLAR PLANT (YSPPAR)
      I        913938.81 MWHe   I    6018.10 BASELINE  (YPMPAR)
      I-------------------------I
0.175                          ( 101374.78 TOTAL AUX ENERGY (YPARN))

0.175 OVERALL PLANT EFFICIENCY (TOTAL NET ELECTRICITY/TOTAL DNI ON FIELD)
```

Figure 30. Annual energy flows within the supercritical plant with dry cooling as predicted by SOLERGY.

```
EFFICIENCY        (MWHRS)           ENERGY LOSSES
        I------------------------I   (MWHRS)
        I     TOTAL INSOLATION    I
        I       5273817.00        I
        I------------------------I
                     V
        I------------------------I OUTAGE LOSSES
  1.000 I     AVAILABLE ENERGY    I        .00 (YEOUTAGE)
        I       5273817.00        I
        I------------------------I
                     V
        I------------------------I FIELD LOSSES
    .990 I    REDIRECTED ENERGY    I   52738.12 HELIOSTAT UNAVAILABILITY LOSS
    .523 I       2728992.00        I 2492087.00 REFLECTANCE, COSINE, SHADOWING, BLOCKING,
        I------------------------I              SPILLAGE,TRANSMISION (OPERATION LIMITS=2089.33)
                     V
        I------------------------I STORAGE FULL
    .953 I  RCVR INCIDENT ENERGY   I  127897.40 DEFOCUS HELIOSTATS (YSUPTR)
        I       2601095.00        I
        I------------------------I
                     V
        I------------------------I RECEIVER LOSSES
        I        RECEIVER         I   66978.60 RCVR MIN FLOW      (YPLRMF)
        I     ABSORBED ENERGY     I   12878.65 SURPLUS ENERGY TO  RCVR DEFOCUS HELIOSTATS (YSPTR)
    .833 I                        I        .00 ABSORPTANCE(INCLUDED IN FIELD)
        I       2167631.00        I  236794.50 THERMAL LOSS        (RADIATION AND CONVECTION)
        I------------------------I  116812.00 RCVR STARTUP       (YRSTRT)
                     V
        I------------------------I PIPING LOSSES
  1.000 I    ENERGY TO STORAGE    I     902.50
        I       2166729.00        I
        I------------------------I
                     V
        I------------------------I STORAGE LOSSES
        I                        I
        I        ENERGY TO       I
    .993 I         TURBINE*       I    9198.04 TANK LOSS          (YTNKLOS)
        I       2150999.00        I        .00 STEAM GENERATOR STARTUP (INCLUDED IN TURBINE SYNC)
        I------------------------I    6544.75 LOSS FROM STEAM    GEN (YTPLDD)
                     V               *  -12.52 MWHRS IN STORAGE AT END OF DAY 365
                     V
        I------------------------I EPGS LOSSES
    .496 I      GROSS ENERGY       I   15867.46 TURBINE SYNC LOSS (YTSTRT)
        I       1067413.00        I 1067718.00 RANKINE LOSS        (APPROX)
        I------------------------I
                     V
        I------------------------I AUXILIARY ENERGY
        I       NET ENERGY        I
    .910 I         OUTPUT         I   57373.47 TURBINE PLANT      (YTPPAR)
        I                         I   32798.57 SOLAR PLANT        (YSPPAR)
        I        971222.60 MWHe   I    6018.10 BASELINE           (YPMPAR)
        I------------------------I
    .184                          (   96190.09 TOTAL AUX ENERGY (YPARN))

.184 OVERALL PLANT EFFICIENCY (TOTAL NET ELECTRICITY/ TOTAL DNI ON FIELD)
```

Figure 31. Annual energy flows within the ultrasupercritical plant with wet cooling as predicted by SOLERGY.

```
EFFICIENCY        (MWHRS)           ENERGY LOSSES
        I------------------------I   (MWHRS)
        I     TOTAL INSOLATION    I
        I       5273817.00        I
        I------------------------I
                     V
        I------------------------I OUTAGE LOSSES
  1.000 I     AVAILABLE ENERGY    I       0.00 (YEOUTAGE)
        I       5273817.00        I
        I------------------------I
                     V
        I------------------------I FIELD LOSSES
  0.990 I    REDIRECTED ENERGY    I   52738.12 HELIOSTAT UNAVAILABILITY LOSS
  0.523 I       2728992.25        I 2492086.75 REFLECTANCE, COSINE, SHADOWING, BLOCKING,
        I------------------------I              SPILLAGE, TRANSMISION (OPERATION LIMITS=2089.33)
                     V
        I------------------------I STORAGE FULL
  0.953 I  RCVR INCIDENT ENERGY   I  127889.23 DEFOCUS HELIOSTATS (YSUPTR)
        I       2601103.00        I
        I------------------------I
                     V
        I------------------------I RECEIVER LOSSES
        I        RECEIVER         I   66696.56 RCVR MIN FLOW (YPLRMF)
        I     ABSORBED ENERGY     I   12878.65 SURPLUS ENERGY TO  RCVR DEFOCUS HELIOSTATS (YSPTR)
  0.833 I                         I       0.00 ABSORPTANCE(INCLUDED IN FIELD)
        I       2167800.25        I  236855.81 THERMAL LOSS (RADIATION AND CONVECTION)
        I------------------------I  116871.68 RCVR STARTUP (YRSTRT)
                     V
        I------------------------I PIPING LOSSES
  1.000 I    ENERGY TO STORAGE    I     902.25
        I       2166898.00        I
        I------------------------I
                     V
        I------------------------I STORAGE LOSSES
        I                        I
        I        ENERGY TO       I
  0.993 I         TURBINE*        I    9198.04 TANK LOSS (YTNKLOS)
        I       2151167.25        I       0.00 STEAM GENERATOR STARTUP (INCLUDED IN TURBINE SYNC)
        I------------------------I    6545.25 LOSS FROM STEAM GEN (YTPLDD)
                     V               *  -12.52 MWHRS IN STORAGE AT END OF DAY 365
                     V
        I------------------------I EPGS LOSSES
  0.484 I      GROSS ENERGY       I   15867.46 TURBINE SYNC LOSS (YTSTRT)
        I       1041057.44        I 1094241.62 RANKINE LOSS (APPROX)
        I------------------------I
                     V
        I------------------------I AUXILIARY ENERGY
        I       NET ENERGY        I
  0.906 I         OUTPUT          I   59522.58 TURBINE PLANT (YTPPAR)
        I                         I   32803.83 SOLAR PLANT (YSPPAR)
        I        942713.12 MWHe   I    6018.10 BASELINE  (YPMPAR)
        I------------------------I
  0.179                          (  98344.48 TOTAL AUX ENERGY (YPARN))

  0.179 OVERALL PLANT EFFICIENCY (TOTAL NET ELECTRICITY/TOTAL DNI ON FIELD)
```

Figure 32. Annual energy flows within the ultrasupercritical plant with dry cooling as predicted by SOLERGY.

The category "GROSS ENERGY" includes losses incurred during startup of the steam generator and turbine and during the Rankine-cycle conversion of thermal energy to electric energy. The annual efficiencies for the wet-cooled subcritical, supercritical, and ultrasupercritical cases are calculated to be 43.1%, 48.4%, and 49.6%, respectively. The annual efficiencies for the dry-cooled subcritical, supercritical, and ultrasupercritical cases are calculated to be 41.5%, 47.1%, and 48.4%, respectively. The results portray the expected behavior that high-temperature cycles have the highest efficiency and that wet-cooled cycles are more efficient than dry-cooled ones.[28] However, it is interesting to note that the annual efficiency of the wet-cooled supercritical case (using 600 ^{o}C salt and 591 ^{o}C steam) is the same as the dry-cooled ultrasupercritical case (using 650 ^{o}C salt and 630 ^{o}C steam).

The category "NET ENERGY OUTPUT" includes parasitic electrical losses throughout power-production periods and during shutdown. Comparing the case studies indicates that dry-cooled plants have more parasitic losses than wet-cooled plants. Even though dry-cooled plants do not need operation of a circulating-water pump (like wet plants do), the increased cooling-tower fan parasitics throughout the year in the dry plant more than compensates for the savings. In addition, comparing the parasitic consumption between subcritical and supercritical plants indicates that subcritical plants have a higher parasitic efficiency; the feedwater pump parasitics are significantly lower in the subcritical plant because of the lower operating pressure.

The annual efficiencies for all the case studies are compared in Table 16. An interesting insight from this comparison is that ~80% of the efficiency improvement identified in this study is achieved by just raising salt temperature from 565 ^{o}C to 600 ^{o}C. Thus, before raising salt temperature to 650 ^{o}C, a detailed evaluation of the additional problems/costs associated with raising the temperature should be performed to determine if it is worth pursuing the remaining 20%.

Table 16. Comparison of Annual Efficiencies for the Six Case Studies.

	Sub-Wet	Sub-Dry	SC-Wet	SC-Dry	USC-Wet	USC-Dry
Redirected Energy	0.520	0.520	0.519	0.519	0.518	0.518
RCVR Incident Energy	0.951	0.951	0.953	0.953	0.953	0.953
Receiver Absorbed Energy	0.858	0.858	0.843	0.844	0.833	0.833
Energy to Storage	1.00	1.00	1.00	1.00	1.00	1.00
Energy to Turbine	0.993	0.993	0.993	0.993	0.993	0.993
Gross Energy Conversion	0.431	0.415	0.484	0.471	0.496	0.484
Net Energy Conversion	0.922	0.915	0.905	0.900	0.910	0.906
Total Annual Efficiency	0.167	0.160	0.181	0.175	0.184	0.179

[28] Carnot efficiency is $(T_H-T_L)/T_H$. Thus, efficiency will increase for a given T_L if T_H increases. Also, efficiency will increase for a given T_H if T_L decreases. The latter occurs with wet cooling.

Chapter 4
Reliability Analysis

Equipment malfunctions will cause a solar power tower to be unavailable for power production during a certain fraction of the calendar year. In this chapter the reliability of the subcritical salt plant design is analyzed in order to estimate this unavailability fraction. Reasons for unavailability are also identified and discussed.

4.1 Overview of Pro-Opta Reliability Analysis Software

SNL's Pro-Opta software [17] was used to predict plant unavailability. As shown in Figure 33, this software has many capabilities that allow a detailed evaluation of the reliability of existing power plants as well as the optimization of proposed future plant designs. The package is currently being used to evaluate and improve the reliability of wind-turbine power plants [57]. The analysis presented in this chapter is the first time the software has been used to evaluate a solar power tower.

To run the software, the analyst must provide a logic model and reliability data for the power plant components and/or subsystems. The logic model (called a "fault tree" or "reliability block diagram") relates the series-parallel arrangement of the plant components. For example, the diagram in Figure 34 shows a series relationship between subsystems; if any of these subsystems fail, the plant becomes unavailable for power production. Two pieces of reliability data are input for each plant component: (1) the mean time between failures (MTBF), and (2) the mean downtime (MDT). Given this information, component availability (i.e. 1-unavailability) is calculated from the following equation:

$$A = MTBF/(MTBF + MDT). \quad (14)$$

The numerator of this equation represents the hours the component is available for service, and the denominator represents total clock hours. The component availabilities for the individual components are combined via the logic model to calculate the availability for the total power plant. In addition to plant availability, the code provides other figures of merit regarding the plant. Some of these additional measures are discussed later in this chapter.

4.2 Validation of Pro-Opta with Solar One Data

In order to gain confidence that the software could predict the availability of a solar power plant, a Pro-Opta model of the Solar One Pilot Plant was created to see if it could predict the actual value recorded at the plant from 1984 through 1987. The reliability of the Solar One plant was studied in depth [58] and MTBF and MDT parameters were generated for the plant components. The parameters for the components reported in Reference 58 were combined with the following equations to develop subsystem level MTBFs and MDTs:

$$MTBF_{sys} = (1/\Sigma_i(1/MTBF_i)), \quad (15)$$

$$MDT_{sys} = (\Sigma_i(MDT_i/MTBF_i))/(\Sigma_i(1/MTBF_i). \quad (16)$$

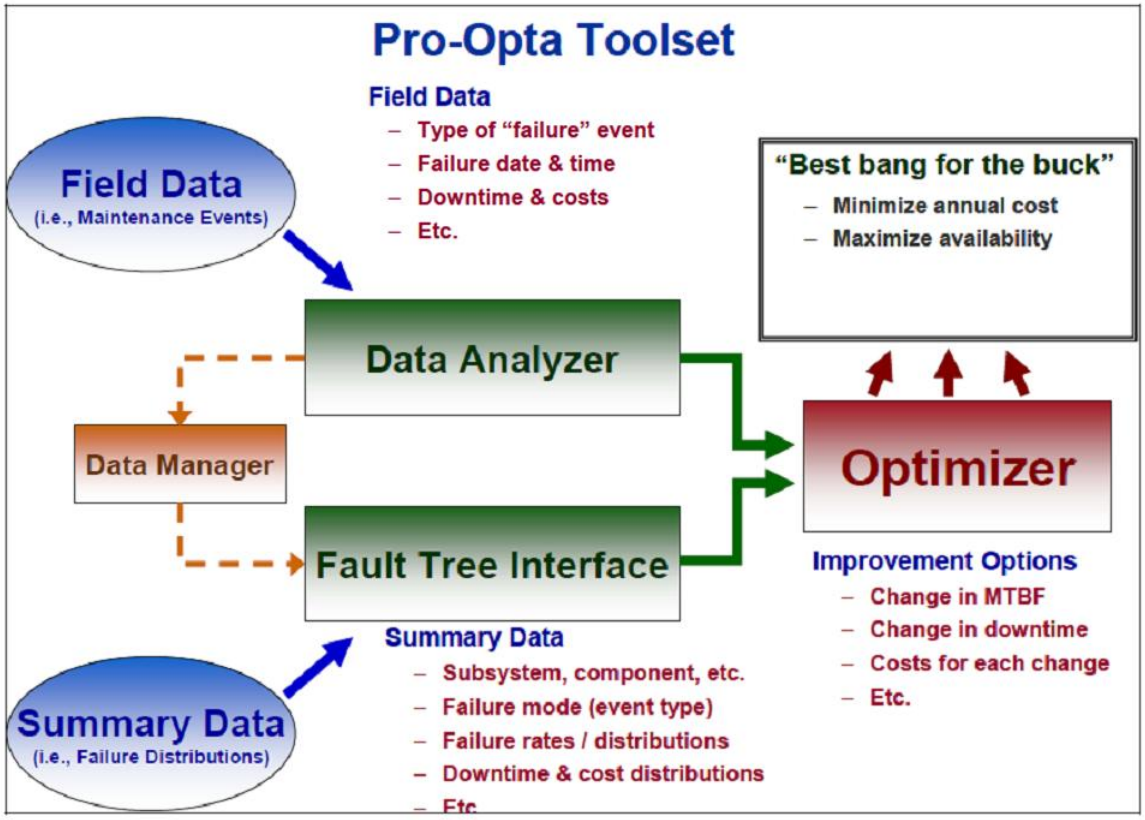

Figure 33. Pro-Opta tool set.

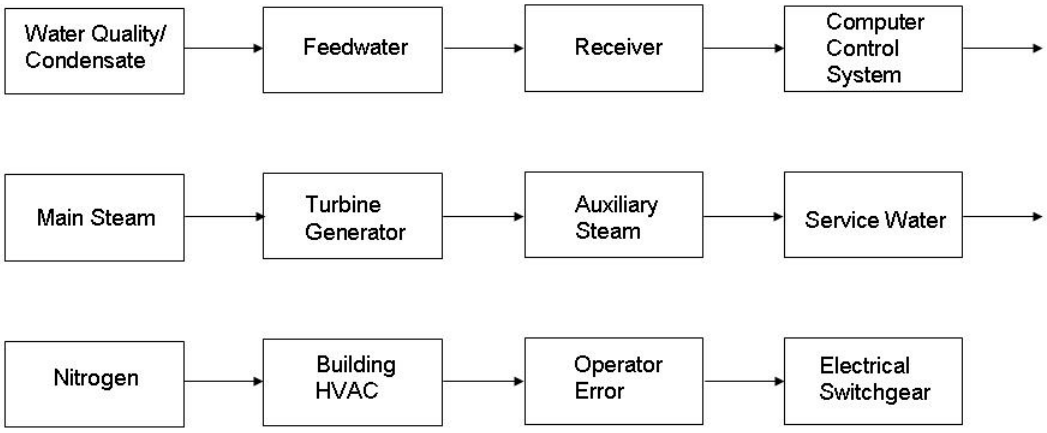

Figure 34. Reliability block diagram for the Solar One Pilot Plant (system boundaries are defined in Reference 58).

These equations are appropriate for combining components exhibiting a series logic relationship. They can be used because there was little component redundancy within the Solar One subsystems. The reliability parameters for the subsystems that were derived with these equations are presented in Table 17, and the series relationship among the subsystems is depicted in Figure 34.

Using the data in Table 17, Pro-Opta predicts the availability due to forced outages to be 87.7%. Combining this with the fact that Solar One was down for scheduled outages an average of three weeks per year, a plant availability of 82.6% during the three-year power production phase is predicted (i.e., 0.877*49/52). The actual availability recorded at Solar One during this interval due to forced outages and scheduled outages was 82% [51].

Table 17. Forced-Outage Reliability Data for Solar One [58].

System	MTBF (hrs)	MDT (DNI hrs)
Receiver	57.0	4.8
Main Steam	1150.0	2.6
Turbine/Generator	490.0	1.3
Aux Steam	5770.0	2.0
Feedwater	825.0	1.6
Condensate	2887.0	1.6
Water Quality	2887.0	1.9
Service Water	5774.0	15.7
Nitrogen	5774.0	1.0
HVAC	5774.0	5.8
Switchgear	1154.0	14.8
Master Control	100.0	2.9
Operator Error	2887.0	1.2
Grid	2887.0	3.8

4.3 Reliability Analysis of a Molten-Salt Power Tower

4.3.1 Logic Model Development

The reliability model for the molten-salt power tower is loosely based on the configuration at Solar Two. Equipment redundancy was virtually nonexistent at Solar Two. There were two parallel cold salt pumps and two parallel hot salt pumps, but each pump provided 50% flow. There were also two parallel receiver flow control valves within each receiver flow loop, but experience at the plant indicated that failure of one of these was not automatically backed up by operation of the other. A Design Basis Document [11] was published after Solar Two that recommended a configuration for a commercial-scale plant. Rather than the two 50% cold pumps and two 50% hot pumps used at Solar Two, a single 100% hot pump and a single 100%

cold pump are suggested. Furthermore, rather than using Solar-Two-type pumps that draw salt from separate sumps located below the hot and cold salt storage tanks, the document promotes elimination of the sumps and the use of long-shafted hot and cold pumps that are installed directly within the storage tanks. It is important to note that the reliability model analyzed here is not based on the salt pump configuration recommended in the Design Basis Document for two reasons:

1. Use of sumps is retained because short-shafted pumps can be used and the operation of the salt pumps at Solar Two was flawless. There is no need to change a design configuration that worked so well.
2. Redundant 100% pumps rather than 50% pumps are also assumed to give the Solar Two approach more flexibility when repair of the salt pumps is required.

The reliability block diagram for the molten-salt plant is presented in Figure 35. It was prepared by modeling the equipment installed at Solar Two [59] and by examining the causes of forced outages during operation of the plant [60]. It can be noted that in some cases the blocks in the diagram represent individual components, while in others they represent entire subsystems. The reason for this apparent inconsistency is because reliability data are obtainable at different levels of detail. Below each block is a list of failures that will cause the block to be unavailable.

Each of the failure modes listed in Figure 35 is quantified in the next section. This is followed by a quantification of the entire reliability block diagram in Section 4.3.3.

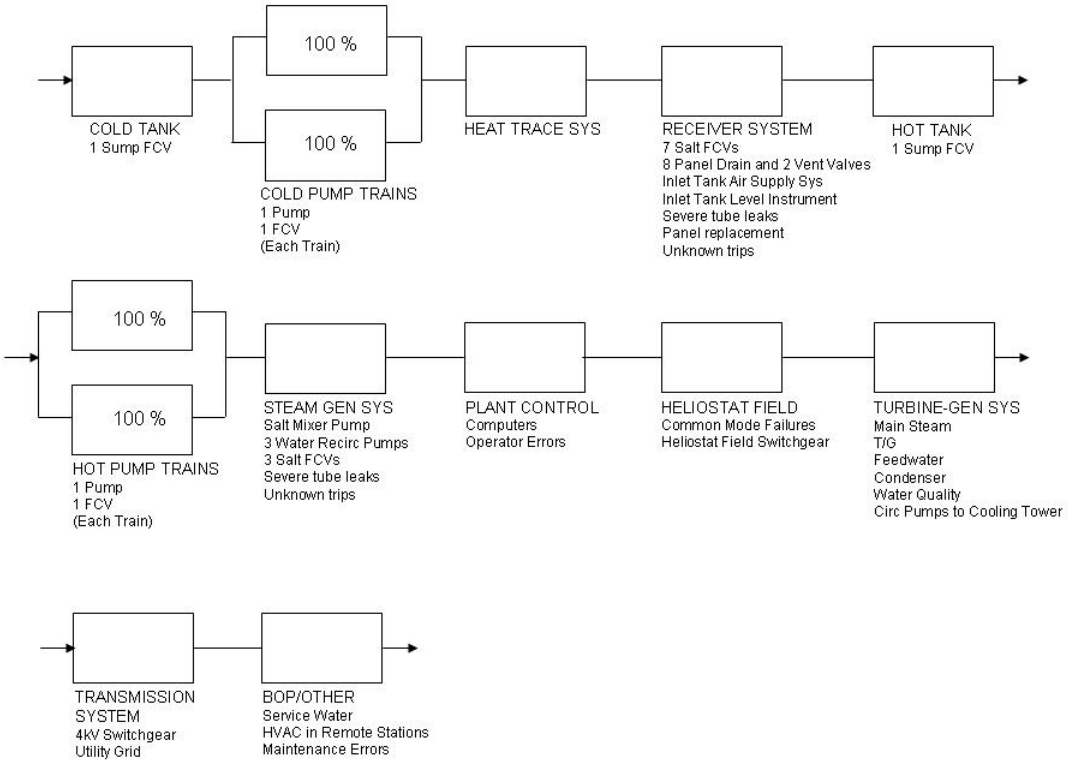

Figure 35. Reliability block diagram for a molten-salt central receiver power plant.

4.3.2 Reliability Data Base

The data sources used to estimate the MTBFs and MDTs needed to predict plant availability were (1) Solar Two daily logs [Reference 60, Appendix A], (2) Solar One [58], (3) Themis [61], and (4) power block data collected by EPRI [62]. Before presenting the data base, a few general remarks regarding these data sources are in order.

The Solar Two plant operated about 2000 hours during the three-year project and daily logs that describe the reliability experience exist for only 1470 hours. An abbreviated summary of the logs covering the period from January 1998 to April 1999 can be found in Appendix A. As described within documents published shortly after plant shutdown [13], Solar Two experienced several problems attributed to design flaws within the steam generator, heat-trace system, downcomer, and receiver that severely limited the total number of operating hours. Fixes for all these "infant-mortality-type" problems were identified [13, 24] but all were not fully implemented at the plant before it was shut down in April 1999. Consequently, many of the forced outages that appear in the logs are classified as "infant mortality" type failures and are removed from the reliability data base used in this analysis. The only failures that have been kept are those that are believed to be applicable to future molten-salt power towers. Another caveat on use of Solar Two data is the fact that the plant did not operate long enough to reach mature operation. Thus, the Solar Two MTBFs and MDTs are believed to be conservative relative to what could be accomplished after Operations and Maintenance (O&M) is optimized. For example, as stated previously, Solar One achieved an average availability of 82% during a three-year period. However, in its final year a 95% availability was achieved due to optimizations in O&M strategy [63] (e.g., the equivalent of much more nighttime maintenance was performed).

An infant mortality problem that plagued Solar Two throughout its entire life was freezing of salt within several tubes on the windward side of the receiver during startup. The problem and its solution are understood, but the fix (i.e., removal of tube clip and installation of heat trace at the receiver/oven interface) was not fully implemented before plant shutdown. This problem delayed startup on many days while the operators waited for the frozen salt to thaw. In addition, this problem was the cause of several severe tube leaks when a tube without salt flow was exposed to too much solar power. This infant mortality problem was not included in the data base, but it is unrealistic to assume that forced outages caused by tube leaks will never occur. For example, the Solar One steam receiver experienced several significant tube leaks that led to outages in its 10,000-hour operating life. A receiver that more closely resembles Solar Two was the Themis salt receiver that operated in France from 1983 through 1986. The tubes within the Themis had wall thicknesses that were similar to Solar Two's. This receiver operated more than 3000 hours and experienced no outages due to tube leaks [61]. Thus, the Themis experience was used to estimate the MTBF for tube leaks. Given a tube leak, the MDT from Solar One is used.

It is assumed in the analysis that, on average, there are ~2500 hours during the year in which the insolation is high enough to operate the receiver. This equates to ~7 hours per day. This is consistent with Solar One data and the SOLERGY calculations that were performed to define the annual-electricity production goal for Solar Two [13]. Therefore, an MTBF of 2500 hours within the solar collection systems (receiver and heliostat field) means the component will fail approximately once per calendar year. In addition, since the MDT is based on solar-outage

hours, a value of 7 hours means that it could have taken up to 24 clock hours for the plant technicians to return the component to service (i.e., additional repair done at night).

Since the plants analyzed in this report have near-base-load capacity factors of ~70%, it is not appropriate to use the steam power block reliability data from Solar One or Two, designed for a capacity factor of ~20%. EPRI has shown that fossil-fired power plants with high-capacity factors have a much longer MTBF than plants with low-capacity factors, attributed to less thermal cycling. Thus, reliability data for commercial steam plants with ~70% capacity factor were used in the analysis [61][29] and, for example, an MTBF for the steam generator and turbine system of 6130 hours (0.7*8760) means that these systems fail approximately once per calendar year.

The EPRI reliability data are based on the analysis of subcritical steam-Rankine cycles. Since this analysis of next-generation power towers is also investigating supercritical steam-Rankine cycles, an attempt was made to obtain reliability data for supercritical plants. SNL's technical librarian searched several data bases and could not find MTBF data for fossil-fired supercritical steam plants.[30]

Scheduled outages were deleted from the data bases and only data for unscheduled (or forced) outages are included. This was done because it is assumed the plant will be shut down for a total of one or two weeks per year to perform scheduled maintenance. This length of time is typical for commercial solar trough plants and appears to be more appropriate than the scheduled outage time at Solar One/Two. (Solar One and Two were first-of-a-kind plants and scheduled outages were conducted more often to check the status of the plant components.) Examples of scheduled maintenance activities include repainting of the receiver tubes and turbine overhaul.

The MTBFs and MDTs derived from the four data sources are presented in Table 18. The columns are explained below:

Component/subsystem – Each of these items can be found on the reliability block diagram shown in Figure 35.
# of events – The number of times the component/subsystem led to a forced outage of the power plants shown in the Reference column.
Fault Exposure Time (FET) (hrs) – The number of hours the component/subsystem was successfully operating at the power plant. If there were multiple similar components operating at the same time in the plant (e.g., pumps and valves), the value shown in the table is (FET)*(number of components).

[29] EPRI studied seven combined cycle plants. Only data for the bottoming steam cycles were used. Typical steam turbine size was ~100 MW_e.

[30] However, the availability/reliability of supercritical plants is expected to be high. According to Chandra Shekhar (http://www.scribd.com/doc/3019711/Comparative-study-on-Subcritical-and-Super-Critical-Power-Cycles)"units installed in Japan over the past 10 years have achieved availabilities in the range of 98% to almost 100% with the exclusion of planned outages." Also, according to Burns and McDonnell, "the availability of supercritical units built since 1990 is every bit as high as the subcritical units." (www.massengineers.com/Documents/article-therankinecycle-013.pdf).

Table 18. Reliability Data for Molten-Salt Plant Analysis.

Component or Subsystem	# of Events	Fault Exposure Time (hrs)	MTBF Nominal (hrs)	MDT Nominal (hrs)	Downtime Data (hrs)	Ref
Salt Flow Control Valves	3	19071	6357	8	1,8,15	Solar 2
Cold Salt Pumps	0	2934	Assume 2934	Assume 16	None	Solar 2
Hot Salt Pumps	0	2934	Assume 2934	Assume 16	None	Solar 2
Heat Trace System	2	1467	734	9	9(2)	Solar 2
Rcvr Panel Drain Valves	1	17604	17604	3	3	Solar 2
Rcvr Inlet Tank Air System	5	1467	293	4	1,4(3),7	Solar 2
Rcvr Inlet Tank Level Instrument	1	1467	1467	3	3	Solar 2
Rcvr Tube Leak	0	3000	Assume 3000	14	0.7,3,6,13(2) 16,22(4)	Solar 1 Themis
Rcvr Panel Replacement			Assume 15000	Assume 20	None	
Rcvr Trips – Unknown Cause	6	1467	241	1.3	0.5(3),1.5, 2,3	Solar 2
Steam Gen Pumps	1	4401	4401	4	4	Solar 2
Steam Gen Tube Leak			Assume 61320	Assume 235	None	
Steam Gen Trips – Unknown Cause	1	1467	1467	4	4	Solar 2
Plant Control Computers	8	1467	183	1.3	0.5,1(5),2, 2.5	Solar 2
Operator Error	2	1467	734	3	2,4	Solar 2
Heliostat Field Common Mode	2	1467	734	6.8	3.5,10	Solar 2
Heliostat Field Switchgear	1	5774	5774	7	7	Solar 1
Rankine Turbine	10	131470	13147	98	9.8(2),61(6), 300(2)	EPRI
Rankine Control System	11	131470	11952	5.8	4(2),6.4(2), 6(7)	EPRI
Rankine Circ Water Pumps	14	131470	9391	39	4,38(2), 43(11)	EPRI
Rankine Lube Oil System	2	131470	65736	125	125(2)	EPRI

Table 18. Reliability Data for Molten-Salt Plant Analysis (continued).

Component or Subsystem	# of Events	Fault Exposure Time (hrs)	MTBF Nominal (hrs)	MDT Nominal (hrs)	Downtime Data (hrs)	Ref
Rankine Electric Generator	16	131470	8217	17	19(10), 14(6)	EPRI
Rankine Condensate Pump	2	131470	65736	83	83(2)	EPRI
Rankine Condenser	6	131470	21912	12	1.2,4.8(4),50	EPRI
Service Water Sys	1	5774	5774	16	16	Solar 1
HVAC	3	1467	489	4.1	2,3.3,7	Solar 2
Maintenance Error	3	1467	489	6.2	2,6.5,10	Solar 2
Plant 4-kV Switchgear	1	5774	5774	0.4	0.4	Solar 1
Utility Grid	2	5774	2887	3.8	0.2,7.4	Solar 1

References – Solar Two [Appendix A], Solar One [58], Themis [61], EPRI [62].

MTBF Nominal (hrs) – The nominal value of MTBF is calculated as MTBF=FET/(# of events). If (# of events) is zero or assumed to be 1, a first-order MTBF based on engineering judgment is shown.
MDT Nominal (hrs) – The nominal value of MDT is calculated as (Sum of downtime data)/(# of events). If no downtime data exist, a first-order MDT based on engineering judgment is shown.
Downtime Data (hrs) – The downtime for each individual event is listed. The number of occurrences of the same downtime appears in parentheses. The downtimes listed are the number of hours solar energy collection was lost. For example, if the solar receiver failed one hour before sunset and it took 6 clock hours to repair the receiver, the downtime is 1 hour. However, because the steam-Rankine cycle is assumed to run 24/7 throughout much of the year, failures that occur after dark could cause the solar receiver to be shut down the next day due to a full hot tank.[31] Thus, steam-Rankine downtimes are conservatively assumed to be based on clock hours.

4.3.3 Plant Availability Prediction

Using the nominal MTBF and MDT values, Pro-Opta predicts a plant availability of 88.5% due to forced outages. Adding two weeks of scheduled outages would further reduce the overall annual availability to 85% = 88.5*(50/52).

Pro-Opta can also be run to estimate the uncertainty associated with the availability prediction. Probability distributions are assigned to each MTBF and MDT and a sampling scheme is employed to propagate uncertainties through the logic model (fault tree or reliability block diagram). For cases with little failure data (like Solar Two) in which data are expressed as "X failures in Y hours of operation," use of the gamma distribution is recommended by the guidance contained in the Pro-Opta User's Manual. The "X" is the gamma-shape parameter and the "Y"

[31] This occurred at Solar Two on a few occasions.

is the gamma-scale parameter. The mean of the gamma distribution is X/Y, which is convenient. However, the guidance warns the user that:

"...it is important to realize that we are not trying to fit a gamma distribution to our data or implying that a gamma distribution is necessarily a good representation of the variability we might expect in failure rates. We recommend the gamma distribution in this situation because it reproduces the mean of our observations and gives us a reasonable representation of uncertainty. The gamma distribution is also easy to update if additional data become available."

To estimate the variability in MDT, the guidance in the Pro-Opta User's Manual was followed:

- Given three or more downtime events, express the spread in downtimes as an empirical distribution. (For example, salt flow control valves [FCVs] in Table 18 have downtimes of 1, 8, and 15 hrs. A discrete-probability was created and each downtime was sampled with a 33.3% probability.)
- If just two downtimes are available, use a uniform distribution between high and low. (For example, see "Operator Errors" in Table 18).
- If a single downtime is all that is available, use the observed value as the best estimate in a triangular distribution and use judgment to add minimum and maximum values. (There are several cases like this in Table 18. The min/max values were assumed to be plus/minus a factor of 2.)

The result of the uncertainty analysis is shown in Figure 36. The mean plant availability due to forced outages is 88.3%, with a standard deviation of 1.8 points.

4.3.4 Plant Availability Improvement Opportunities

The 85% nominal availability prediction is below the 90% goal established for initial commercial plants [3]. To achieve the goal requires an understanding of the most important contributors to the plant unavailability and an engineering evaluation of the most practical improvements.

Pro-Opta was run to indentify the most important causes of plant unavailability. Table 19 displays the ranking according to system and Table 20 displays the ranking according to the basic failure event. As shown, the receiver system is expected to be the most important contributor to outages in a molten-salt plant. However, other systems and components are also predicted to be significant contributors.

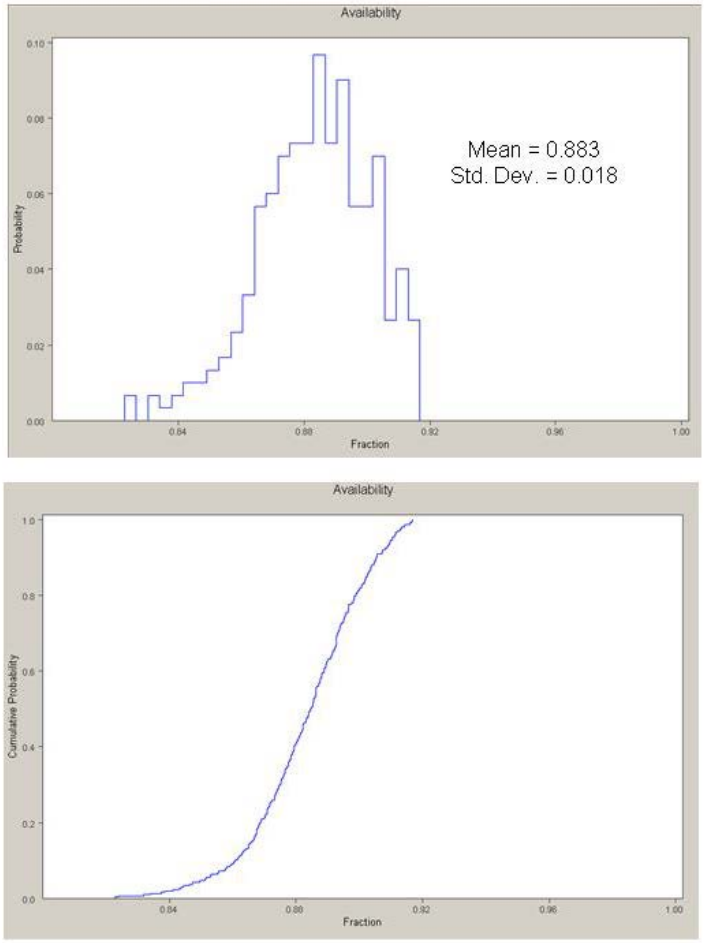

Figure 36. Results from Pro-Opta uncertainty analysis of forced-outage availability.

Table 19. Contributors to Forced Outages Ranked by Systems Defined in Figure 35.

	System	Mean Fraction
1	Receiver	0.3125
2	Turbine Gen	0.1442
3	BOP/Other	0.1339
4	Steam Gen	0.1111
5	Heat Trace	0.1041
6	Plant Control	0.0858
7	Heliostat Field	0.0782
8	Transmission	0.0106
9	Hot Tank	0.0100
10	Cold Tank	0.0096
11	Cold Pump Trains	<0.0005
12	Hot Pump Trains	<0.0005
		1.0000

Table 20. Contributors to Forced Outages Ranked by Basic Event.

	Events	Mean Fraction
1	Rcvr Inlet Tank Air System	0.12280
2	Heat Trace System	0.10407
3	Maintenance Error	0.09470
4	Heliostat Field Common Mode Failures	0.06711
5	Rankine Turbine	0.06091
6	Control System Computers	0.05437
7	Rcvr Trips from Unknown Causes	0.04651
8	Steam Gen Tube Leak	0.03439
9	Rcvr Tube Leak	0.03244
10	Operator Error	0.03142
11	Rankine Circ Water Pump	0.03060
12	Service Water System	0.02382
13	Steam Gen Trips from Unknown Causes	0.02355
14	Rcvr Inlet Tank Level xmitter	0.01785
15	Rankine Lube Oil System	0.01694
16	Remote Heating Ventilation and Cooling	0.01536
17	Rankine Electric Generator	0.01526
18	Rcvr Panel Replacement	0.01210
19	Rankine Condensate Pump	0.01152
20	Heliostat Interface Switchgear	0.01112
21	Hot Sump Flow Control Valve	0.00998
22	Utility Grid	0.00996
23	Rcvr Flow Control Valve 7	0.00995
24	Rcvr Flow Control Valve 1	0.00982
25	Rcvr Flow Control Valve 2	0.00981
26	Rcvr Flow Control Valve 6	0.00979
27	Rcvr Flow Control Valve 5	0.00976
28	Rcvr Flow Control Valve 3	0.00974
29	Steam Gen Salt Flow Control Valve 3	0.00969
30	Steam Gen Salt Flow Control Valve 2	0.00962
31	Steam Gen Salt Flow Control Valve 1	0.00962
32	Rcvr Flow Control Valve 4	0.00960
33	Cold Sump Flow Control Valve	0.00956
34	Steam Gen Water Mix Pump 2	0.00830
35	Steam Gen Water Mix Pump 3	0.00798
36	Steam Gen Water Mix Pump 1	0.00797
37	Rankine Condenser	0.00537
38	Rankine Control System	0.00366
39	Rcvr Panel Drain Valve 2	0.00160
40	Rcvr Panel Drain Valve 5	0.00157
41	Rcvr Panel Drain Valve 1	0.00155
42	Rcvr Panel Drain Valve 6	0.00155
43	Rcvr Panel Drain Valve 3	0.00153
44	Rcvr Panel Drain Valve 7	0.00153
45	Rcvr Panel Drain Valve 4	0.00152
46	Rcvr Panel Drain Valve 8	0.00150
47	4 kV Switchgear	0.00063
48	Redundant Cold Salt Pumps	<0.0005
49	Redundant Hot Salt Pumps	<0.0005
		1.00000

The ranking within these tables, as well as further review of the Solar Two MTBF and MDT data, can be used to identify reliability improvement opportunities to achieve the 90% availability goal. For example, lengthening the MTBF of the following events by a factor of 2 appears plausible and would likely have occurred naturally due to learning and optimization if Solar Two would have operated as long as Solar One.

- Receiver Inlet Tank Air System
- Maintenance Error
- Heat Trace System
- Heliostat Field Common Mode Failures
- Remote Station Heating Ventilation and Cooling
- Control System Computers
- Operator Error

It is also believed that more nighttime maintenance could reduce the average downtimes (MDTs) of the following items by 50%.

- Salt Flow Control Valves
- Receiver Tube Leaks
- Receiver Inlet Tank
- Maintenance Errors
- Heat Trace
- Heliostat Field Common Mode Failures

In addition, more maintenance during nighttime and weather outages could reduce the needed annual scheduled outage time from two weeks to almost one week.[32] Making all these changes to the data used in the analysis results in an annual availability of >90%. Pro-Opta was rerun to again determine the most important contributors to plant outages after the reliability improvements listed above are made. Table 21 gives the revised ranking.

[32] Achieving one week scheduled outage per year may sound optimistic. However, the reduction in availability due to the assumed one week of scheduled outages (51/52 = 0.98) can also be accomplished by scheduling nearly three weeks of outages in December and January since days are much shorter and weather is worse than an average week.

Table 21. Contributors to Forced Outages Assuming Reliability Improvements.

	Events	Mean Fraction
1	Rankine Turbine	0.08257
2	Rcvr Inlet Tank Air System	0.06523
3	Rcvr Trips from Unknown Causes	0.06399
4	Maintenance Error	0.06025
5	Heat Trace System	0.05834
6	Remote Heating Ventilation and Cooling	0.05609
7	Control System Computers	0.05064
8	Steam Gen Tube Leak	0.04669
9	Heliostat Field Common Mode Failures	0.04402
10	Rankine Circ Water Pump	0.04225
11	Service Water System	0.03318
12	Steam Gen Trips from Unknown Causes	0.03258
13	Rcvr Tube Leak	0.03250
14	Operator Error	0.02928
15	Rcvr Inlet Tank Level xmitter	0.02461
16	Rankine Lube Oil System	0.02335
17	Rankine Electric Generator	0.02110
18	Rcvr Panel Replacement	0.01659
19	Rankine Condensate Pump	0.01589
20	Heliostat Interface Switchgear	0.01506
21	Utility Grid	0.01376
22	Steam Gen Water Mix Pump 2	0.01153
23	Steam Gen Water Mix Pump 1	0.01097
24	Steam Gen Water Mix Pump 3	0.01097
25	Hot Sump Flow Control Valve	0.00916
26	Rcvr Flow Control Valve 7	0.00907
27	Rcvr Flow Control Valve 1	0.00903
28	Rcvr Flow Control Valve 2	0.00903
29	Rcvr Flow Control Valve 3	0.00902
30	Rcvr Flow Control Valve 6	0.00902
31	Steam Gen Salt Flow Control Valve 1	0.00902
32	Rcvr Flow Control Valve 5	0.00900
33	Steam Gen Salt Flow Control Valve 3	0.00897
34	Steam Gen Salt Flow Control Valve 2	0.00895
35	Rcvr Flow Control Valve 4	0.00895
36	Cold Sump Flow Control Valve	0.00879
37	Rankine Condenser	0.00745
38	Rankine Control System	0.00507
39	Rcvr Panel Drain Valve 2	0.00219
40	Rcvr Panel Drain Valve 6	0.00216
41	Rcvr Panel Drain Valve 5	0.00216
42	Rcvr Panel Drain Valve 4	0.00214
43	Rcvr Panel Drain Valve 3	0.00214
44	Rcvr Panel Drain Valve 1	0.00214
45	Rcvr Panel Drain Valve 7	0.00213
46	Rcvr Panel Drain Valve 8	0.00209
47	4 kV Switchgear	0.00087
48	Redundant Cold Salt Pumps	<0.0005
49	Redundant Hot Salt Pumps	<0.0005
		1.00000

Chapter 5
Levelized-Energy Cost Calculations

In this chapter the data presented in the previous chapters regarding performance and reliability are brought together with costs from the DOE Power Tower Roadmap to calculate an LCOE. The LCOE is the levelized 30-year price that would have to be charged for the electricity by an IPP given the financing parameters required by the debt and equity investors as defined in the project proforma. The financing parameters selected for this analysis were those used within the DOE Power Tower Roadmap [3]. They are summarized in Table 22.

The LCOE for the central receiver plants were calculated with the following simple equation:

$$\text{LCOE} = \frac{\text{FCR}*\text{Installed Capital Costs} + \text{Annual O\&M Costs}}{\text{Annual Energy} * \text{Plant Availability}} \quad (17)$$

Table 22. IPP Financing Parameters.

General	
Analysis Period	30 yrs
Inflation Rate	2.5%
Taxes and Insurance	
Federal Tax	35%/yr
State Tax	8%/yr
Property Tax	0.5%/yr
Sales Tax	7.75%/yr
Insurance	0.5%/yr
Salvage Value	0
Construction Period	Overnight
IPP Financing Parameters	
Loan term	20 yrs
Loan rate	8%/yr
Debt/equity fraction	54/46 (optimized)
Equity required IRR	14%
Minimum debt coverage ratio	1.4
Cashflows all positive?	Yes
PPA escalation rate	1.2%/yr
Tax Incentives (Equity Measures[33])	
Investment tax credit (ITC)	10%
Accelerated depreciation	5-yr MACRS

The fixed charge rate (FCR) is a single parameter that represents all the capital-financing-related assumptions in the analysis. The value used in the analysis was 7.5% based on the financial

[33] Detailed studies performed by the California Energy Commission [64, 65] have shown that a combination of the permanent federal ITC of 10%, 5-year or shorter accelerated depreciation, and property tax reductions, approximately equalizes the tax burden paid by solar power plants and fossil-fired plants of similar size. Thus, the "tax incentives" are actually "tax equity measures."

parameters listed in Table 22. It was estimated by solving for FCR in Equation (17) given the 30-yr cash-flow analysis conducted by SAM in support of the Power Tower Roadmap.[34] It is a constant-dollar value, i.e., the effects of inflation are removed.

The annual energy was predicted by the SOLERGY calculations presented in Chapter 3. This estimate was then reduced by the plant availability factor estimated in Chapter 4.

The capital and O&M costs used in the calculations were primarily taken from the DOE Power Tower Roadmap [3] (see Table 23). As described in the Roadmap, industry input obtained during a two-day workshop was combined with data from several cost studies to develop the estimates. "Today's Baseline" represents what can be accomplished in early commercial-scale plants that are currently planned or are under construction. The "Workshop Goal" costs are consensus values that were believed to be plausible given improvements in manufacturing and a more mature power tower industry. Since the plants investigated in this study are possible future-generation plants that will not come online for several years, the Workshop-Goal costs were generally assumed to be applicable. However, there were two exceptions:

1. Storage costs were assumed to be \$25 rather than \$20/kWh$_t$ Roadmap value because the lower value assumes use of thermocline-type storage system; the analysis in this study assumes use of a more costly two-tank storage.
2. Receiver costs were assumed to be \$150 rather than \$170/kWh$_t$ Roadmap value because the higher value applies to a receiver that is about ½ the size of the 1000-MW$_t$ receivers studied here; cost is expected to be reduced through an improved economy of scale.

Table 23. Baseline Costs and Roadmap Workshop Cost Goals for Commercial Power Towers.

	Solar Field	Solar Receiver	Thermal Storage	Power Block	Steam Generation	O&M
Today's Baseline	\$200/m^2	\$200/kW$_t$	\$30/kWh$_t$	\$1000/kW$_e$	\$350/kW$_e$	\$65/kW-yr
Workshop Goal	\$120/m^2	\$170/kW$_t$	\$20/kWh$_t$	\$800/kW$_e$	\$250/kW$_e$	\$50/kW-yr

[34] For example, inserting the year 2013 case 1.1 (100 MWe plant, 48% capacity factor) study values in Equation 17 yields 0.15=[FCR*(743E6)+7.8E6]/423E6. Solving for FCR produces 0.075. Inserting the year 2020 case 3.1 (150 MWe plant, 72% capacity factor) study values in Equation (17) yields: 0.078=[FCR*(850E6)+10.35E6]/950E6. Solving for FCR also produces 0.075.

The Roadmap capital costs only represent direct costs. To convert to "Installed Costs" several indirect-type costs must be added. Indirects include Engineering, Procurement, and Construction costs, as well as other items such as project development costs and sales tax. Historical studies have shown that Indirects can be 40% or more of the direct costs, especially for early commercial power plants. However, as the technology matures and after several similar plants are deployed, the indirect-cost multiplier can be substantially reduced. In this study, this factor is assumed to be 1.25.

Results of LCOE Calculations

A summary of the LCOE calculations for all six case studies is presented in Table 24. The example below shows how Equation (17) was used to calculate the LCOE for the case entitled "subcritical wet."

Installed Capital Costs = (Direct Capital Costs) * Indirect Cost Multiplier
= ($693E6) * 1.25
= $867E6

Annual O&M Costs = Fixed O&M Cost + Variable O&M Cost
Fixed O&M Cost = $50/$kW_e$-yr * 145000 kWe = $7.3E6/yr
Variable O&M Cost = $3/$MWh_e$ * 775000 MWh_e/yr = $2.3E6/yr
Annual O&M Cost = $9.6E6/yr
Plant Availability = 90% appears to be feasible from reliability analysis in Chapter 4
Annual Energy = 861E6 kWh from SOLERGY analysis in Chapter 3

$$\text{LCOE} = \frac{0.075*\$867E6 + \$9.6E6}{861E6\ \text{kWh} * 0.9} = 0.096\ \$/kWh_e$$

The other LCOEs found in Table 24 were calculated in a similar fashion. These LCOEs are "point estimates" and do not include the uncertain nature of the parameters used in the calculations. As shown in the next chapter, the parameter uncertainties can have a significant impact on LCOE.

Table 24. Data Used in LCOE Calculations.

	Units	Subcritical Wet	Subcritical Dry	Supercritical Wet	Supercritical Dry	Ultra-supercritical Wet	Ultra-supercritical Dry	Roadmap Goals	
Turbine Output (gross)	MWe	145	139	163	158	167	162		
Turbine Output (net)	MWe	131	125	147	142	150	146		
Heliostat Field Size	m2	1.90E+06	1.90E+06	1.93E+06	1.93E+06	1.95E+06	1.95E+06		
Receiver Size	MWt	1000	1000	1000	1000	1000	1000		
Storage Size	MWhrt	5000	5000	5000	5000	5000	5000		
Site Improvements	$M	38	38	39	39	39	39	20	$/m2
Heliostat Field	$M	228	228	232	232	234	234	120	$/m2
Receiver/Tower/Cold Pumps	$M	150	150	150	150	150	150	150	$/kWt
Steam Generator/Hot Pumps	$M	36	36	36	36	36	36	250	$/kWe
Thermal Storage	$M	125	125	125	125	125	125	25	$/kWht
Power Block	$M	116	116	130	130	134	134	800	$/kWe
Supercritical Increment	$M	0	0	4.6	4.6	4.7	4.7		3.5% of PB
Dry Cooling Increment	$M	0	19.7	0	22.9	0	23.5		17% of PB+SCI
Total Direct Cost	$M	693	713	716	739	723	746		
Indirect Costs	$M	173	178	179	185	181	187		25% of Direct
Installed Capital Cost	$M	867	891	896	924	903	933		
Fixed O&M Cost	$M	7.3	7.3	8.2	8.2	8.4	8.4	50	$/kWe-yr
Variable O&M Cost	$M	2.3	2.2	2.6	2.5	2.6	2.5	3	$/MWhe
Electricity Production Given 100% Plant Availability	GWhre	861	822	946	914	971	943		
Electricity Production Given 90% Plant Availability	GWhre	775	740	851	823	874	849	0.90	Plant Availability
Capacity Factor		0.68	0.68	0.66	0.66	0.66	0.66		
LCOE	**$/kWhe**	**0.096**	**0.103**	**0.091**	**0.097**	**0.090**	**0.095**		

Notes:

1. Fixed O&M costs are assumed to be the same for each pair of case studies. For example, fixed O&M for subcritical wet and subcritical dry are the same. According to References 66 and 67, this is a good assumption.
2. The "Dry-Cooling Incremental" cost is based on analysis performed by Worley Parsons for NREL [68] in which the capital cost of a dry-cooled condenser with an ITD of 14 ^{o}C (i.e., the value assumed in this analysis) was compared to a wet-cooled condenser. The capital cost was 7 times higher. A wet-cooling system is about 2.8% of the total power block cost [16]. Increasing this portion by a factor of 7, increases cost of the power block by ~17%, i.e., [100%-2.8%+7*2.8%]/100%.
3. The cost of supercritical steam power blocks are typically 2 to 5% higher than subcritical power blocks of similar size [67]. An average incremental cost of 3.5% was selected for the analysis.
4. The 90% plant availability was estimated in Chapter 4 to be feasible, but is higher than the 85% value suggested by the Solar Two experience.

Chapter 6
Uncertainty Analysis

The parameters employed in the analysis of plant performance, cost, and reliability are not known precisely. In this chapter, uncertainty ranges are estimated for the parameters associated with the subcritical plant with dry cooling, followed by a determination of each parameters effect on the overall uncertainty in LCOE. As will be shown, this type of analysis is useful to planning and prioritizing future central receiver research.

6.1 Goal and Philosophy

R&D programs for central receiver technology are conducted to reduce uncertainty regarding performance, cost, etc., so that more credible predictions of economic viability can be made. The systems analysis presented in this report attempts to integrate all the major parameters that have an influence on economic predictions. Therefore, if it can be determined that the parameters are most important to the uncertainty in the predictions of LCOE, this information can be used to help identify and prioritize future central receiver research. This is the goal of the work presented in this chapter.

Uncertainty ranges were placed on the basic analysis parameters and these ranges were combined through the analytical models and a constrained sampling technique to obtain an uncertainty range on LCOE. This uncertainty was then decomposed, using linear regression techniques, to determine the influence of the individual analysis parameters.

Financial parameters, such as FCR, can have a large impact on LCOE. However, uncertainty limits were not placed on them because they are not engineering-related and even if they were identified to be important to uncertainty, they could not be addressed by an R&D program.

Based on the above discussion, it is evident the uncertainty analysis does not represent a rigorous statistical treatment. However, it represents the current state of knowledge regarding the uncertainties associated with the technology and the method appears useful to help plan and prioritize future R&D activities.

6.2 Methodology

The analysis methodology steps are shown in Figure 37 and explained below.

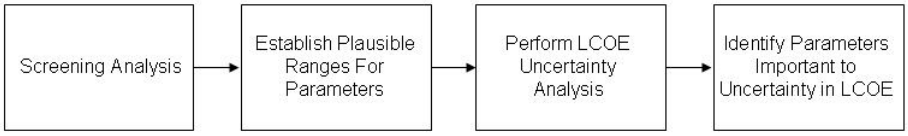

Figure 37. Methodology used in uncertainty analysis.

Screening Analysis

A screening analysis was conducted first. The goal was to reduce the several hundred parameters in the study to a smaller number more tractable for analysis. The number was reduced by (1) grouping the parameters, (2) treating parameters that are highly certain as point values or equations with no uncertainty, and (3) ignoring uncertainties associated with parameters that have been shown by other studies to have a small effect on LCOE.

An example of parameter grouping is heliostat costs. Rather than subdividing heliostat costs into mirror costs, drive costs, motor costs, etc., these parameters were treated as a single parameter.

An example of a set of parameters treated as an equation with no uncertainty is gross steam-Rankine-cycle efficiency. For a given plant design, known heat inputs, and ambient conditions, professional computer software used to predict steam-plant efficiency (such as the GateCycle code used here) have been validated with data collected at many different steam plants over the years.

Reliability parameters were screened using the Pro-Opta importance ranking presented in Table 20. Based on that ranking, it was decided to input the plausible ranges for the reliability parameters associated with the top 20 components and to ignore the rest.[35] Since each component is characterized by a MTBF and MDT, 40 reliability parameters are included.

Experience gained during the modeling of Solar Two was used to screen the uncertain annual performance parameters used by SOLERGY. The nine parameters listed in Table 25 were selected.

Uncertainty limits were placed on all capital cost and O&M parameters. Limits were even placed on low-cost items that would not have a significant impact on the results. This was done to test the predictive capability of the computer code employed in the analysis. The nine cost parameters listed in Table 26 were selected.

The screening analysis identified 58 parameters for further study: 40 reliability, 9 annual performance, and 9 cost.

Establishing Plausible Ranges for Parameters

The 58 parameters and associated ranges are summarized in Tables 25, 26, and a subset of Table 18. The values presented in previous chapters for performance, cost, and reliability were taken to be "best-estimate" values within a plausible range of values. Plausible ranges on the parameters were established through use of experimental evidence and expert judgment. The plausible range is expressed by a probability distribution. In general, the distributions assigned to each parameter followed the guidance given in the Pro-Opta user's guide [17]. For example, when actual X/Y data were available (i.e., X results in Y tests), gamma and discrete-probability

[35] The Pro-Opta uncertainty analysis described in Chapter 4 included plausible ranges for all the reliability parameters.

distributions (DPDs) were used. However, if little or no data are available, experience is used to estimate lower and upper bounds for the parameters. If only the bounds can be estimated, a uniform probability distribution is assumed. If a most likely value is known to exist within the bounds, a triangular distribution is used. Also stated in the tables are the rationales used to establish the ranges. The information presented is sufficient to understand the rationales; if more detail is needed, the reader should refer to the discussion of these parameters in Chapters 3 and 4.

Table 25. Uncertainty Distributions for SOLERGY Parameters.

Parameter	Best Estimate	Distribution	Rationale
Receiver Absorptance	0.94	Triangular 0.91-0.95	Upper bound was measured at Solar One during its final three years [51]. Lower bound is plausible because salt receiver has higher flux level and salt leaks can cause Pyromark coating to degrade.
Heliostat Cleanliness	0.95	Triangular 0.93-0.97	Best estimate is typical value at Kramer Junction trough plants [50]. Upper bound may be achievable with more frequent washes. Lower bound assumed symmetric to upper bound.
Receiver Turn Down	16%	Triangular 10%-16%	Best estimate based on data from Solar Two [13]. It is feasible that a more aggressive operating procedure and/or design could reduce the turndown ratio.
Heliostat Availability	0.99	Triangular 0.970-0.995	Best estimate based on Solar One data [51]. Upper and lower bounds are plausible depending on the design of the heliostat and the field control system.
Receiver Thermal Losses	30 kW_t/m^2	Triangular 20 to 30kW_t/m^2	Best estimate based on Solar Two data [15]. The radiation and convection model in SAM predicts lower thermal losses for Solar Two. The difference between model and data is unresolved.
Parasitic Multiplier	1	Uniform ±20%	Since the SOLERGY and GateCycle parasitic power models were based on generic information, it was judged they could be in error by +/- 20%.
Unusable DNI	0%	Triangular 0% to 40%	Solar Two demonstrated that the receiver can operate through very rapid insolation transients. Thus, the best estimate is that plant operators do not defocus field during cloudy weather. However, to reduce thermal fatigue the operators may decide to defocus in some cloud situations; 40% implies that operators will shut down if average DNI is less than 40% of clear-sky value within a 15-minute period.
Heliostat Stow Wind Speed	40 mph	Triangular 25 to 40 mph	Best estimate is from Solar One operations experience [51]. However, industry is currently considering designs that may stow as low as 25 mph.
Wind Effect on Beam Spillage	Not significant	Uniform 0 to 1.5%	Best estimate assumes very rigid heliostats. If heliostats are designed to meet minimum wind specs in Design Basis Document [11] up to ~1.5% annual loss could occur for Barstow-type weather based on DELSOL/SOLERGY sensitivity study.

Table 26. Uncertainty Distributions for Cost Parameters.

Parameter	Best Estimate	Distribution	Rationale
Site Improvements	$\$20/m^2$	Uniform $\$10-\$30/m^2$	Best estimate is SAM default value. Upper and lower bounds are +/- 50%.
Heliostat Field	$\$120/m^2$	Triangular $\$100-\$180/m^2$	Best estimate is Roadmap plausible goal. Lower bound is for advanced heliostats studied in 2006 [22]. Upper bound represents a pessimistic view of future achievable costs relative to today's baseline of $\$200/m^2$.
Receiver/Tower System	$\$150/kW_t$	Triangular $\$125-\$180/kW_t$	Best estimate is Roadmap plausible goal extended to very large receivers. Lower bound is from Abengoa study of a 910 MW_t receiver/tower as shown in Roadmap. Upper bound represents a pessimistic view of future achievable costs relative to today's baseline of $\$200/kW_t$.
Steam Gen. System	$\$250/kW_e$	Triangular $\$170-\$300/kW_e$	Best estimate is Roadmap plausible goal. Lower bound is from Abengoa study of a larger subcritical steam generator as shown in Roadmap. Upper bound is a pessimistic view of future achievable costs relative to today's baseline of $\$350/kW_e$.
Thermal Storage System	$\$25/kWh_t$	Triangular $\$20/kWh_t$-$\$40/kWh_t$	Best estimate is Roadmap plausible goal for two-tank system. Lower bound similar to $\$22/kW_t$ from Abengoa study of a larger two-tank storage system as shown in Roadmap. Upper bound is a pessimistic view of future achievable costs relative to today's baseline of $\$30/kWh_t$. Solar salt prices vary from year to year, which could affect the storage system cost.
Power Block with Dry Cooling	$\$835/kW_e$	Triangular $\$600$-$\$1000/kW_e$	Best estimate is Roadmap plausible goal. Lower bound is a value that might be achieved if more suppliers compete in the 100 to 200 MW_e market. Value is suggested by Sargent and Lundy Study [69]. Upper bound is a pessimistic view of future achievable costs relative to today's baseline of $\$1000/kW_e$.
Indirect Cost Multiplier	1.25*direct	Triangular 1.2-1.35	Best estimate is Roadmap plausible goal. Lower bound might be achieved if multiple standard plants can be built, which reduces engineering costs. Upper bound is a pessimistic view of future achievable costs relative to today's baseline of ~1.4.
Fixed O&M	$\$50/kW_e$-yr	Triangular $\$35-\$60/kW_e$-yr	Best estimate is Roadmap plausible goal. Lower bound might be achieved if multiple standard plants can be collocated within a power park so that O&M costs can be shared. Upper bound is a pessimistic view of future achievable costs relative to today's baseline of $65/kW-yr.
Variable O&M	$\$3/MWh_e$	Uniform $1.5 to $4.5/MWh	Best estimate is SAM default value. Upper and lower bounds are +/- 50%.

Performing LCOE Uncertainty Analysis

The LCOE for the plant can be expressed by the following equation:

$$LCOE = \frac{FCR * IND* (DC_1 + DC_2 + ... DC_9) + O\&M_F + O\&M_V*AE*AVAIL}{AE(P_1, P_2, ... P_9) * AVAIL(R_1, R_2, ... R_{40})} \quad (18)$$

where

FCR = fixed charge rate = 0.075,
IND = Indirect cost multiplier,
DC_x = Direct costs associated with system X,
$O\&M_F$ = Fixed O&M costs,
$O\&M_V$ = Variable O&M costs,
AE = SOLERGY prediction of annual energy given variations in performance parameters P_1 through P_9, and
AVAIL = Pro-Opta prediction of plant availability given variations in reliability parameters R_1 through R_{40}.

To obtain uncertainty limits on LCOE, the probability distributions associated with each of the 58 parameters must be convolved via the above function. This was done through use of Latin-Hypercube sampling (LHS) [21]. Unlike the Monte Carlo approach, which employs random sampling, LHS uses a constrained sampling scheme. LHS requires a fewer number of computer runs than Monte Carlo and can yield more precise estimates.

The LHS computer code was used to sample the ranges of the 58 parameters. This sampling produced 301 different combinations of parameter values. Equation (18) was then solved for each combination to produce 301 values of LCOE.[36] The LCOE values were then grouped to produce a cumulative distribution function (CDF), as shown in Figure 38. The analysis was performed two times assuming two different sets of reliability parameters, as explained in Section 6.3.

[36] SOLERGY was run 301 times. Siri Khalsa developed a routine for another project to automate this process [70].

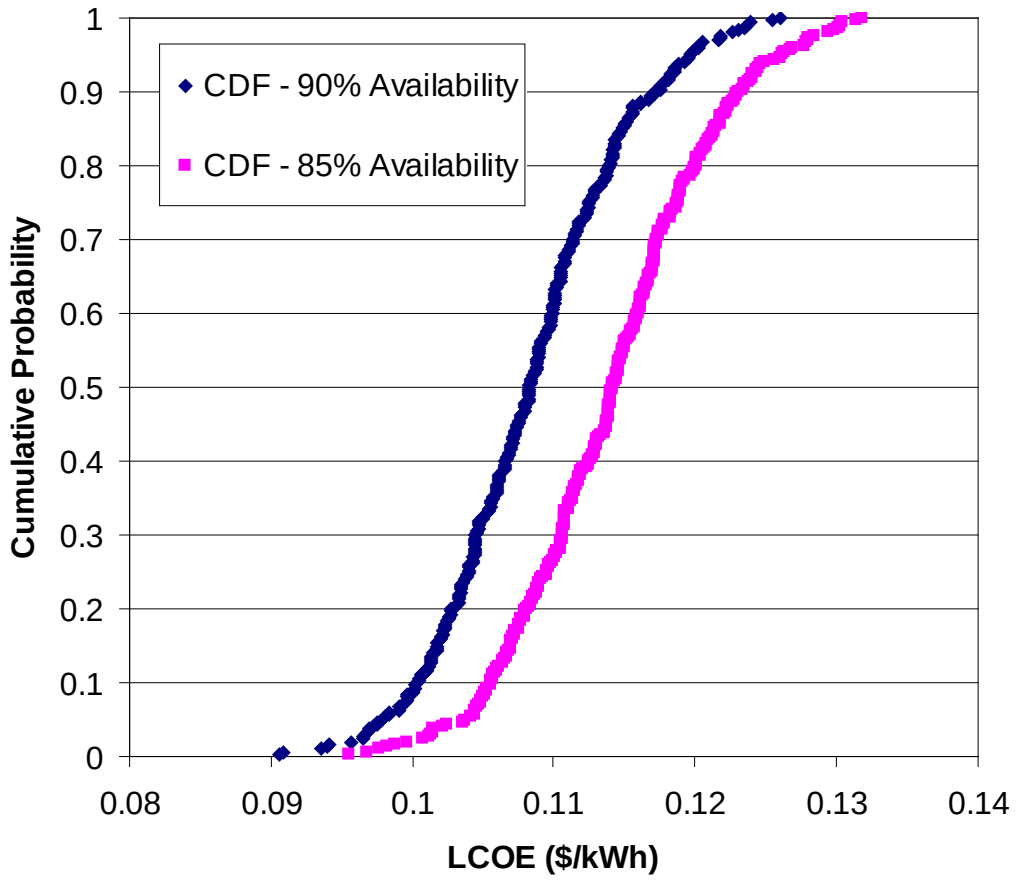

Figure 38. LCOE CDFs for the subcritical plant with dry cooling.

Identifying Parameters Important to Uncertainty in LCOE

The Statisica computer code was used to identify and rank the parameters that are important to LCOE uncertainty [20] (called "stepwise rank regression"). The code attempts to fit a linear regression model to data sets of dependent versus independent variables and contains algorithms that protect against overfit of the data. In the case analyzed here, each of the 301 solutions to Equation (18) constituted a data set. The model is of the form:

$$Y = B_0 + \sum_j B_j * X_j \tag{19}$$

where

Y = dependent variable (LCOE),
B_0 = intercept,
B_j = regression coefficients, and
X_j = independent variables (the 58 parameters).

The independent variables that are most important to the predictive capability of the regression model are brought into the model first, followed by variables of less importance. An R^2 statistical test is performed to determine the goodness of fit. The R^2 value varies between zero and one and should be close to one if the model predicts the observed values adequately.

In addition to the intercept and regression coefficients, the code also calculates standardized regression coefficients (SRCs) for each independent variable. The SRCs are used to rank the independent variables in terms of their effect on uncertainty, and have the following physical interpretation: if all independent variables are increased or decreased by the same fraction of their standard deviation, the SRC is a relative ranking of how the dependent variable changes.

The SRCs are presented in Figure 39. The linear regression models identified by Statistica are very good since the R^2 values (~0.95) are close to unity for both analyses. SRC values have positive and negative signs. If the SRC has a positive value, an increase in the value of the independent variable will cause an increase in the dependent variable. If SRC is negative, an increase in the independent variable will cause a decrease in the dependent. Examples are: since collector cost is positive, an increase in this parameter will cause an increase in LCOE; since heliostat cleanliness is negative, an increase in this parameter will cause a decrease in LCOE. Please note that the inverse of MTBF (also called “failure rate”) is plotted.

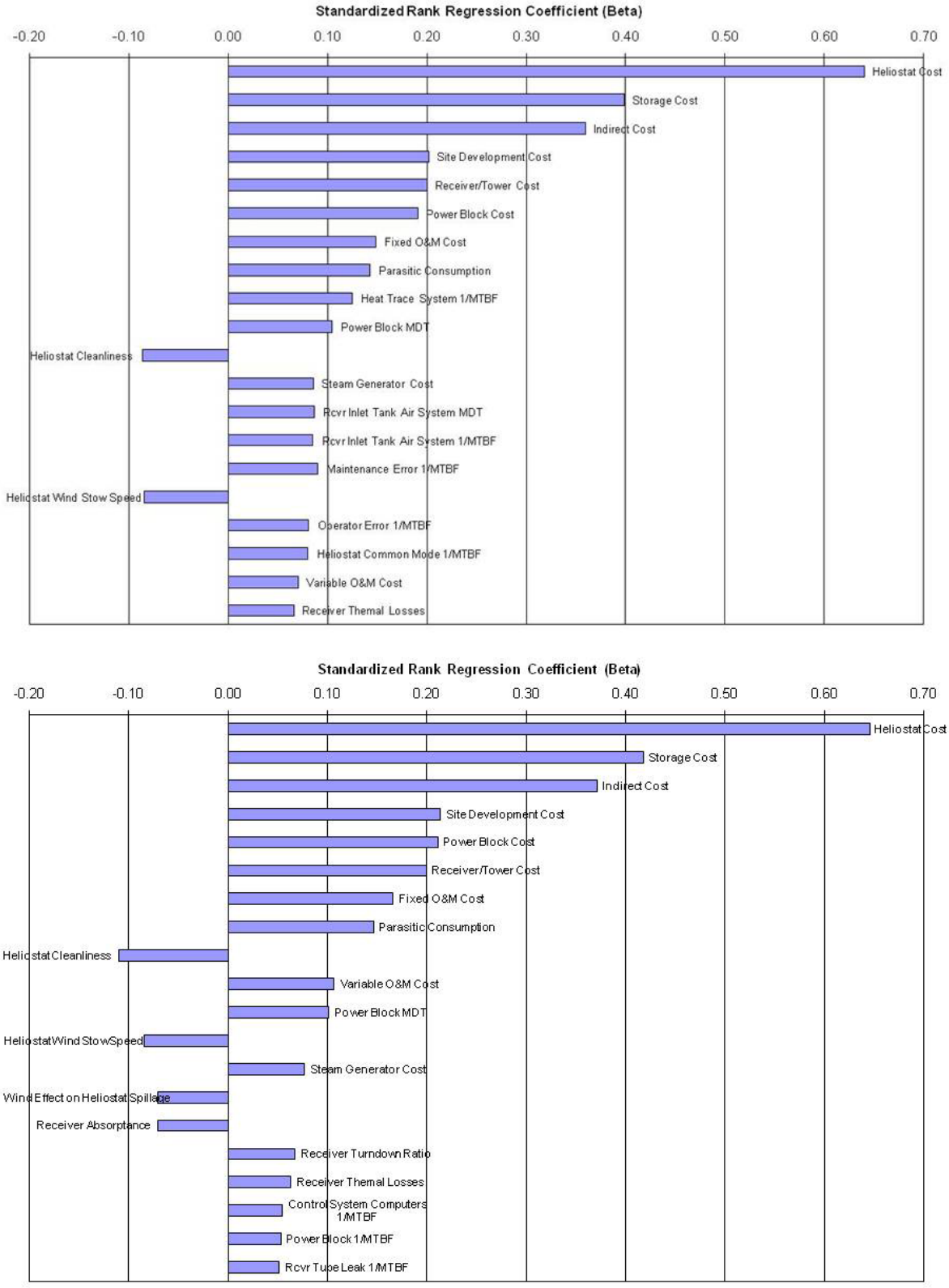

Figure 39. Top 20 contributors to LCOE uncertainty given 85% (top) and 90% (bottom) plant availability parameters.

6.3 Results

Two separate analyses were run to represent the two different plant-availability studies described in Chapter 4: an 85% availability case study and a 90% case study.

According to Figure 38, the LCOE for the subcritical plant with dry cooling is between 9 and 12.5 cents/kWh, given a nominal plant availability of ~90%. This range is applicable if reliability improvements relative to the Solar Two experience can be achieved. These improvements were described in Chapter 4 and are summarized in Table 27. It is interesting to compare this CDF with the 10.3-cent/kWh point estimate calculated for this case study in Chapter 5 (see Table 24). According to the CDF, the probability of achieving 10.3 cents or less is only ~20%; the more likely median value is shown to be ~10.8 cents. This occurred because several of the uncertainty distributions were not symmetric about the nominal value. For example, heliostat costs were characterized by a triangular distribution with upper and lower bounds of \$100 and \$180/m^2, but with a most likely value of \$120/m^2. This comparison clearly shows that it is important to include uncertainties when estimating LCOE.

For the 85% plant availability case, the MTBF and MDT uncertainty distributions based on the Solar Two reliability experience were used (see Table 18). Combining these reliability distributions with the performance and cost distributions described in Tables 25 and 26, respectively, yielded the ranking shown at the top of Figure 39. This figure indicates that heliostat cost (1) has the most important influence on LCOE uncertainty with the following parameters having approximately one-half to one-sixth the influence: storage cost (2), indirect cost (3), site development cost (4), receiver/tower cost (5), power block cost (6), fixed O&M cost (7), parasitic consumption (8), heat trace MTBF (9), and power block MDT (10). Other parameters in the analysis were ranked below these ten.

Since heliostats comprise more than 1/3 of the total plant cost and have a large uncertainty in future cost, it is not surprising they dominate. Other studies have concluded the same [1, 71].

For the 90% plant availability case, the MTBF and MDT uncertainty distributions described in Table 27 were used. Combining these reliability distributions with the same performance and cost distributions yielded the ranking shown at the bottom of Figure 39. Comparison of the top versus bottom shows the top eight parameters to be the same. However, the ranking below that is different. Noticeably absent are the following reliability parameters that were assumed to be improved in the 90% plant availability case study: heat-trace MTBF, receiver inlet tank MDT and MTBF, maintenance error and operator error MTBFs, and heliostat field common-mode failure MTBF. Since the influences of these parameters are now much less, other uncertain parameters such as “wind-effect on heliostat spillage” and “receiver absorptance” have moved up the top-20 list.

Since the purpose of central receiver R&D is to reduce the uncertainty associated with predictions of the economic viability of the technology, this importance ranking should help prioritize future central receiver research. The analysis indicates that primary emphasis should be placed on narrowing the uncertainty limits associated with several capital cost categories, especially heliostats.

Table 27. Changes to Uncertainty Distributions for Improved Plant Availability Study.

Parameter	Best Estimate (hrs)	Distribution	Rationale
Receiver Inlet Tank MTBF	586	Triangular 293 to 586	Lengthening MTBF by a factor of 2 appears plausible through learning. Worst-case bound is Solar Two experience.
Maintenance Error MTBF	978	Triangular 489 to 978	
Heat Trace System MTBF	1468	Triangular 734 to 1468	
Heliostat Field Common Mode Failure MTBF	1468	Triangular 734 to 1468	
Remote Station HVAC MTBF	978	Triangular 489 to 978	
Control System Computers MTBF	366	Triangular 183 to 366	
Operator Error MTBF	1468	Triangular 734 to 1468	
Receiver Tube Leak MDT	7	Triangular 7 to 14	Reducing MDT by a factor of 2 appears plausible through learning. Worst-case bound is Solar Two experience.
Salt Flow Control Valve MDT	4	Triangular 4 to 8	
Receiver Inlet Tank MDT	2	Triangular to 4	
Maintenance Error MDT	3.1	Triangular 3.1 to 6.2	
Heat Trace MDT	4.5	Triangular 4.5 to 9	
Heliostat Field Common Mode Failure MDT	3.4	Triangular 3.4 to 6.8	
Scheduled Outages	1 week	None	Reducing scheduled outage from 2 to 1 weeks/yr could happen with more nighttime scheduled maintenance.

Chapter 7
Conclusions

Since completion of the Solar Two molten-salt power tower demonstration in 1999, the solar industry has been developing initial commercial-scale projects that are 3 to 14 times larger. The first commercial plant, Gemasolar, began operating in Spain in 2011 and the first commercial U.S. plant is now under construction near Tonopah, Nevada. Like Solar Two, these initial plants will power subcritical steam-Rankine cycles using molten salt with a temperature of 565 °C. Several of these plants are expected to be built over the next decade.

The main question explored in this study is whether there is significant economic benefit to develop future molten-salt plants that operate at a higher receiver outlet temperature. Higher temperatures would allow the use of supercritical steam cycles that achieve an improved efficiency relative to today's subcritical cycle (~50% versus ~42%). The 2010 DOE/Industry Roadmap also suggested that future molten salts could benefit from higher operating temperatures. Thus, the LCOE of a 565 °C subcritical baseline plant was compared with possible future-generation plants that operate at 600 or 650 °C. The receiver thermal ratings of the plants that were studied are the maximum practical size originally identified by the DOE program in the late 1980s (~1000 MW_t). This is 1.7X scaleup of the Tonopah plant. In addition, like Gemasolar, all plants incorporate 15 hours of thermal storage to achieve high solar-only capacity factors.[37]

The seven major conclusions of the study are underlined and discussed below.

Significant economic benefit is realized by increasing salt temperature from 565 to 600 °C. There is no compelling argument to increase salt temperature to 650 °C.

The analysis showed that increasing salt temperature from 565 to 650 °C should reduce LCOE by ~8%. However, ~80% of that reduction can be achieved by raising the temperature to only 600 °C. LCOE is direct function of power block efficiency. As shown in the analysis, raising salt temperature to 600 °C increases the design-point efficiency from 43% to 48.4% and raising it to 650 °C results in 49.6% (wet cooling cases). Thus, ~80% of the efficiency improvement is achieved by increasing the temperature to 600 °C. Figure 40 is helpful in understanding this nonlinear behavior of temperature versus efficiency.

Figure 40 compares the steam cycles powered by the three salt temperatures on a temperature-entropy (TS) diagram. The efficiency of a particular steam cycle is the ratio of the area enclosed by the cycle (A_{encl}) divided by the total area (defined as A_{encl} plus the area of the rectangle below A_{encl} extrapolated to absolute zero). It can be seen that a significant increase in A_{encl} occurs when switching from a subcritical to a supercritical cycle because the thermodynamic cycle "jumps over the steam dome." However, after jumping over the dome, only a small incremental increase in A_{encl} occurs when increasing temperatures from supercritical to ultra-supercritical.

[37] DOE is currently directing a large R&D program to develop baseload solar technology that is a direct replacement of coal-fired power plants. Coal produces 50% of the power in the United States.

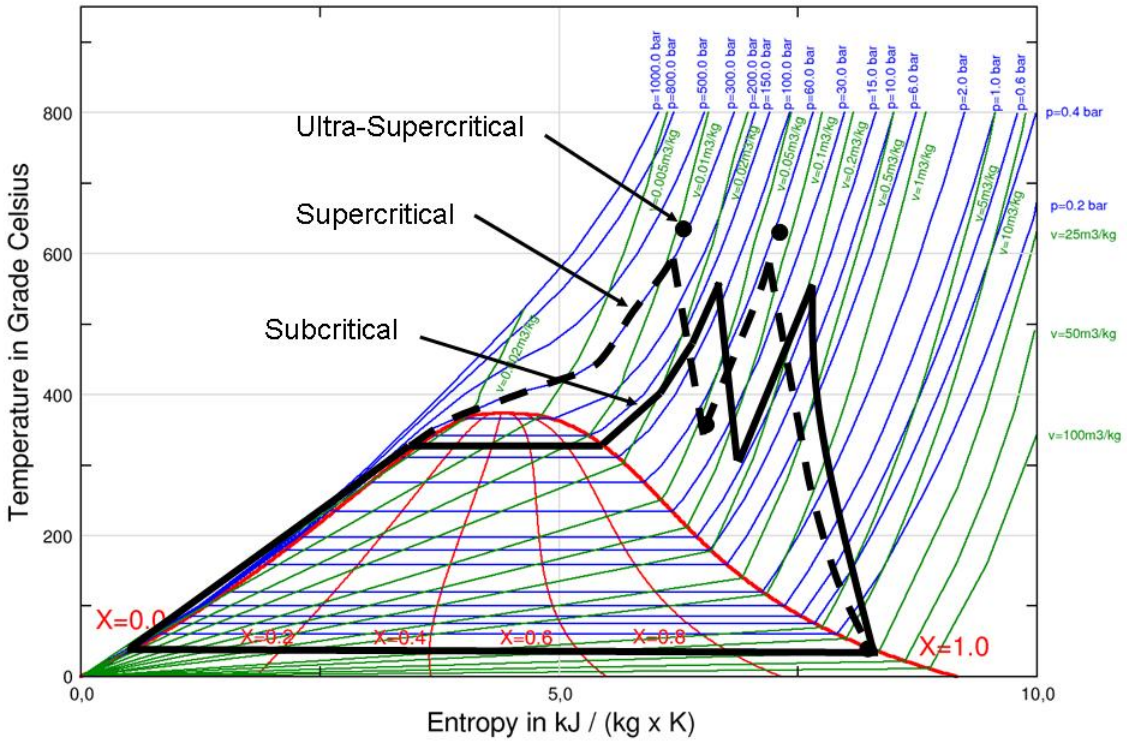

Figure 40. Comparison of steam-Rankine thermodynamic cycles. The subcritical cycle is powered by 565 °C salt. The supercritical and ultra-supercritical cycles are powered by 600 and 650 °C salt, respectively. To improve clarity, only the extremes (i.e., dots) of the ultra-supercritical cycle are shown; the full-cycle shape is similar to the supercritical cycle.

Limiting salt temperatures to 600 °C avoids several technical issues that would need to be addressed if it was desired to operate at 650 °C. For example, salt corrosion of receiver materials is fairly well understood at 600 °C, but not at 650 °C. Operation at 650 °C would likely require the development of a new solar salt, new receiver materials, and/or the inclusion of an oxygen-blanking system to reduce the rate of corrosion. This could increase costs beyond the estimates provided in this report, which could easily eliminate the remaining possible reduction in LCOE.

<u>To achieve the LCOE reduction possible with supercritical power towers will likely require a scale-up of today's solar technology and a scale-down of today's steam-power blocks.</u>

All the subcritical and supercritical plants investigated in this study are comprised of a 1000-MW_t receiver, 15 hours of storage (5000 MWh_t), and a steam power block with a nominal rating between 140 and 165 MW_e. Not all the technologies needed to build these plants currently exist. For example, the world's largest molten-salt power tower now under construction in Nevada consists of a 585-MW_t receiver and a 2900-MWh_t thermal storage system. Thus, the receiver/storage technologies studied here are 1.7X larger than today's technology. Subcritical

steam-power blocks with an output of ~150 MW_e currently exist. However, the smallest supercritical power blocks available today are ~450 MW_e. Thus, the supercritical power blocks studied here are about 1/3 the size of today's technology.

An important assumption was made that it is not practical to thermally cycle a supercritical-power block on a daily basis; it will need to operate nearly 24/7, much like it does in a coal plant. The much higher steam pressures (≥300 bar supercritical versus 125 bar subcritical) will result in very thick pipe walls and turbine casings, which should greatly increase startup time relative to a subcritical plant. The 1000-MW_t receiver size was selected as a "happy medium" to meet the technological and economic constraints that could likely be required to deploy a successful supercritical power tower. That is, the 1000-MW_t size has been predicted in previous studies to result in a lower LCOE due to an improved economy of scale relative to ~500-MW_t receivers. Also, preliminary discussions with supercritical power block providers suggest that scaling down by a factor of 3 may be feasible. Combining these two statements with the expected need to run baseload results in the 1000 MW_t/5000 MWh/~150 MW_e combination recommended here.

A salt receiver with a flux limit that is 25% higher than demonstrated at Solar Two can likely be built to achieve a 30-year lifetime.

The peak flux at Solar Two was 800 suns. The receivers investigated in this study increased the peak flux to 1000 suns. A higher flux receiver is desirable because less heat-exchange area is needed to absorb a given amount of power. A reduction in area reduces heat loss (improves efficiency) as well as the cost of the receiver. The recommended receiver tube materials are different than the 316SS used at Solar Two. Depending on the receiver outlet temperature, the following materials were investigated and appear to be possible: (1) 565 °C – Incoloy 800, Inconel 625-LCF, and Haynes 230, (2) 600 °C – Incoloy 800 and Haynes 230, and (3) 650 °C – perhaps Haynes 230. Further analysis and experiments are recommended, but the analysis conducted here suggests that these tube materials are appropriate and meet the 30-year lifetime requirements dictated by low-cycle thermal fatigue, salt corrosion, and strength as specified in the ASME boiler and pressure vessel code.

Reliability improvements relative to the experience at Solar Two need to occur to achieve the 90% plant availability goal.

Several problems and design flaws identified during startup and commissioning led to significant downtime at Solar Two. Consequently, the plant operated for less than 2000 total hours during the project lifetime. This short time precluded the achievement of a mature operating mode. Thus, even after correcting for known infant-mortality problems, an analysis of the existing data suggests ~85% plant availability, which is short of the 90% goal for the technology. Several of the remaining reliability problems would likely have been resolved through the natural course of learning if the plant would have run longer, but that is conjecture. (For example, Solar One operated for 10,000 hours and plant availability steadily improved from an initial value of 82% to 95%.) Several plant systems and components were targeted for improvement to achieve the 90% goal.

The LCOE of dry-cooled power tower is ~0.6 cents/kWh higher than a wet-cooled power tower.

Critics of solar power towers often state the technology is not sustainable because they consume a large amount of water and are installed in desert regions that do not have this resource. Dry cooling of the condenser can reduce water consumption by more than 90%. A detailed comparison of wet versus dry cooling in this study suggests that LCOE will increase by ~0.6 cents/kWh if dry cooling is used. The incremental capital cost to implement dry cooling is insignificant relative to the total cost of the plant. However, LCOE is increased because annual efficiency is degraded from 16.7% to 16.0% for the subcritical plant using 565 ^{o}C salt and from 18.1% to 17.5% for the supercritical plant using 600 ^{o}C salt.

The LCOE of future molten-salt power towers is uncertain and that uncertainty is dominated by the predicted cost for heliostats.

Heliostats now being deployed within initial commercial projects cost about \$200 to \$250/m^2. Significant cost reductions are predicted as the power-tower industry matures due to increases in manufacturing volume and technology improvements. But there is a large variation in expected future costs. An analysis of the causes of LCOE uncertainty found that heliostats had the dominant influence, followed by several other capital cost categories. Since heliostats comprise more than 1/3 of the total plant cost and have a large uncertainty in future cost, it is not surprising they dominate. Uncertainties in several performance and reliability parameters were also found to have a significant influence on LCOE uncertainty. Since the purpose of R&D is to reduce the uncertainty associated with predictions of the economic viability of the technology, the developed importance ranking can help prioritize future central receiver research.

The Pro-Opta reliability software tool was validated with power tower data and is a useful power-tower analysis tool.

Most of the software tools used in this study (DELSOL, SOLERGY, SAM, GateCycle, and Statistica) have been used within previous studies of power towers. However, this is the first study to use Pro-Opta software to analyze power tower reliability issues. To ensure its validity, software predictions were compared with reliability data collected during the Solar One project. The prediction of plant availability was very close to the data. Pro-Opta has also been used to study wind-farm power plants. This SNL-developed tool is easy to use and is available for free upon request.

References

1. M. Becker and P. Klimas (editors), J. Chavez, G. Kolb, and W. Meinecke (authors), *Second Generation Central Receiver Technologies – A Status Report*, Sandia National Laboratories (SNL) and Deutsche Forschungsanstalt fur Luft-und Raumfahrt (DLR), Verlag C. F. Muller, Karlsruhe, April 1993.
2. Pacific Gas & Electric Company, *Solar Central Receiver Technology Advancement for Electric Utility Applications, Phase 1 Topical Report*, Report No. 007.2-88.2, San Francisco, CA, September 1988.
   Arizona Public Service Company, *Utility Solar Central Receiver Study*, Report No. DOE/AL/38741-1, November 1988.
   Alternate Utility Team, *Utility Solar Central Receiver Study*, Report No. DOE/AL/38741-2, September 1988.
3. G. J. Kolb, C. K. Ho, T. R. Mancini, and J. A. Gary, *Power Tower Technology Roadmap and Cost Reduction Plan*, SAND2011-2419. Sandia National Laboratories, Albuquerque, NM, April 2011.
4. G. J. Kolb, "STAMP Work Package 9.2 – Model Benchmarking," Presentation to SolarPACES Task Meeting, Granada, Spain, February 2011.
5. K. Miner, "Pratt & Whitney Rocketdyne Receiver Overview," CSP Program Review Meeting, February 9-11, 2010, Albuquerque, NM, http://www1.eere.energy.gov/solar/past_meetings_workshops.html.
6. C. Turchi, M. Mehos, C. K. Ho, and G. J. Kolb, Current and Future Costs for Parabolic Trough and Power Tower Systems in the US Market, *Proceedings of the SolarPACES 2010 Conference*, Perpignan, France, September 21-24, 2010.
7. GE Energy, *GateCycle™ Ver: 6.00 SP4*, General Electric Company, Copyright 2010.
8. Rajesh Gupta (SPX), Air Cooled Condenser Using SRC™, Single Row Aluminized Carbon Steel Tube/Aluminum Fin Tube Bundle, memorandum to Babul Patel (Nexant Inc.), August 31, 2007, SRX Cooling Technologies, Overland Park, KS.
9. WorleyParsons Group, Inc., *Analysis of Wet and Dry Condensing 125 MW Parabolic Trough Power Plants*, NREL-2-ME-REP-0002 Rev 0, September 29, 2009. Also found in *Water Use in Parabolic Trough Power Plants: Summary Results from Worley Parsons' Analysis*, by C. S. Turchi, M. J. Wagner, and C. F. Kutscher, National Renewable Energy Laboratory, NREL/TP-5500-49468, December 2010.
10. B. L. Kistler, *A User's Manual for DELSOL3--A Computer Code for Calculating the Optical Performance and Optimal System Design for Solar Thermal Central Receiver Plants*, SAND86-8018. Sandia National Laboratories, Livermore, CA, November 1986.
11. A. B. Zavoico, *Solar Power Tower Design Basis Document, Rev. 0*, SAND2001-2100. Sandia National Laboratories, Albuquerque, NM, July 2001.
12. D. J. Alpert and G. J. Kolb, *Performance of the Solar One Power Plant as Simulated by the SOLERGY Computer Code*, SAND88-0321. Sandia National Laboratories, Albuquerque, NM, April 1988.

13. H. E. Reilly and G. J. Kolb, *Evaluation of Molten Salt Power Tower Technology Based on Experience at Solar Two*, SAND2001-3674. Sandia National Laboratories, Albuquerque, NM, November 2001.
14. M. J. Wagner, Simulation and Predictive Performance Modeling of Utility Scale Central Receiver System Power Plants, Master's Thesis, University of Wisconsin, Madison, Wisconsin, 2008.
15. J. E. Pacheco (editor), *Final Test and Evaluation Results from the Solar Two Project*, SAND2002-0120. Sandia National Laboratories, Albuquerque, NM, January 2002.
16. B. D. Kelly, *Advanced Thermal Storage for Central Receivers with Supercritical Coolants*, DOE Grant DE-FG36-08GO18149, Abengoa Solar Inc., Lakewood, CO, June 15, 2010.
17. Sandia Corporation, *Design for Reliability User Guide for: Pro-Opta Fault Tree Interface, Pro-Opta Data Manager, Pro-Opta Results Module,* Version 2.1.0, Sandia National Laboratories, Albuquerque, NM, copyright 2007.
18. R. Wiser and E. Kahn, *Alternative Windpower Ownership Structures Financing Terms and Project Costs*, LBNL-38921 UC-1321. Lawrence Berkeley National Laboratory, Berkeley, CA, May 1996.
19. National Renewable Energy Laboratory, *System Advisor Model, Ver. 2010 11.9*, Golden, CO, 2010.
20. Statistica, Statsoft, Inc., Tulsa, OK.
21. G. D. Wyss and K.H. Jorgensen, A User's Guide to LHS: Sandia's Latin Hypercube Sampling Software, Sandia National Laboratories, Albuquerque, NM, 1988.
22. G. J. Kolb, S. A. Jones, M. W. Donnelly, D. Gorman, R. Thomas, R. Davenport, and R. Lumia, *Heliostat Cost Reduction Study*, SAND2007-3293. Sandia National Laboratories, Albuquerque, NM, June 2007.
23. D. C. Smith and J. M. Chavez, *A Final Report on the Phase 1 Testing of a Molten-Salt Cavity Receiver - Volume 1 - A Summary Report*, SAND87-2290. Sandia National Laboratories, Albuquerque, NM, 1988.
24. B. Kelly, *Lessons Learned, Project History, and Operating Experience of the Solar Two Project*, SAND2000-2598. Sandia National Laboratories, Albuquerque, NM, November 2000.
25. R. W. Bradshaw and S. H. Goods, *Accelerated Corrosion Testing of a Nickel-Base Alloy in a Molten Salt*, SAND2001-8758. Sandia National Laboratories, Albuquerque, NM, November 2009.
26. Special Metals, "Incoloy® alloy 800H & 800HT®," Under "Products" at www.specialmetals.com.
27. Special Metals, "Inconel® alloy 625LCF®," Under "Products" at www.specialmetals.com.
28. Haynes International, "Haynes® 230® Alloy," Under "Products" at www.haynesintl.com.
29. D. C. Smith, Design and Optimization of Tube-Type Receiver Panels for Molten Salt Application, *Solar Engineering 1992 - Vol. 2*, American Society of Mechanical Engineers, New York, NY, 1992.

30. Memo from Metcut Research Associates Incorporated to Cabot Corporation Haynes International Attn: George Lai, Number 330-44169-2, Project: Low Cycle Fatigue Testing of (30) Haynes Alloy 230 Smooth Bar Specimens Manufactured by Metcut Research from Material Supplied and Identified by Cabot Corporation, Frequency 0.33 Hz, July 22, 1987.
31. J. B. Conway and J. T. Berling, A New Correlation of Low-Cycle Fatigue Data Involving Hold Periods, *Metallurgical Transactions,* Vol. 1, pp. 324-325, January 1970.
32. J. B. Conway, J. T. Berling, and R. H. Stentz, "Low-Cycle Fatigue and Cyclic Stress-Strain Behavior of Incoloy 800," *Metallurgical Transactions,* Vol. 3, pp. 1633-1637, June 1972.
33. S. Majumdar, *Compilation of Fatigue Data for Incoloy 800 Alloys,* ANS/MSD-78-3. Argonne National Laboratory, Argonne, Illinois, March 1978.
34. R. Bui-Quoc, R. Gomuc, A. Biron, H. L. Nguyen, and J. Masounave, "Elevated Temperature Fatigue-Creep Behavior of Nickel-Base Superalloy IN 625," *Low Cycle Fatigue, ASTM STP 942,* H. D. Solomon, G. R. Halford, L. R. Kaisand, and B. N. Leis, Eds., American Society for Testing and Materials, Philadelphia, pp. 470-486, 1988.
35. B. L. Kistler, *Fatigue Analysis of a Solar Central Receiver Design Using Measured Weather Data,* SAND86-8017. Sandia National Laboratories, Livermore, CA, November 1986.
36. W. C. Young, R. J. Roark, and R. G. Budynas, *Roark's Formulas for Stress and Strain,* 7th Edition, McGraw-Hill Book Company, 2003.
37. American Society of Mechanical Engineers, *2007 ASME Boiler and Pressure Vessel Code – Section I-Rules for Construction of Power Boilers and Section II-Materials,* New York, NY, 2007.
38. R. W. Bradshaw and S. H. Goods, *Corrosion Resistance of Nickel-Base Alloys in Molten Alkali Nitrates,* SAND2000-8240. Sandia National Laboratories, Livermore, CA, November 2009.
39. J. R. Slusser, J. B. Titcomb, M. T. Heffelfinger, and B. R. Dunbobbin, Corrosion in Molten Nitrate-Nitrite Salts, Air Products Corporation, *J. Metals,* pp. 24-27, July 1985.
40. R. W. Bradshaw, *A Thermal Convection Loop Study of Corrosion of Alloy 800 in Molten NaNO3-KNO3,* SAND82-8911. Sandia National Laboratories, Livermore, CA, January 1983.
41. R. W. Bradshaw, *Oxidation and Chromium Depletion of Alloy 800 and 316SS by Molten NaNO3-KNO3 at Temperatures Above 600 Degrees Centigrade,* SAND86-9009. Sandia National Laboratories, Livermore, CA, January 1987.
42. R. W. Bradshaw, *Thermal Convection Loop Corrosion Tests of 316SS and In800 in Molten Nitrate Salts,* SAND82-8210. Sandia National Laboratories, Livermore, CA, February 1982.
43. C. Singer, R. Buck, R. Pitz-Paal, and H. Muller-Steinhagen, Assessment of Solar Power Tower Driven Ultrasupercritical Steam Cycles Applying Tubular Central Receivers with Varied Heat Transfer Media, *Journal of Solar Energy Engineering,* Vol. 132, November 2010.

44. F. Lippke, *Solar Two Overall Efficiency at Reduced Receiver Outlet Temperatures,* SAND2009-2437P. Sandia National Laboratories, Albuquerque, NM, April 1995.
45. Babcock and Wilcox, *Molten Salt Electric Experiment Steam Generator Subsystem, Final Report,* contractor report, SAND85-8181. Sandia National Laboratories, Albuquerque, NM, April 1986.
46. M. C. Stoddard, S. E. Faas, C. J. Chiang, and J. A. Dirks, *SOLERGY - A Computer Code for Calculating the Annual Energy from Central Receiver Power Plants,* SAND86-8060. Sandia National Laboratories, Livermore, CA, May 1987.
47. W. Marion and S. Wilcox, *Solar Radiation Data Manual for Flat-Plate and Concentrating Collectors,* NREL/TP-463-5607. National Renewable Energy Laboratory, Golden, CO, April 1994.
48. C. M. Randall, *Barstow Insolation and Meteorological Data Base,* Aerospace Report Number ATR-78 (7695-05)-2. The Aerospace Corporation, El Segundo, CA, March 1978 (Data from 1977 were provided in personal communications).
49. J. W. Strachan and R. M. Houser, *Testing and Evaluation of Large-Area Heliostats for Solar Thermal Applications,* SAND92-1381. Sandia National Laboratories, Albuquerque, NM, February 1993.
50. G. E. Cohen, D. W. Kearney, and G. J. Kolb, *Final Report on the Operation and Maintenance Improvement Program for Concentrating Solar Power Plants,* SAND99-1290. Sandia National Laboratories, Albuquerque, NM, June 1999.
51. L. G. Radosevich, *Final Report on the Power Production Phase of the 10 MW_e Solar Thermal Central Receiver Pilot Plant,* SAND87-8022. Sandia National Laboratories, Livermore, CA, March 1988.
52. C. J. Chiang, *SUNBURN: A Computer Code for Evaluating the Economic Viability of Hybrid Solar Central Receiver Electric Power Plants,* SAND86-2165. Sandia National Laboratories, Albuquerque, NM, June 1987.
53. Bechtel Corporation, *Investigation of Thermal Storage and Steam Generator Issues,* contractor report, SAND93-7084. Sandia National Laboratories, Albuquerque, NM, August 1993.
54. Southern California Edison Company, *Solar 100 Conceptual Study - Final Report,* August 3, 1982.
55. D. Gorman, Advanced Thermal Systems, Englewood, CO, personal communication, 1990.
56. S. Lazarkiewicz and A. T. Troskolanski, *Impeller Pumps - First Edition,* Pergamon Press Inc., New York, NY, 1965.
57. R. R. Hill, J. A. Stinebaugh, D. Briand, A. Benjamin, and J. Linsday, *Wind Turbine Reliability: A Database and Analysis Approach,* SAND2008-0983. Sandia National Laboratories, Albuquerque, NM, February 2008.
58. G. J. Kolb and C. W. Lopez, *Reliability of the Solar One Plant During the Power Production Phase,* SAND88-2664. Sandia National Laboratories, Albuquerque, NM, October 1988.

59. Bechtel Corporation, “Solar Two Project Piping and Instrumentation Diagrams – Revised and Reissued for Construction,” dated May 15, 1998, San Francisco, CA.
60. Sandia National Laboratories, “Solar Two Data and Daily Reports – January 1998 – April 1999,” multiple binders.
61. B. Bonduelle et al., Themis Evaluation Report, Centre National de la Recherche Scientifique, *Proceedings of the Third International Workshop on Solar Thermal Central Receiver Systems: Volume 1*, Springer-Verlag Publishing Co., 1986.
62. Electric Power Research Institute, *Reliability and Availability Assessments of Selected Domestic Combined-Cycle Power-Generating Plants*, EPRI AP-2536, Palo Alto, CA, August 1982.
63. G. J. Kolb and C. W. Lopez, Reliability of the Solar One Plant During the Power Production Phase, *Proceedings of the 16th Inter-RAM Conference for the Electric Power Industry*, Monterey, CA, May 30 – June 2, 1989.
64. A. F. Jenkinsand H. E. Reilly, Tax Barriers to Solar Central Receiver Generation Technology, *Solar Engineering 1995*, American Society of Mechanical Engineers, New York, NY, 1995.
65. A. F. Jenkins, R. A. Chapman, and H. E. Reilly, Tax Barriers to Four Renewable Electric Generation Technologies, *Solar Engineering 1996*, American Society of Mechanical Engineers, New York, NY, 1996.
66. N. Spring, Supercritical Plants to Come Online in 2009, *Power Engineering*, July 2009.
67. M. Alf and J. Kern, “Primer on supercritical steam,” Siemens Power Generation, http://www.elp.com/index/display/article-display/165839/articles/electric-light-power/volume-81/issue-1/power-pointers/primer-on-supercritical-steam.html
68. C. S. Turchi, *Parabolic Trough Reference Plant for Cost Modeling with the Solar Advisor Model (SAM)*, NREL/TP-550-47605, July 2010.
69. Sargent and Lundy, *Assessment of Parabolic Trough and Power Tower Solar Technology Cost and Performance Forecasts*, prepared for Department of Energy and National Renewable Energy Laboratory, SL-5641, Chicago, IL, May 2003.
70. C. K. Ho, S. S. Khalsa, and G. J. Kolb, Methods for Probabilistic Modeling of Concentrating Solar Power Plants, *Solar Energy*, vol. 85, pp. 669-675, 2011.
71. C. K. Ho and G. J. Kolb, Incorporating Uncertainty into Probabilistic Performance Models of Concentrating Solar Power Plants, *J. Solar Energy Engr.*, vol. 132, pp. 031012-1 – 0131012-8, 2010.

APPENDIX A – Analysis of Operating Hours and Failures at Solar Two from January 14, 1998, to April 8, 1999

Date	DNI (kWh/m2)	Outage Category	Solar Outage Hrs	RCVR Salt Flow Time (hr)	Steam Gen Run Time (hr)	Notes
1/14/1998	6.24			5.7	5.5	Start of detailed logs that describe daily issues
1/15/1998	2.59			0.0	0.0	
1/16/1998	4.12			5.5	2.1	
1/17/1998	4.17			3.9	2.9	
1/18/1998	6.47			4.7	2.6	
1/19/1998	2.98			0.0	2.7	
1/20/1998	0.89			0.0	0.0	
1/21/1998	8.19			9.1	10.1	
1/22/1998	8.19			7.7	5.8	
1/23/1998	6.04			5.4	5.6	
1/24/1998	8.35			0.0	0.0	Planned no operation -- no problems, measuring rcvr absorp
1/25/1998	8.46			0.0	0.0	Planned no operation -- no problems, measuring rcvr absorp
1/26/1998	1.59			0.0	0.0	Planned no operation -- no problems, measuring rcvr absorp
1/27/1998	5.42			2.4	0.0	Special RCVR testing
1/28/1998	5.76			6.1	3.1	Proves RCVR can operate through harsh cloud transitions all day
1/29/1998	1.9			0.0	0.0	
1/30/1998	8.1			9.3	7.5	
1/31/1998	0.367			0.0	0.0	
2/1/1998	2.34			0.0	0.0	
2/2/1998	0.57			0.0	0.0	
2/3/1998	0.4			0.0	0.0	
2/4/1998	7.21	Infant Mortality		0.0	0.0	Low RCVR oven temps due to high winds prevented operation
2/5/1998	4.41			6.5	4.4	Harsh cloud transition today but RCVR met collection goal
2/6/1998	0.79			0.0	0.0	
2/7/1998	3.78			0.0	0.0	
2/8/1998	3.84			0.0	0.0	
2/9/1998	8.53			9.1	7.7	Good run
2/10/1998	6.07			7.4	5.8	High thins all day -- good run
2/11/1998	6.26			5.1	4.3	Delayed start due to morning clouds
2/12/1998	3.37			5.6	2.8	Good run
2/13/1998	8.62			9.2	8.4	Good run
2/14/1998	0.03			0.0	0.0	Rain wash the collector field
2/15/1998	7.78			0.0	0.0	High wind stow of heliostat field
2/16/1998	5.85			7.6	5.1	Good run
2/17/1998	0.39			0.0	0.0	
2/18/1998	8.86			9.4	8.9	**Bechtel turns over plant to ESI - good run**
2/19/1998	0.12			0.0	0.0	
2/20/1998	5.91			0.0	0.0	Windy in AM precludes op
2/21/1998	2.37			0.0	0.0	
2/22/1998	3.03			0.0	0.0	
2/23/1998	1.4			0.0	0.0	Rain in PM
2/24/1998	6.05	Infant Mortality		0.0	0.0	Rains led to non-op of heliostat field
2/25/1998	8.17			8.0	5.7	Good RCVR run but shutdown early in PM due to clouds
2/26/1998	6.71			5.0	4.2	
2/27/1998	8.59	Rcvr Inlet Tank Air	4	8.6	4.6	UNSCH OUT - HP air regulator in RCVR blown diphragm - 2 HR OUT to restart RCVR
2/28/1998	8.76	Included Above		7.8	6.4	UNSCH OUT - HP air regulator in RCVR not completely repaired from previous day, another 2 hrs to repair delays startup
3/1/1998	8.32			9.8	8.2	
3/2/1998	8.73	Rankine Steam Sys	2	10.0	6.3	No RCVR problems but there was a 2-hr RCVR shutdown in middle of the day -- turbine trip (hi vacuum press) causes full hot tank?
3/3/1998	9.18	Operator Err	2	7.8	7.0	UNSCH OUT - Operator error caused RCVR trip - 2 hr outage
3/4/1998	7.77	Infant Mortality		0.2	0.0	UNSCH OUT - Tube rupture on W5 (4th tube from left) during startup
3/5/1998	7.55			0.0	0.0	Repairing the tube
3/6/1998	7.03			0.0	0.0	Hi winds are delaying tube repair
3/7/1998	9.3			0.0	0.0	Problem with welder is delaying repair - ask for outside help to arrive tomorrow
3/8/1998	8.99			0.0	0.0	Complete tube repair
3/9/1998	9.2			0.0	0.0	Clean tubes and Sandia installs 5 thermocouples on receiver panel that failed
3/10/1998	10.29	Control Computer	1	4.1	0.0	2 UNSCH OUTS - RCVR tripped 2due to computer problems(1 hr OUT), RCVR could not start due to OP ERR with RCVR air purge system (4 hr OUT)
3/10/1998		Operator Err	4	0.0	0.0	
3/11/1998	10.12	Infant Mortality		0.0	0.0	UNSCH OUT of SGS due to Operator Error on low evap level during SU precluded RCVR operation - need to change startup procedures
3/12/1998	6.46	Utility Grid		2.6	5.9	Limited run because of offsite transmission line restriction
3/13/1998	0.99			0.0	0.0	
3/14/1998	1.84			0.0	0.0	
3/15/1998	9.33			0.0	0.0	No reasons given for why plant did not operate today
3/16/1998	4.01			0.0	0.0	
3/17/1998	8.83			9.1	8.5	Output lower than SOLERGY due to heliostat control problems
3/18/1998	10.05			5.7	4.8	Output lower than SOLERGY due to receiver fill testing
3/19/1998	9.33			8.9	7.1	Testing continues
3/20/1998	8			4.4	0.0	Testing continues
3/21/1998	6.17			1.5	2.0	
3/22/1998	6.76			0.0	0.0	Conservative no-run due to overcast conditions
3/23/1998	9.36	Utility Grid		9.1	9.4	Limited run because of offsite transmission line restriction
3/24/1998	10.25	Control Computer	1	8.0	9.2	UNSCH OUT - DAPS erroneously pulled off heliostats during startup (1 hr OUT)
3/25/1998	1.56			1.1	0.0	
3/26/1998	1.78			0.0	0.0	
3/27/1998	1.68			0.0	0.0	
3/28/1998	2.37			0.0	0.0	Rain and wind
3/29/1998	9.41	Rankine Steam Sys	9	3.1	0.0	UNSCH OUT of SGS on low evap level during SU limited RCVR operation due to hot tank full (18 ft) - steam dump valve PV-1001 Failed
3/30/1998	10.7			3.5	7.2	Scheduled Outage of RCVR in morning to inspect the vent lines on the west panels
3/31/1998	4.99			3.1	2.3	

4/1/1998	6.32			0.0	0.0	Converative no operation due to many passing clouds
4/2/1998	8.72	Infant Mortality		4.5	3.4	UNSCH OUT - Heliostat field burned the RCVR over covers - Lost ~4 hrs of RCVR operation
4/3/1998	4.37			0.0	0.0	Continue to perform oven repair - removed to ground level
4/4/1998	6.07			0.0	0.0	Continue to perform oven repair in shop
4/5/1998	5.15			0.0	0.0	Continue to perform oven repair in shop
4/6/1998	3.12			0.0	0.0	High winds hampers over repair
4/7/1998	8.19			0.0	0.0	Continue to perform oven repair in shop
4/8/1998	10.23			0.0	0.0	Continue to perform oven repair in shop
4/9/1998	9.29			0.0	0.0	Continue to perform oven repair in shop
4/10/1998	9.97			0.0	0.0	Continue to perform oven repair in shop
4/11/1998	3.97			0.0	0.0	Finishing receiver oven and other work
4/12/1998	10.02			0.0	0.0	High Winds all day prevented operation of heliostat field
4/13/1998	5.36			0.0	0.0	Receiver returned to service today, but high winds kept heliostat field stowed
4/14/1998	6.84			0.0	0.0	Looks like BCS work and winds prevented operation. Perhaps checking aim of heliostats to prevent reburn of ovens?
4/15/1998	8.26			0.0	0.0	Continuing to check heliostats with BCS
4/16/1998	10.3	Heat Trace Sys	9	0.0	0.0	UNSCH OUT - Riser plugged - 2 heat trace circuits found off. Perhaps riser strainer was frozen? Soaked riser at 600 F all day to recover.
4/17/1998	9.99	Infant Mortality		0.4	0.0	UNSCH OUT - Small tube leak on W5 (5th tube from left) noticed during startup
4/18/1998	10.85			0.0	0.0	Completed tube repair and other misc jobs
4/19/1998	10.26	HVAC	3.25	5.4	0.8	2 UNSCH OUTS - ILS link caused field to defocus (15 min OUT). Then SG tripped due to cold salt in hot-pump sump (lost 5 hrs of collection because hot tank full)
4/19/1998		Infant Mortality		0.0	0.0	
4/20/1998	10.03	Included Above		5.5	8.6	UNSCH OUT - ILS tripped heliostat field again (same problem as yesterday). Cause is failure of HVAC in remote station #1 (3 hr OUT)
4/21/1998	10.22	Infant Mortality		1.1	8.8	UNSCH OUT - Oven covers are burning again due to aiming problem - shutdown receiver most of day.
4/22/1998	9.93			9.9	13.1	
4/23/1998	10.37	Infant Mortality		2.3	0.0	UNSCH OUT - Oven covers are oveheating due to aiming problem
4/24/1998	9.78			0.0	0.0	Continue to troubleshoot aiming problem
4/25/1998	4.52			0.0	0.0	Aiming issue semi resolved. See discussion in SAND2002-0120
4/26/1998	7.81			7.6	6.8	
4/27/1998	9.68	Infant Mortality		9.9	6.5	UNSCH OUT - Operator error caused SGS trip - procedures were not properly followed. RCVR offline due to hot tank full
4/28/1998	9.23	Infant Mortality		4.4	3.6	UNSCH OUT - Oven covers are oveheating once again
4/29/1998	9.35			0.0	0.0	Repaired oven cover brackets
4/30/1998	9.26			4.6	3.3	Receiver aimpoint testing continues
5/1/1998	9.22			6.2	8.7	
5/2/1998	9.77			0.0	0.0	Receiver aimpoint testing continues by Sandia's Bob Edgar and Ken Stone (MDAC)
5/3/1998	9.08			7.5	7.7	Good run but early conservative shutdown due to many puffy clouds
5/4/1998	6.75	Infant Mortality		0.0	0.0	High winds precluded RCVR preheat
5/5/1998	4.12			0.0	0.0	
5/6/1998	2.73			0.0	0.0	
5/7/1998	4.94			3.4	0.0	
5/8/1998	9.93			2.2	2.7	Aimpoint testing
5/9/1998	8.22	Infant Mortality		3.7	0.0	UNSCH OUT - RCVR plugged tube on W5 identified during startup. RCVR operated in preheat only.
5/10/1998	10.01			1.0	0.0	The W5 tube plug ruptured today (5th tube from North). High winds.
5/11/1998	7.17			0.0	0.0	Started to replace tube.
5/12/1998	3.94			0.0	0.0	High winds are hampering tube repair
5/13/1998	3.43			0.0	0.0	
5/14/1998	9.35			0.0	0.0	Lowered panel W5 to ground
5/15/1998	10.44			0.0	0.0	
5/16/1998	8.82			0.0	0.0	
5/17/1998	11.01			0.0	0.0	
5/18/1998	9.58			0.0	0.0	
5/19/1998	8.33			0.0	0.0	Winds hampering reinstall of W5
5/20/1998	10.07			0.0	0.0	Winds hampering reinstall of W5 - start to schedule 430 am work to avoid winds
5/21/1998	11.33			0.0	0.0	
5/22/1998	10.95			0.0	0.0	Winds in morning slowing work
5/23/1998	9.93			0.0	0.0	
5/24/1998	10.36			0.0	0.0	Receiver repairs completed
5/25/1998	7.26			0.0	0.7	Spent most of the day reheating the steam generator after long outage
5/26/1998	6.62	Infant Mortality		0.0	0.0	UNSCH OUT? See 7/8 - RCVR bypass valve (HV5020) heat trace cable and spare are both burned out. Don't start RCVR until fixed - Conservative?.
5/27/1998	11.05			0.0	0.0	Installed new heat trace. Used heliostats to try and thaw a plug in W8 first noted on 5/9
5/28/1998	9.52	Infant Mortality		0.0	0.0	UNSCH OUT - Could not thaw plug in W8
5/29/1998	4.06			0.0	0.0	Too windy to thaw W8 - decide to install new heat trace on W8 to help with thaw
5/30/1998	11.03			0.0	0.0	Installed heat trace to help with thaw
5/31/1998	7.48			0.0	0.0	Complete install of heat trace and test W8 temperatures

6/1/1998	11.12	Rcvr Trip - Unk	1.5	7.3	5.5	UNSCH OUT - Receiver trip, cause unknown (OUT 1.5 hrs). Tube thawed mid day
6/2/1998	10.82	Steam Gen Trip - Unk	4	4.5	7.7	UNSCH OUT - SGS tripped (cause unknown). Hot Tank full thus trip receiver. (OUT ~4hrs)
6/3/1998	9.48			0.0	0.0	High winds during preheat and then stowed field rest of day
6/4/1998	10.83			9.1	11.8	Several tube plugs on W6 delayed startup until mid day.
6/5/1998	10.63	Rcvr Trip - Unk	2	9.6	13.3	UNSCH OUT - 2 Receiver ILS trips (unknown cause) (OUT 2 hr)
6/6/1998	9.42			8.3	13.9	Station blackout during night (when SGS operating?). Safely shutdown systems. Wind caused.
6/7/1998	10.54	Helio Field Common Mode	10	0.0	0.0	UNSCH OUT - Last nights blackout caused many heliostat control strings to fail. All day to recover.
6/8/1998	8.94			7.6	15.6	
6/9/1998	8.8	Rcvr Panel Drain Valves	3	6.7	7.2	UNSCH OUT - RCVR drain valve solenoid failure delayed startup (gummed up, clean/reinstall) (OUT 3 hrs)
6/10/1998	5.59	Control Computer	0.5	6.1	9.2	UNSCH OUT - ILS trip (unknown) (OUT 30 min)
6/11/1998	10.12			0.0	0.0	Scheduled Outage to install to replace RCVR ball valves with gate valves
6/12/1998	7.21			0.0	0.0	Tried to test new gates valves but clouds hampered test
6/13/1998	11.01			10.2	14.1	First ever SGS run through the night
6/14/1998	10.98	Control Computer	1	9.7	24.0	UNSCH OUT - Master Control Computer failed delaying RCVR startup, needed to reboot (OUT 1 hr)
6/15/1998	10.43			11.6	24.0	Good run
6/16/1998	10.41	Infant Mortality		2.5	9.4	UNSCH OUT - Several plugged tubes in W8 - high winds. Ended ~70 hr SGS run.
6/17/1998	11.64			6.6	4.5	Plugs cleared but SU delayed to repair air tank to reduce air consumption - could have done this repair at night?
6/18/1998	11.32			13.1	16.6	Good run
6/19/1998	11.26	Infant Mortality		6.4	3.2	UNSCH OUT see 7/8? - RCVR bypass valve (HV5020) heat trace cable and spare are both burned out. Delayed startup (4hrs) of RCVR (conservative decision?) -ordered cables
6/20/1998	11.16			12.3	15.3	Good run
6/21/1998	11.61	Infant Mortality		10.9	9.6	UNSCH OUT - RCVR plug in W5 delayed startup by 2 hr
6/22/1998	11.5	Heat Trace Sys	9	0.0	0.0	UNSCH OUT - Inlet tank vent valve (PV5003) obstructed with salt - cleaned and stoked (OUT 9hrs) valve heat trace failure??
6/23/1998	11.25	Infant Mortality		11.5	15.0	UNSCH OUT - RCVR plug in W7 with 25 mph wind delayed startup ~2 hr. Removed PV5003 after run and found plug in pipe, not valve
6/24/1998	10.88			8.6	9.7	Dispatchability testing (25%, 50%, 75%)
6/25/1998	10.8	Infant Mortality		1.9	0.0	UNSCH OUT - RCVR plug in W7 on SU with high winds - no run
6/26/1998	11.08			10.2	9.8	Good run
6/27/1998	11.22			9.4	11.5	Dispatchability test
6/28/1998	11.54			8.7	12.4	Dispatchability test
6/29/1998	11.41	Infant Mortality		11.1	15.9	UNSCH OUT - RCVR plug delayed SU by ~30 minutes
6/30/1998	11.2	Infant Mortality		4.2	14.4	UNSCH OUT - RCVR plug delayed SU until afternoon
7/1/1998	11.12	Infant Mortality		11.7	16.8	UNSCH OUT - RCVR plug delayed SU a few hours
7/2/1998	10.79	Infant Mortality		12.3	24.0	UNSCH OUT - RCVR plug delayed SU ~2 hours
7/3/1998	10.83			12.5	24.0	Good run
7/4/1998	11.05			12.2	24.0	Good run
7/5/1998	10.35	Rcvr Inlet Tank Air	1	11.0	24.0	UNSCH OUT - Unknown problem caused spill through inlet tank vent (OUT 1 hr) - supect inlet tank air valve malfunction
7/6/1998	9.4			11.5	24.4	Good run
7/7/1998	7.52			9.0	18.8	
7/8/1998	7.76			9.2	9.3	HV5020 thermocouple connection failed but did not impact operation
7/9/1998	9.98	Rankine Steam Sys	1.5	11.2	8.5	UNSCH OUT - Turbine control problem caused SU failure. Hot tank full (OUT 1.5 hr)
7/10/1998	11.08	Infant Mortality		11.4	14.9	UNSCH OUT - RCVR plug on W7 delayed SU ~2 hours
7/11/1998	11.86	Infant Mortality		9.2	0.0	UNSCH OUT - RCVR plug on W5 prevented operation - cold tank was heated to 600 F due to salt circulation
7/12/1998	11.94	Infant Mortality		9.1	8.7	UNSCH OUT - RCVR plug on W5 delayed SU ~3 hours
7/13/1998	11.86	Infant Mortality		12.1	11.1	UNSCH OUT - RCVR plug on W7 delayed SU ~0.5 hours
7/14/1998	11.41	Steam Gen Water Pump	4	11.4	7.9	UNSCH OUT - SGS water pump P853 tripped 2 times on hi temperature. Hot Tank full. (OUT 4 hr)
7/15/1998	11.23	Rankine Steam Sys	4	7.6	8.0	UNSCH OUT - Turbine tripped. Exhaust instrument recalibration fixed the problem (OUT 4 hr)
7/16/1998	10.77	Salt FCVs	15	0.0	0.0	UNSCH OUT - Repair salt valve leak (PSV5071) piping (cold pump recirc line) - out all day
7/17/1998	8.72	Included Above		1.8	0.0	UNSCH OUT - Complete repair of PSV5071 - reheat the valve with heat trace. Total OUT was 15 hrs.
7/18/1998	7.15			8.2	4.0	Firecracker 250 race puts much dust in the air
7/19/1998	7.1	Maintenance Err	10	0.0	0.0	UNSCH OUT - PV5003 Inlet Tank Vent Valve did not close during morning fill. Operations found no problem but nightshift found valve open. (OUT 10 hr)
7/20/1998	1.83			0.0	0.0	
7/21/1998	6.8	Rcvr Inlet Tank Air	4	4.6	1.8	UNSCH OUT - Inlet tank pressure control failed (OUT 4 hr)
7/22/1998	4.59			0.0	0.0	SCHED OUT - Inspecting/cleaning internals of SGS Preheater.
7/23/1998	6.96			0.0	0.0	SGS outage continues. Much other work being done, e.g. cold pump motors were sent off site
7/24/1998	10.34			0.0	0.0	
7/25/1998	10.92			0.0	0.0	
7/26/1998	11.06			0.0	0.0	
7/27/1998	10.63			0.0	0.0	Inspected Evaporator today. Took many days to cool down the kettle.
7/28/1998	8.75			0.0	0.0	Evaporator temperature and pressure coming up slowly. Emergency diesel failed several start attempts
7/29/1998	10.56			0.0	2.3	Testing SGS after heating up. Outage ends.
7/30/1998	11.19			4.4	1.4	Short run today but no report is available to explain why
7/31/1998	11.39	Rcvr Inlet Tank Air	4	8.2	13.3	UNSCH OUT - Late start - looks like to adjust inlet vessel vent valve PV5003 to ensure tight closure

8/1/1998	11.32	Rankine Steam Sys	5	6.7	2.9	UNSCH OUT - Unknown turbine trips led to hot tank full and shutdown of receiver. (OUT 5 hr)
8/2/1998	11.01			10.3	10.4	Delayed start 3.5 hr to resolve previous day problem. Control logic changed so that trip cause cannot happen again.
8/3/1998	10.87	Infant Mortality		11.2	8.6	UNSCH OUT - RCVR plug on W3 delayed SU 1 hour
8/4/1998	10.66	HVAC	7	3.5	0.9	UNSCH OUT - HVAC failure (see comments on 8/5 daily report) on Load Center A prevented turbine startup. (OUT 7 hr)
8/5/1998	10.25			12.1	13.4	Good run
8/6/1998	7.71			7.3	4.7	
8/7/1998	7.79			8.0	6.9	
8/8/1998	8.97			8.0	6.3	
8/9/1998	7.2			5.1	4.7	
8/10/1998	0.39			0.0	0.0	
8/11/1998	6.62			3.8	1.6	Conservative SU delay due to lightning in the area.
8/12/1998	8.51			5.5	11.7	
8/13/1998	5.65			7.8	6.0	
8/14/1998	7.01	Rankine Steam Sys	2	6.5	0.0	UNSCH OUT - SGS main boiler feed pump seal replaced (OUT 2 hr)
8/15/1998	7			4.0	5.4	Late startup. Looks like operators were busy operating the SGS/turbine
8/16/1998	7.74			6.9	14.6	
8/17/1998	10.21			9.3	11.0	
8/18/1998	11.03	Infant Mortality		5.5	6.7	UNSCH OUT - Several RCVR plugs (OUT 4 hr)
8/19/1998	9.63			1.9	2.3	Pre test part day run
8/20/1998	10.06			3.2	0.0	Serpentine fill tests that were directed by me
8/21/1998	10.75			0.4	0.0	Serpentine tests concluded. Hot Tank inspection kept RCVR down rest of day.
8/22/1998	8.73			0.0	0.0	SCHED OUT - Hot tank cool down begins for inspection of internals
8/23/1998	7.04			0.0	0.0	
8/24/1998	7.59			0.0	0.0	
8/25/1998	8.14			0.0	0.0	
8/26/1998	10.23			2.1	0.0	Short run to keep cold tank warm -- outage continues
8/27/1998	8.83			0.0	0.0	Inspection performed today - Everything inside tank looks good
8/28/1998	9.95	Infant Mortality		0.0	0.0	UNSCH OUT - Failed RCVR vent valve heat trace found yesterday - no spares, ordered new due tomorrow
8/29/1998	6.68			3.7	2.4	Limited receiver run because of hot tank rate limit of 100 F/hr
8/30/1998	4.97			3.1	0.0	Finished the limited receiver run because of hot tank rate limit of 100 F/hr
8/31/1998	4.77	Helio Field Common Mode	3.5	1.9	0.0	UNSCH OUT - Startup delayed due to inability of heliostats to wakeup easily after turning off power. Power off because of lightning last night.
9/1/1998	4.69			5.2	3.2	**Begin campaign to reduce parasitics**
9/2/1998	5.4			4.4	3.3	
9/3/1998	2.83			0.0	0.0	
9/4/1998	1.42			0.0	0.0	Rain caused some RCVR heat trace problems
9/5/1998	4.36	Infant Mortality		0.0	0.0	UNSCH OUT - Rain-induced RCVR heat trace failures are being fixed (OUT 4 hr)
9/6/1998	1.41			0.0	0.0	Weather outage - still working on failed heat trace
9/7/1998	4.51	Infant Mortality		0.0	0.0	UNSCH OUT - Heat trace still failing (OUT 2 hr)
9/8/1998	5.59			6.4	3.9	Ran in AM. Could have run in PM for a couple of hours but RCVR not restart after 3 hrs of cloud cover.
9/9/1998	8.44	Infant Mortality		0.0	0.0	UNSCH OUT - RCVR controls failure. Looks like rain intrusion into cabinet (OUT 8 hr)
9/10/1998	9.01	Maintenance Err	2	8.8	5.1	2 UNSCH OUTS - 1)MAINT ERR cooling water to water-side SGS pumps inadvert valved out (OUT 2 hr). 2) RCVR salt safety lift tripped rcvr (OUT 0.5 hr)
9/10/1998		Rcvr Trip - Unk	0.5	0.0	0.0	
9/11/1998	9.77			4.0	10.9	UNSCH OUT - Hot tank full, apparently to complete SGS repairs (OUT 3 hr)
9/12/1998	9.51			7.6	13.9	
9/13/1998	9.62			9.8	19.3	
9/14/1998	7.4			6.6	7.5	
9/15/1998	6.9			5.8	8.3	
9/16/1998	8.73			7.0	14.5	Ran in AM. Could have run in PM for a couple of hours but RCVR not restart after 2 hrs of cloud cover.
9/17/1998	9.47	Maintenance Err	6.5	2.7	0.3	UNSCH OUT - MAINT ERR resulted in MCS computer lockup and inadvertant fill/freeze in the RCVR (OUT 6.5 hr)
9/18/1998	10.56			8.0	10.9	
9/19/1998	9.88	Control Computer	2.5	6.8	5.5	UNSCH OUT - MCS reboot needed to gain control of heliostat field (OUT 2.5 hr)
9/20/1998	9.5	Infant Mortality		6.8	5.8	UNSCH OUT - Many RCVR tubes plugged during windy fill (OUT 3 hr)
9/21/1998	9.14	Infant Mortality		9.5	6.3	UNSCH OUT - Many RCVR tubes plugged during windy fill (OUT 4 hr)
9/22/1998	8.26			2.1	0.0	Testing the Serpentine fill procedure all day
9/23/1998	9.16			8.8	8.3	
9/24/1998	8.94	Infant Mortality		7.1	7.0	UNSCH OUT - RCVR plugs during startup (OUT 1 hr)
9/25/1998	8.53	Rcvr Trip - Unk	0.5	9.6	7.3	UNSCH OUT - RCVR cold pump unknown trip (OUT 0.5 hr)
9/26/1998	8.75			9.8	8.1	Good run
9/27/1998	7.11			7.2	5.7	Good run - overnight thermal conditioning test is underway
9/28/1998	9.16			9.5	8.7	
9/29/1998	8.34			6.9	5.4	
9/30/1998	8.19			8.9	8.5	Good run

10/1/1998	9.32	Control Computer	1	4.1	5.1	2 UNSCH OUTS - 1) MCS lockup delayed RCVR SU (OUT 1 hr) 2) Main steam bypass valve erratic causes SGS trip (OUT 4 hr)
10/1/1998		Rankine Steam Sys	4	0.0	0.0	
10/2/1998	9.55			9.0	8.9	
10/3/1998	8.45	Infant Mortality		0.0	0.0	UNSCH OUT - high winds preclude RCVR preheat - cold ovens
10/4/1998	9.11	Infant Mortality		9.6	7.7	UNSCH OUT - plugged tubes during RCVR SU (OUT 2 hr)
10/5/1998	9.84	HVAC	2	7.0	7.0	UNSCH OUT - RCVR remote station HVAC problem delayed SU (OUT 2 hr)
10/6/1998	9.25			10.7	9.0	Good run
10/7/1998	6.73			9.9	7.9	Outstanding demonstration of energy collection during difficult cloud conditions
10/8/1998	8.54			9.9	8.9	Good run
10/9/1998	9.19			9.4	8.9	Good run
10/10/1998	9.13	Infant Mortality		8.5	7.2	UNSCH OUT - plugged tubes during RCVR SU (OUT 2 hr)
10/11/1998	8.18	Infant Mortality		9.5	7.7	UNSCH OUT - plugged tubes during RCVR SU (OUT 0.5 hr)
10/12/1998	5.61			5.8	6.0	Good run
10/13/1998	8.61			9.6	7.8	Good run
10/14/1998	6.63	Infant Mortality		6.1	0.0	UNSCH OUT - plugged tubes during RCVR SU (OUT 2 hr)
10/15/1998	6.67	Infant Mortality		0.0	0.0	UNSCH OUT - high winds preclude RCVR preheat - cold ovens
10/16/1998	8.13	Rcvr Trip - Unk	3	4.8	7.9	UNSCH OUT - RCVR tripped due to erroneous salt flow transmitter, but no problem found (OUT 3 hr)
10/17/1998	8.96			10.2	5.8	
10/18/1998	8.85			10.0	8.2	Good run
10/19/1998	8.01	Control Computer	2	7.9	7.3	UNSCH OUT - MCS anomaly delayed SU of RCVR (OUT 2 hr)
10/20/1998	8.28			10.0	9.0	Good run
10/21/1998	8.3	Salt FCVs	1	8.3	7.4	UNSCH OUT - RCVR flow control valve 5302A problem. Adjust and continue SU. B valve is not auto backup. (OUT 2 hr)
10/22/1998	9.32			0.0	0.0	SCHED OUT - Installing heat trace on lower tube clip area to mitigate plugged tube problem W3, W5, W7
10/23/1998	7.07			0.0	0.0	Outage continues - 24 hr average parasitic power is reduced to 416 kW
10/24/1998	1.76			2.1	0.0	Receiver ran on a bad weather day
10/25/1998	6.48			7.1	7.1	Good run
10/26/1998	7.42			6.1	4.5	
10/27/1998	8.36			0.0	0.0	SCHED OUT - Installing heat trace on lower tube clip area to mitigate plugged tube problem W4, W6, W8,
10/28/1998	7.37			0.0	0.0	Outage continues - 24 hr average parasitic power is 446 kW
10/29/1998	2.91			0.0	0.0	
10/30/1998	3.21			0.0	0.0	
10/31/1998	8.91	Infant Mortality	2.5	5.1	0.7	UNSCH OUT - RCVR Backtube TC fails causing RCVR trip lock in -Heliostats would not go to preheat (OUT 2.5 hr). Remove TC from scan.
11/1/1998	7.76			7.7	13.6	
11/2/1998	6.6			8.7	6.6	Good run
11/3/1998	8.27			9.7	8.0	Good run
11/4/1998	7.69			9.3	7.8	Good run
11/5/1998	7.25	Infant Mortality		8.2	4.0	UNSCH OUT - plugged tubes in W5, W7 during RCVR SU (OUT 4.5 hr)
11/6/1998	7.79	Infant Mortality		8.8	7.4	UNSCH OUT - plugged tubes during RCVR SU (OUT 0.5 hr)
11/7/1998	5.96	Infant Mortality		0.0	0.0	UNSCH OUT - high winds preclude RCVR preheat - too cold to fill
11/8/1998	4.06			0.0	0.0	
11/9/1998	7.37	Infant Mortality		4.7	4.4	UNSCH OUT - plugged tubes (W4, W5, W6, W7) during RCVR SU (OUT 2 hr)
11/10/1998	7.19			5.1	5.4	
11/11/1998	0.33			0.0	0.0	
11/12/1998	8.57			8.8	7.2	Receiver efficiency test run today
11/13/1998	8.51			6.6	5.4	Receiver efficiency test run today
11/14/1998	8.6			0.0	0.0	No run today (Weekend) lack of manpower
11/15/1998	8.13			0.0	0.0	No run today (Weekend) lack of manpower
11/16/1998	6.57	Infant Mortality		1.2	0.0	UNSCH OUT - DOWNCOMER RUPTURED
				0.0	0.0	
2/23/1999	8.67			3.8	0.0	Short receiver run after returning from long outage
2/24/1999	7.42			3.6	2.5	Short run with many restart problems that were resolved
2/25/1999	7.45			6.3	4.8	
2/26/1999	8.18	Salt FCVs	8	2.6	0.0	UNSCH OUT - Flow control problems in RCVR (OUT 8 hr), SEGS 1 Storage System destroyed today.
2/27/1999	8.2			0.0	0.0	Budget prohibits run on weekend - Smoke from SEGS 1 fire
2/28/1999	8			0.0	4.5	Budget prohibits run on weekend - Ran SGS to get ready for Monday run

3/1/1999	7.63			8.3	5.2	Receiver efficiency test. Defocussing lead to an E that is 75% of SOLERGY
3/2/1999	8.38			10.2	8.8	Receiver efficiency test. Defocussing lead to an E that is 90% of SOLERGY
3/3/1999	8.54			5.6	4.8	Receiver drain/fill test in high winds - Receiver did not meet refill temperature requirements
3/4/1999	8.93	Infant Mortality		8.1	3.9	UNSCH OUT - High AM winds caused numerous RCVR plugs on SU -- W4, 5, 7, and 8 (OUT 3 hr)
3/5/1999	9.56	Infant Mortality		9.9	8.3	UNSCH OUT - High AM winds caused RCVR plugs (OUT 1 hr), Receiver efficiency testing continues
3/6/1999	7.09			0.0	0.0	Budget prohibits run on weekend
3/7/1999	6.63			0.0	0.0	Budget prohibits run on weekend
3/8/1999	8.52	Rcvr Inlet Tank Air	7	3.0	0.0	UNSCH OUT - Air inlet valve to inlet vessel. Valve OK but no signal to computers (OUT 7 hr)
3/9/1999	7.02	Rcvr Inlet Tank Level Inst	3	1.5	3.2	UNSCH OUT - Nuclear level detector for inlet vessel repaired and calibrated (OUT 3 hr)
3/10/1999	5.66	Rcvr Trip - Unk	0.5	6.5	3.9	UNSCH OUT - 2 RCVR trips for unknown reasons (OUT 0.5 hr)
3/11/1999	5.9			2.7	0.0	Receiver fill and drain tests during cloudy/windy weather - good results
3/12/1999	8.41			10.4	9.5	Receiver efficiency test. Defocussing lead to an E that is 85% of SOLERGY
3/13/1999	7.41			0.0	0.0	Budget prohibits run on weekend
3/14/1999	2.74			0.0	0.0	Budget prohibits run on weekend
3/15/1999	5.67			0.0	0.0	High winds and clouds prevented operation
3/16/1999	1.05			0.0	0.0	
3/17/1999	9.31			10.0	8.3	Receiver efficiency test. Defocussing lead to an E that is 85% of SOLERGY
3/18/1999	8.23			9.6	9.4	Receiver efficiency test. Defocussing lead to an E that is 89% of SOLERGY
3/19/1999	2.82			0.0	0.0	Performed some scheduled maintenance during bad weather
3/20/1999	9.77			0.0	0.0	Budget prohibits run on weekend
3/21/1999	9.38			0.0	0.0	Budget prohibits run on weekend
3/22/1999	7.88			8.1	8.3	Receiver efficiency test. Defocussing lead to an E that is 75% of SOLERGY
3/23/1999	8.43			9.4	9.5	Receiver efficiency test. Defocussing lead to an E that is 75% of SOLERGY
3/24/1999	8.41			9.4	10.7	Receiver efficiency test. Defocussing lead to an E that is 82% of SOLERGY
3/25/1999	0.14			0.0	0.0	
3/26/1999	9.04	Infant Mortality		4.2	2.0	UNSCH OUT - Operator Error led to SGS trip - Conservative shutdown since turbine insulation is soaked with oil (OUT 6 hr)
3/27/1999	9.35			1.0	6.7	Budget prohibits run on weekend - but running turbine in steam dump mode because of oil in insulation
3/28/1999	8.01			0.0	0.0	Budget prohibits run on weekend
3/29/1999	8.41	Control Computer	1	9.7	8.9	UNSCH OUT - Receiver tripped 2 time due to ILS problems (OUT 1 hr). Turbine idle due to oil. E is 86% of SOLERGY.
3/30/1999	7.7			9.1	8.9	Receiver efficiency test. Defocussing lead to an E that is 75% of SOLERGY. Turbine idle due to oil.
3/31/1999	3.75			0.0	0.0	Weather outage. Winds ~ 50 mph.
4/1/1999	5.82			6.2	6.3	Receiver testing. E is 94% of SOLERGY.
4/2/1999	9.47			0.3	0.0	Receiver test. Studied the discharge of the inlet tank during blackout conditions with no RCVR pump. Looks good.
4/3/1999	2.33			0.0	0.0	Budget prohibits run on weekend
4/4/1999	5.05			0.0	0.0	Budget prohibits run on weekend
4/5/1999	8.77			4.3	0.0	Short run. No daily report to say why.
4/6/1999	1.33			0.0	0.0	
4/7/1999	6.96			1.8	0.0	Receiver blackout test. Looks good.
4/8/1999	8.21			11.4	9.2	Ran aimpoint test for T&E group. RCVR shut down for last time at 7 pm.
				1460	1474	

DISTRIBUTION

Internal distribution *(distributed electronically unless otherwise noted)*:

1 MS0899 RIM-Reports Management 9532 *(electronic copy)*


Sandia National Laboratories